VOLCANIC EVIDENCE FOR A COMPOSITIONAL CONTRAST IN THE LITHOSPHERIC UPPER MANTLE ACROSS THE TINTINA TRENCH, SOUTHEASTERN YUKON, CANADA

Valérie Hasik
McGill University, Montréal
June 1994

A thesis submitted
to the Faculty of Graduate Studies and Research
in partial fulfilment of the requirements for the
M.Sc. degree in Geology

Nom VALÉRIE HASIK

Dissertation Abstracts International est organisé en catégories de sujets Veuillez s v p choisir le sujet qui décrit le mieux votre thèse et inscrivez le code numérique approprié dans l'espace réservé ci-dessous

GÉOLOGIE — SUJET

0372 — CODE DE SUJET

U·M·I

Catégories par sujets

HUMANITÉS ET SCIENCES SOCIALES

COMMUNICATIONS ET LES ARTS

Architecture	0729
Beaux arts	0357
Bibliothéconomie	0399
Cinéma	0900
Communication verbale	0459
Communications	0708
Danse	0378
Histoire de l'art	0377
Journalisme	0391
Musique	0413
Sciences de l'information	0723
Théâtre	0465

ÉDUCATION

Généralités	515
Administration	0514
Art	0273
Collèges communautaires	0275
Commerce	0688
Économie domestique	0278
Éducation permanente	0516
Éducation préscolaire	0518
Éducation sanitaire	0680
Enseignement agricole	0517
Enseignement bilingue et multiculturel	0282
Enseignement industriel	0521
Enseignement primaire	0524
Enseignement professionnel	0747
Enseignement religieux	0527
Enseignement secondaire	0533
Enseignement spécial	0529
Enseignement supérieur	0745
Évaluation	0288
Finances	0277
Formation des enseignants	0530
Histoire de l'éducation	0520
Langues et littérature	0279
Lecture	0535
Mathématiques	0280
Musique	0522
Orientation et consultation	0519
Philosophie de l'éducation	0998
Physique	0523
Programmes d'études et enseignement	0727
Psychologie	0525
Sciences	0714
Sciences sociales	0534
Sociologie de l'éducation	0340
Technologie	0710

LANGUE, LITTÉRATURE ET LINGUISTIQUE

Langues	
Généralités	0679
Anciennes	0289
Linguistique	0290
Modernes	0291
Littérature	
Généralités	0401
Anciennes	0294
Comparée	0295
Médiévale	0297
Moderne	0298
Africaine	0316
Américaine	0591
Anglaise	0593
Asiatique	0305
Canadienne (Anglaise)	0352
Canadienne (Française)	0355
Germanique	0311
Latino américaine	0312
Moyen orientale	0315
Romane	0313
Slave et est européenne	0314

PHILOSOPHIE, RELIGION ET THÉOLOGIE

Philosophie	0422
Religion	
Généralités	0318
Clergé	0319
Études bibliques	0321
Histoire des religions	0320
Philosophie de la religion	0322
Théologie	0469

SCIENCES SOCIALES

Anthropologie	
Archéologie	0324
Culturelle	0326
Physique	0327
Droit	0398
Économie	
Généralités	0501
Commerce-Affaires	0505
Économie agricole	0503
Économie du travail	0510
Finances	0508
Histoire	0509
Théorie	0511
Études américaines	0323
Études canadiennes	0385
Études féministes	0453
Folklore	0358
Géographie	0366
Gérontologie	0351
Gestion des affaires	
Généralités	0310
Administration	0454
Banques	0770
Comptabilité	0272
Marketing	0338
Histoire	
Histoire générale	0578
Ancienne	0579
Médiévale	0581
Moderne	0582
Histoire des noirs	0328
Africaine	0331
Canadienne	0334
États Unis	0337
Européenne	0335
Moyen orientale	0333
Latino américaine	0336
Asie, Australie et Océanie	0332
Histoire des sciences	0585
Loisirs	081
Planification urbaine et régionale	0999
Science politique	
Généralités	0615
Administration publique	0617
Droit et relations internationales	0616
Sociologie	
Généralités	0626
Aide et bien être social	0630
Criminologie et établissements pénitentiaires	0627
Démographie	0938
Études de l'individu et de la famille	0628
Études des relations interethniques et des relations raciales	0631
Structure et développement social	0700
Théorie et méthodes	0344
Travail et relations industrielles	0629
Transports	0709
Travail social	0452

SCIENCES ET INGÉNIERIE

SCIENCES BIOLOGIQUES

Agriculture	
Généralités	0473
Agronomie	0285
Alimentation et technologie alimentaire	0359
Culture	0479
Élevage et alimentation	0475
Exploitation des pâturages	0777
Pathologie animale	0476
Pathologie végétale	0480
Physiologie végétale	0817
Sylviculture et faune	0478
Technologie du bois	0746
Biologie	
Généralités	0306
Anatomie	0287
Biologie (Statistiques)	0308
Biologie moléculaire	0307
Botanique	0309
Cellule	0379
Écologie	0329
Entomologie	0353
Génétique	0369
Limnologie	0793
Microbiologie	0410
Neurologie	0317
Océanographie	0416
Physiologie	0433
Radiation	0821
Science vétérinaire	0778
Zoologie	0472
Biophysique	
Généralités	0786
Médicale	0760

SCIENCES DE LA TERRE

Biogéochimie	0425
Géochimie	0996
Géodésie	0370
Géographie physique	0368
Géologie	0372
Géophysique	0373
Hydrologie	0388
Minéralogie	0411
Océanographie physique	0415
Paléobotanique	0345
Paléoécologie	0426
Paléontologie	0418
Paléozoologie	0985
Palynologie	0427

SCIENCES DE LA SANTÉ ET DE L'ENVIRONNEMENT

Économie domestique	0386
Sciences de l'environnement	0768
Sciences de la santé	
Généralités	0566
Administration des hôpitaux	0769
Alimentation et nutrition	0570
Audiologie	0300
Chimiothérapie	0992
Dentisterie	0567
Développement humain	0758
Enseignement	0350
Immunologie	0982
Loisirs	0575
Médecine du travail et thérapie	0354
Médecine et chirurgie	0564
Obstétrique et gynécologie	0380
Ophtalmologie	0381
Orthophonie	0460
Pathologie	0571
Pharmacie	0572
Pharmacologie	0419
Physiothérapie	0382
Radiologie	0574
Santé mentale	0347
Santé publique	0573
Soins infirmiers	0569
Toxicologie	0383

SCIENCES PHYSIQUES

Sciences Pures

Chimie	
Généralités	0485
Biochimie	487
Chimie agricole	0749
Chimie analytique	0486
Chimie minérale	0488
Chimie nucléaire	0738
Chimie organique	0490
Chimie pharmaceutique	0491
Physique	0494
PolymÈres	0495
Radiation	0754
Mathématiques	0405
Physique	
Généralités	0605
Acoustique	0986
Astronomie et astrophysique	0606
Électronique et électricité	0607
Fluides et plasma	0759
Météorologie	0608
Optique	0752
Particules (Physique nucléaire)	0798
Physique atomique	0748
Physique de l'état solide	0611
Physique moléculaire	0609
Physique nucléaire	0610
Radiation	0756
Statistiques	0463

Sciences Appliqués Et Technologie

Informatique	0984
Ingénierie	
Généralités	0537
Agricole	0539
Automobile	0540
Biomédicale	0541
Chaleur et thermodynamique	0348
Conditionnement (Emballage)	0549
Génie aérospatial	0538
Génie chimique	0542
Génie civil	0543
Génie électronique et électrique	0544
Génie industriel	0546
Génie mécanique	0548
Génie nucléaire	0552
Ingénierie des systèmes	0790
Mécanique navale	0547
Métallurgie	0743
Science des matériaux	0794
Technique du pétrole	0765
Technique minière	0551
Techniques sanitaires et municipales	0554
Technologie hydraulique	0545
Mécanique appliquée	0346
Géotechnologie	0428
Matières plastiques (Technologie)	0795
Recherche opérationnelle	0796
Textiles et tissus (Technologie)	0794

PSYCHOLOGIE

Généralités	0621
Personnalité	0625
Psychobiologie	0349
Psychologie clinique	0622
Psychologie du comportement	0384
Psychologie du développement	0620
Psychologie expérimentale	0623
Psychologie industrielle	0624
Psychologie physiologique	0989
Psychologie sociale	0451
Psychométrie	0632

ABSTRACT

In the southeastern Yukon Territory, Quaternary continental alkaline basalts have erupted across an important crustal suture, the Tintina Trench, which separates the accreted terranes of the Canadian Cordillera from the ancestral North American craton. The lavas from the Rancheria region from the west side of the Tintina Trench are basanites (BASAN), alkaline olivine basalts (AOB), and hypersthene-normative basalts (HYN). They display fractionated rare earth element (REE) profiles and are enriched in light rare earth elements (LREE) and high field strength elements (HFSE). The compositional spectra of the Rancheria alkaline magmas appears to represent the progressive melting of an amphibole-bearing garnet lherzolite. The involvement of amphibole in the petrogenesis of the Rancheria alkaline magmas indicates that these magmas were generated within the lithosphere. At the eastern end of the Rancheria suite, on the east side of the Tintina Trench, the AOB from Watson Lake have higher Zr contents than Rancheria AOB to the west of the Trench. The high Zr contents of the Watson Lake AOB are similar to those observed in the Hoole Eocene tholeiitic basalts, on the east side of the Tintina Trench, further to the north. The Eocene basalts from the Hoole River region are olivine tholeiites which have experienced closed-system crystal fractionation of olivine at low pressure. The estimated primary magma for these Eocene basalts appears to have been derived by partial melting of an incompatible-element enriched lithospheric mantle source, during which garnet was not a residual phase. The Nb - Zr systematics of the Watson Lake basalts indicate that they may be derived by mixing between melts produced by melting of an amphibole-bearing residue and a lithospheric mantle similar in composition to that of the Hoole basalts. Therefore, these compositional differences in the alkaline basalts across the Tintina Trench appear to reflect the juxtaposition of chemically distinct continental lithospheric mantles, indicating that the Tintina Fault is a steep lithospheric suture.

RESUME

Dans le sud-est du Territoire du Yukon, des basaltes alcalins continentaux d'âge Quaternaire ont érupté de part et d'autre d'une importante suture crustale, la faille Tintina, qui sépare les terranes accrétionnés de la Cordillière canadienne de l'ancien craton de l'Amérique du Nord. Les laves de la région de Rancheria à l'ouest de la faille Tintina sont des basanites (BASAN), des basaltes alcalins à olivine (AOB) et des basaltes normatifs en hypersthène (HYN). Ils montrent des profils de terres rares fractionnés et sont enrichis en terres rares légères et en éléments à charge ionique élevée. Le spectre des compositions des magmas alcalins de la région de Rancheria semble représenter la fusion progressive d'une lherzolite à grenat et amphibole. La présence d'amphibole dans la pétrogénèse des basaltes alcalins de Rancheria nécessite que ces basaltes soient produits dans le manteau lithosphérique. A l'extrémité est de la suite de Rancheria, du coté est de la faille de Tintina, les basaltes alcalins à olivine (AOB) de Watson Lake ont des abondances en Zr plus élevées que celles des AOB de Rancheria à l'ouest de la faille. Ces abondances élevées en Zr sont similaires aux abondances en Zr des basaltes tholéiitiques de Hoole, à l'est de la faille Tintina, plus au nord. Les basaltes d'âge Eocène de la région de la rivière Hoole sont des tholéiites à olivine qui ont expérimenté la cristallization fractionnée de l'olivine en milieu fermé et à basse pression. Le magma primitif calculé de ces tholéiites semble être dérivé de la fusion partielle, sans grenat résiduel, d'une source lithosphérique enrichie en éléments incompatibles. Les variations en Nb et Zr des AOB de Watson Lake indiquent qu'ils peuvent être produits par un mélange de liquides magmatiques provenant de la fusion partielle d'un résidu contenant de l'amphibole et d'un manteau lithosphérique ayant une composition semblable à celui qui a produit les basaltes tholéiitiques de la région de Hoole. Donc, les différences dans la composition des basaltes alcalins d'âge Quaternaire de part et d'autre de la faille Tintina semblent refléter la juxtaposition de manteaux continentaux lithosphériques chimiquement distincts, indiquant, par le fait-même, que la faille Tintina est une suture lithosphérique profonde.

TABLE OF CONTENTS

LIST OF FIGURES

LIST OF TABLES

LIST OF APPENDICES

ACKNOWLEDGEDMENTS

I am grateful to Don Francis for giving me a great opportunity to participate in a great adventure in the Yukon Territory, and for his good advice and constructive reviews of the manuscript. This project is part of a long term study bearing on the nature of the mantle sources in the northern Canadian Cordillera on which Don Francis and John Ludden have already spent many years. Thanks to John Ludden for giving me access to INAA geochemical laboratory at Ecole Polytechique de Montréal, to Jean-Luc Bastien and Brigitte Dionne for assistance in the collection of INAA data, to Glenn Poirier at McGill University for his great technical assistance on the electron microprobe, to Tariq Ahmedali and his technicians who performed the major and trace elements analyses, and to Alexandra Fliszar who has been my field assistant during summer 1991. For support and useful discussions, I would like to thank Anne Charland, Claude Dalpé, and Pierre Hudon. Without them, my stay at McGill would not have been as pleasant.

PREFACE

This thesis is presented in the form of a manuscript entitled "Volcanic evidence for a compositional contrast in the lithospheric upper mantle across the Tintina Trench, southeastern Yukon, Canada." which will be submitted to the journal *Contributions to Mineralogy and Petrology*. An expanded introduction, a general summary, as well as appendices containing a complete geochemical data set are added to the manuscript to complete the thesis. This study will provide constraints on the contribution of the lithospheric upper mantle to the petrogenesis of continental alkaline basalts. In order to do so, petrological and geochemical characteristics of Quaternary alkaline basalts from the Rancheria River region which erupted across a major crustal suture, the Tintina Trench, in the southeastern Yukon Territory, will be described. Eocene tholeiitic basalts from the Hoole River region, which erupted on the east side of the Tintina Trench, are used to constrain the composition of the lithospheric mantle beneath the ancestral North American craton on the east side of the Trench. Seventy-nine samples were used for this study: 9 were collected by Don Francis in the summer of 1990, 63 by Valérie Hasik and Don Francis during the summer field season of 1991, and 7 by Don Francis in the summer of 1993. All the samples were analyzed for major and trace element (Nb, Zr, Y, Sr, Rb, Ba, Ni, V, Cr) chemistry by T. Ahmedali at McGill University by XRF. Twenty-six of those samples have been analyzed by Valérie Hasik for Sc, Hf, Ta, Co, Cs, Th, U, and rare earth elements by INAA at Ecole Polytechnique de Montréal.

GENERAL INTRODUCTION

Much debate surrounds the issue of the relative roles of lithospheric and asthenospheric mantle in the genesis of continental alkaline basalts. In this study, we wanted to constrain the contribution of the lithospheric mantle to the petrogenesis of continental alkaline basalts. In order to do so, a suite of Quaternary continental alkaline basalts was studied which has erupted across a major tectonic suture of the northern Canadian Cordillera, the Tintina Trench. The alkaline volcanics lie at the northern end of the Stikine Volcanic Belt, a series of Tertiary to Recent alkaline volcanic centres, which crosses the Tintina Fault in the southeastern Yukon, near Watson Lake. The Tintina Fault is a right-lateral transcurrent fault stretching more than 1000 km across the Yukon Territory, and extending into British Columbia to join the Rocky Mountain Trench to the south. Dextral displacement of at least 450 km (Roddick 1967), and possibly as much as 750 km (Gabrielse 1985), has occurred along the Tintina Fault during late Cretaceous and early Tertiary time. The Tintina Trench is an elongated topographic depression following the Tintina Fault that formed by younger normal faulting in Pliocene time (Tempelman-Kluit 1980). The Tintina Fault may penetrate the lithosphere, although little is known about its attitude at depth (Clowes 1993 - LITHOPROBE Phase IV Proposal, p. 4-26) and some have proposed it may be listric. If the Tintina Fault does penetrate the subcontinental lithospheric mantle, then it may juxtapose chemically distinct continental lithospheres which may be recorded in the alkaline basaltic lavas which have erupted on both sides of the fault. With this possibility in mind, a series of samples were

collected along the Rancheria River and the Alaska Highway, between the towns of Teslin and Watson Lake. In addition, Eocene tholeiitic basalts were collected in the Hoole River region, further to the north, on the east side of the Tintina Trench, to further constrain the composition of the lithospheric mantle on the east side of the Tintina Fault, beneath the ancestral North American craton.

PREVIOUS WORK

The geochemical variation of mafic alkaline lavas in continental environments has been variously attributed to variable degrees of partial melting of a common mantle source, derivation from different depths, and variable mantle source compositions. The compositional similarity between oceanic and continental alkaline basalts has led some to conclude that asthenospheric mantle is also present beneath some continental areas (Allègre et al. 1981; Fitton and Dunlop 1985; Fitton 1987). Others would derive alkaline magmas by the melting of enriched lithospheric mantle (Bailey 1982, 1987). Geochemical and isotopic studies of mantle xenoliths and continental flood basalts (e.g. Menzies 1983; Hawkesworth et al. 1984) suppport the existence of an enriched lithospheric mantle, but systematic isotopic differences make it difficult to derive the associated alkaline olivine basalts and hypersthene-normative basaltic lavas of alkaline suites from a single enriched mantle source (Miyashiro 1978; Francis and Ludden 1990). The compositional diversity of some continental alkaline magma series has also been modelled in terms of interaction between asthenosphere-derived magmas and the

lithospheric mantle (Chen and Frey 1985; Menzies 1987; Leat et al. 1988). When the effects of crustal contamination can be eliminated, continental intraplate basaltic magmas could represent melts derived from an asthenospheric mantle source mixed with melts generated from enriched lithospheric mantle (Fitton et al. 1988). Such models require very small degrees of partial melting from primitive asthenospheric mantle to obtain trace element enriched magmas with isotopically depleted signatures. Francis and Ludden (1990) have proposed a model in which the nephelinite, basanite, alkaline olivine basalts, and hypersthene-normative basalts at Fort Selkirk, in the Yukon, are derived by the melting of a single heterogeneous lithospheric mantle source consisting of lherzolite cut by amphibole - garnet - clinopyroxene veins. In this model, the composition of the HYN magma end member is buffered by the lherzolite lithosphere while the nephelinite magma end member represents a partial melt of the amphibole-rich veins, which were ultimately derived from the asthenosphere. However, more recently, Francis and Ludden (1994) have observed that trace element systematics at a number of alkaline volcanic centres in the Canadian Cordillera indicate that their compositional spectra could be explained simply in terms of the progressive melting of a homogeneous amphibole lherzolite source. The composition of the subcontinental lithospheric mantle is, however, poorly constrained at present, and likely manifests significant variations on a regional scale.

GEOLOGICAL SETTING

Mid-Tertiary to Quaternary basalts are found at two localities along the Tintina

Trench in the southeastern Yukon Territory. Quaternary alkaline volcanism has occurred along the Yukon - British Columbia border in the Rancheria region, and Eocene tholeiitic volcanism has occurred in the Hoole River region, 250 km to the north. The Rancheria alkaline basalts lie at the northern end of the Stikine Volcanic Belt, a series of Tertiary to Recent alkaline volcanic centres stretching NNE from Mount Edziza in northern British Columbia. In the Rancheria region, along the Alaska Highway, Lord (1944) mapped basalt flows along the valley bottoms and concluded that they ranged in age from the late Tertiary to the Pleistocene. The first detailed geological mappping of the Rancheria region was undertaken by Gabrielse (1966), who mapped flat-lying vesicular olivine basalts along the Little Rancheria River, the Big Creek, the Robert Campbell Highway, the Liard River, and in the vicinity of Watson Lake. Subsequent mapping along the Rancheria River done by Lowey and Lowey (1986) documented Quaternary olivine-phyric basalts as subaerial flows with vesicular ropy flow tops and columnar jointed interiors. While doing the reconnaissance mapping of surficial deposits of the Rancheria region, Klassen (1987) mapped the olivine basalts exposed along the banks of the Rancheria River, the lower part of the Liard River, and in the vicinity of Watson Lake, and he obtained K-Ar dates of 0.765 Ma to 0.232 Ma for the Rancheria basalts.

Basaltic volcanism in the Hoole River region was first reported by Dawson in 1888. He noted discontinuous exposures of dark brown basalt from the mouth of the Hoole River to the Hoole Canyon. Later reconnaissance geologic mapping of the Hoole River region by Wheeler et al. (1960) and Tempelman-Kluit (1972, 1977) documented the

distribution of Tertiary mafic volcanic rocks in the Hoole River region. More recently, Duke and Godwin (1986) undertook a study of the geology and alteration of the Grew Creek gold-silver deposit and obtained an Eocene age (K-Ar) for the basaltic rocks. Jackson et al. (1986) have described and dated Paleocene to Eocene basalt and rhyolite occurrences in the Tintina Trench along the Hoole and Pelly Rivers, and at Starr Creek and Weasel Lake. Based on chemical analyses, they concluded that these volcanic rocks formed a bimodal suite composed of calc-alkaline to transitional tholeiitic basalts and high potassic subaluminous rhyolites, associated with transcurrent slip along the Tintina Fault. Similar conclusions on the nature and tectonic setting of the Eocene basalts in the Grew Creek, Glenlyon, and Ketza River areas, within the Tintina Trench, were reached by Pride (1988). Finally, Christie et al. (1992) have obtained chemical analyses of Eocene basalts associated with the Grew Creek deposit.

THESIS OUTLINE

This thesis reports the results of a study of the geochemistry of a suite of Quaternary continental alkaline basalts across the Tintina Trench, a major tectonic feature of the northern Canadian Cordillera, in the form of a manuscript for publication in **Contributions to Mineralogy and Petrology**. Its major contribution is the identification of a compositional change in the lithospheric component in these lavas across the Tintina Trench. The results of this work not only provide constraints on the relative roles of asthenospheric versus lithospheric mantle sources in the genesis of continental alkaline

basalts, but this work also suggests that the chemistry of the numerous recent alkaline volcanic centres provides a powerful tool with which we can characterize the mantle rocks of the disparate tectonic terranes of the northern Canadian Cordillera.

Volcanic evidence for a compositional contrast in the lithospheric upper mantle across the Tintina Trench, southeastern Yukon, Canada

Valérie Hasik[1], Don Francis[1] and John Ludden[2]

(1) Department of Earth and Planetary Sciences, McGill University, 3450 University Street, Montréal, Québec, Canada H3A 2A7

(2) Département de Géologie, Université de Montréal, CP 6128 A, Montréal, Québec, Canada H3C 3J7

For Submission in

Contributions to Mineralogy and Petrology

June 1994

ABSTRACT

The Quaternary lavas of the Rancheria region, in the southeastern Yukon, constitute the northern end of the Stikine Volcanic Belt, a series of Tertiary to Recent alkaline volcanic centers stretching NNE from Mount Edziza in northern British Columbia. The Rancheria alkaline basalts have erupted across a major crustal feature, the Tintina Trench, which may separate the accreted terranes of the Canadian Cordillera on the southwest from the ancestral North American craton on the northeast. The Tintina Trench constitutes an important crustal suture which is colinear with the Rocky Mountain Trench to the south and may juxtapose distinct continental lithospheres. The study of the petrogenesis of Quaternary continental alkaline basalts on either side of the Tintina Trench enable us to recognize the changes in the composition of the lithospheric component across the Tintina Trench.

Three magma types are recognized in the Rancheria region, on the west side of the Tintina Trench: (1) basanites (BASAN) with normative nepheline between 5 and 15 wt%; (2) alkaline olivine basalts (AOB) with normative nepheline ranging from 0 to 5 wt%; (3) hypersthene-normative basalts (HYN) with 0 to 13 wt% normative hypersthene. They all display fractionated rare earth element (REE) profiles and are enriched in light rare earth elements (LREE) and high field strength elements (HFSE). The systematics of the large ion lithophile elements (LILE) of the Rancheria BASAN magmas require the presence of amphibole as a residual mantle phase in their source. The involvement of amphibole in the petrogenesis of the Rancheria alkaline magmas indicates that these magmas were generated within the lithosphere, where amphibole is a stable phase, and their fractionated heavy rare earth element (HREE) profiles suggest that they were produced in the garnet stability field.

To the north of the Rancheria region, in the vicinity of the Hoole River, Eocene tholeiitic basalts are used to constrain the composition of the subcontinental lithospheric mantle on the east side of the Tintina Trench. They have fractionated LREE, but flat HREE profiles, and relative depletions in Nb, Ta, and Sr. The major and trace elements of the Hoole tholeiitic basalts indicate that they are continental tholeiites which have experienced closed-system crystal fractionation of olivine at low pressure. The estimated primary magma for these Eocene tholeiitic basalts could have been derived by partial melting of an incompatible-element enriched lithospheric mantle source, during which garnet was not a residual phase.

At the eastern end of the Rancheria region, on the east side of the Tintina Trench, the AOB from Watson Lake have distinctive Nb/Zr ratios reflecting higher Zr contents than those of the Rancheria AOB to the west of the Tintina Trench. The high Zr contents of the Watson Lake AOB lavas are similar to those observed in the Eocene tholeiitic basalts on the northeast side of the Tintina Trench. The Nb - Zr systematics of the Watson Lake basalts indicate that they may be derived by mixing between melts produced by melting of an amphibole-dominated residue and a lithospheric mantle similar in composition to that which generated the Eocene tholeiitic basalts which erupted on the eastern side of the Tintina Trench. The compositional differences in the alkaline basalts across the Tintina Trench appears to reflect the contribution of chemically distinct continental lithospheric mantles, indicating that the Tintina Fault is a steep lithospheric-scale suture.

INTRODUCTION

The compositional variation within alkaline magma series has been attributed to variable degrees of partial melting of a common mantle source, derivation from different depths, or variable mantle source compositions. The fact that continental alkaline basalts commonly exhibit close geochemical and isotopic resemblance to oceanic alkaline basalts has been taken as evidence that the mantle source of all alkaline magmas lies in the asthenosphere, and that suboceanic asthenospheric mantle is present beneath some continental areas (Allègre et al. 1981; Fitton and Dunlop 1985; Fitton 1987). Others would derive alkaline magmas by melting of an enriched lithosphere (e.g. Bailey 1987). Trace element and isotopic differences, however, make it unlikely that commonly associated basanites, alkali olivine basalts, and hypersthene-normative basalts can be derived from a single mantle source (Miyashiro 1978; Francis and Ludden 1990), and interaction between asthenosphere-derived magmas and the lithospheric mantle has been proposed as a mechanism for generating the chemical diversity of some continental alkaline magma suites (e.g. Leat et al. 1988; Francis and Ludden 1990). The composition of the lithospheric mantle is, however, poorly constrained, especially in continental settings, and the role of this component in the genesis of continental alkaline basalts is presently unresolved.

In the southeastern Yukon, Quaternary continental alkaline basalts have erupted across a major crustal feature, the Tintina Trench, which separates the accreted terranes

of the Canadian Cordillera from the ancestral North America craton. The Tintina Trench constitutes an important crustal suture which is colinear with the Rocky Mountain Trench to the south and may juxtapose distinct continental lithospheres. A recent alkaline volcanic suite in SE Yukon which crosses the Tintina Trench thus presents a remarkable opportunity to identify and constrain the contribution of continental lithospheric mantle to the petrogenesis of alkaline basalts.

In this paper, we show that the Quaternary alkaline basalts on the east side of the Tintina Trench, the Watson Lake alkaline basalts, differ from contemporaneous alkaline basalts from the west side of the Trench in both Nb - Zr systematics and petrographic features, and necessitate the involvement of a distinct high-Zr component similar to that observed in earlier Eocene tholeiitic lavas on the eastern side of the fault. We propose that the compositional differences in the alkaline basalts across the Tintina Trench reflect the contribution of distinct continental lithospheric mantles.

GEOLOGICAL SETTING

Mid-Tertiary to Quaternary basaltic volcanism has occurred at two localities along the Tintina Trench in the southeastern Yukon Territory. Quaternary alkaline volcanism has occurred along the Yukon - British Columbia border in the Rancheria region (Gabrielse 1966; Lowey and Lowey 1986; Klassen 1987), and Eocene tholeiitic volcanism

has occurred in the Hoole River region, 250 km to the north (Tempelman-Kluit 1972, 1977; Jackson et al. 1986; Pride 1988). The Rancheria alkaline basalts constitute the northern end of the Stikine Volcanic Belt, a series of Tertiary to Recent alkaline volcanic centres stretching NNE from Mount Edziza in northern British Columbia. Basaltic volcanism in the Hoole River region was first reported by Dawson in 1888 and later mapped by Wheeler et al. (1960), and Tempelman-Kluit (1972, 1977). More recently, Jackson et al. (1986), Pride (1988), and Christie et al. (1992) have described Paleocene to Eocene basaltic and rhyolitic occurrences along the Tintina Trench in the Glenlyon, Grew Creek, and Ketza areas, along the Hoole and Pelly Rivers, and at Starr Creek and Weasel Lake. Based on whole rock K-Ar ages and chemical analyses, Jackson et al. (1986) suggested that these volcanic rocks formed a bimodal suite composed of calc-alkaline to transitional tholeiitic basalts and high potassic subaluminous rhyolites which are associated with transcurrent slip along the Tintina Fault.

The Tintina Fault is a right-lateral transcurrent fault stretching more than 1000 km across the Yukon Territory, and extending into British Columbia to join the Rocky Mountain Trench to the south. Dextral displacement of at least 450 km (Roddick 1967), and possibly as much as 750 km (Gabrielse 1985), has occurred along the Tintina Fault during late Cretaceous and early Tertiary time. In the Yukon Territory, the Tintina suture may separate rocks of the ancestral North American craton on the north-east from an assemblage of pericratonic accreted terranes and the ancestral North American basement on the south-west (Fig. 1). The linear extent of the Tintina Fault has lead some to

Figure 1: Location map of the southeastern Yukon showing the Quaternary volcanic suite in the Rancheria River region along the Yukon - British Columbia border, and the Eocene volcanic suite in the Hoole River region 250 km to the north. SM - Slide Mountain terrane, KO - Kootenay pericratonic terrane, DO - Dorsey terrane. Modified from Erdmer (1987) and Wheeler et al. (1991).

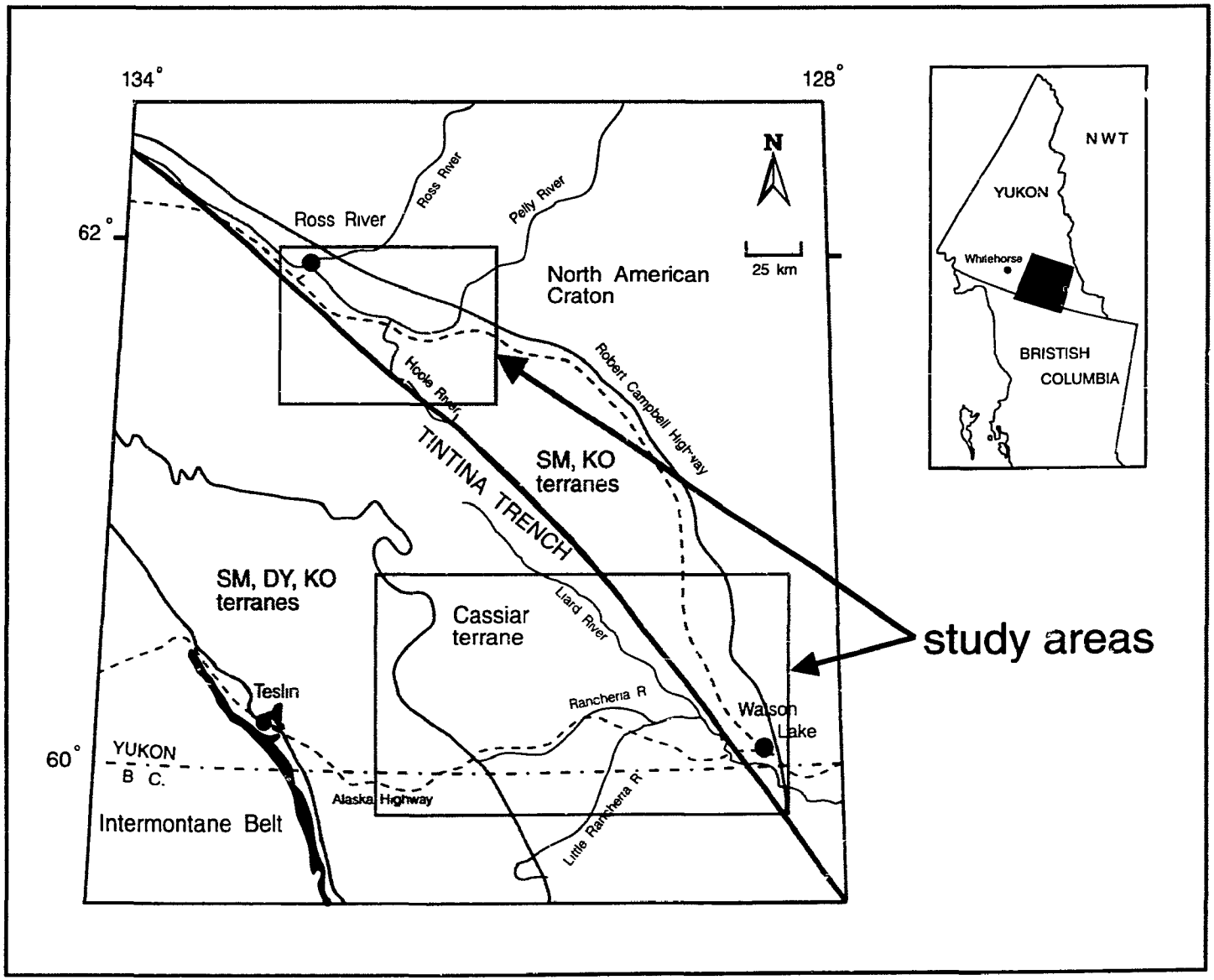
134°
128°
62°
60°
Ross River
Ross River
Pelly River
N
25 km
North American Craton
Hoole River
Robert Campbell Highway
TINTINA TRENCH
SM, KO terranes
SM, DY, KO terranes
Cassiar terrane
Liard River
Rancheria R
Watson Lake
Teslin
YUKON
B C.
Alaska Highway
Intermontane Belt
Little Rancheria R
study areas
NWT
YUKON
Whitehorse
BRISTISH COLUMBIA

consider it as a fundamental crustal fault which may penetrate the lithosphere, although little is known about its attitude at depth (Clowes 1993 - LITHOPROBE Phase IV Proposal, p. 4-26) and some have proposed it may be listric. The Tintina Trench is an elongated topographic depression following the Tintina Fault that formed by younger normal faulting in Pliocene time (Tempelman-Kluit 1980).

Erosional remnants of Quaternary alkaline basalts occur for 150 km along an east-west trend following the Rancheria River and the Alaska Highway between the towns of Teslin and Watson Lake. The Quaternary lavas of the Rancheria region unconformably overlie Upper Proterozoic to Upper Triassic sediments of the Cassiar Terrane, Mesozoic to Cenozoic granodioritic plutons, Carboniferous chert and clastics of the Dorsey terrane, Devonian to Late Triassic oceanic volcanics and sediments of the Slide Mountain terrane, and Proterozoic to Triassic metamorphic rocks of the Kootenay pericratonic terrane (Wheeler et al. 1991). The lavas are in turn partially covered by the Quaternary deposits of the Liard Plain (Figs. 1 and 2). The great majority of the basaltic occurrences lie on the western side of the Tintina Fault, but a number of occurrences, near the town of Watson Lake, lie on the eastern side of the fault. K-Ar dates of 0.765 Ma and 0.232 Ma have been obtained respectively for a basalt erupted near the town of Watson Lake and for a basalt 40 km to the west of the trench near the junction of the Little Rancheria River and the Alaska Highway (Klassen 1987). The volcanism on the west and east sides of the Tintina Trench in the Rancheria and Watson Lake regions is characterized by the effusive eruption of flat-lying valley-filling flows that range in thickness from 1 to 16

Figure 2: Simplified geological map of the Rancheria region modified from Gabrielse et al. (1977) and Souther et al. (1974) showing the outcrops of basalt and the sampled sites. The site 'A' refers samples located outside the Cassiar terrane.

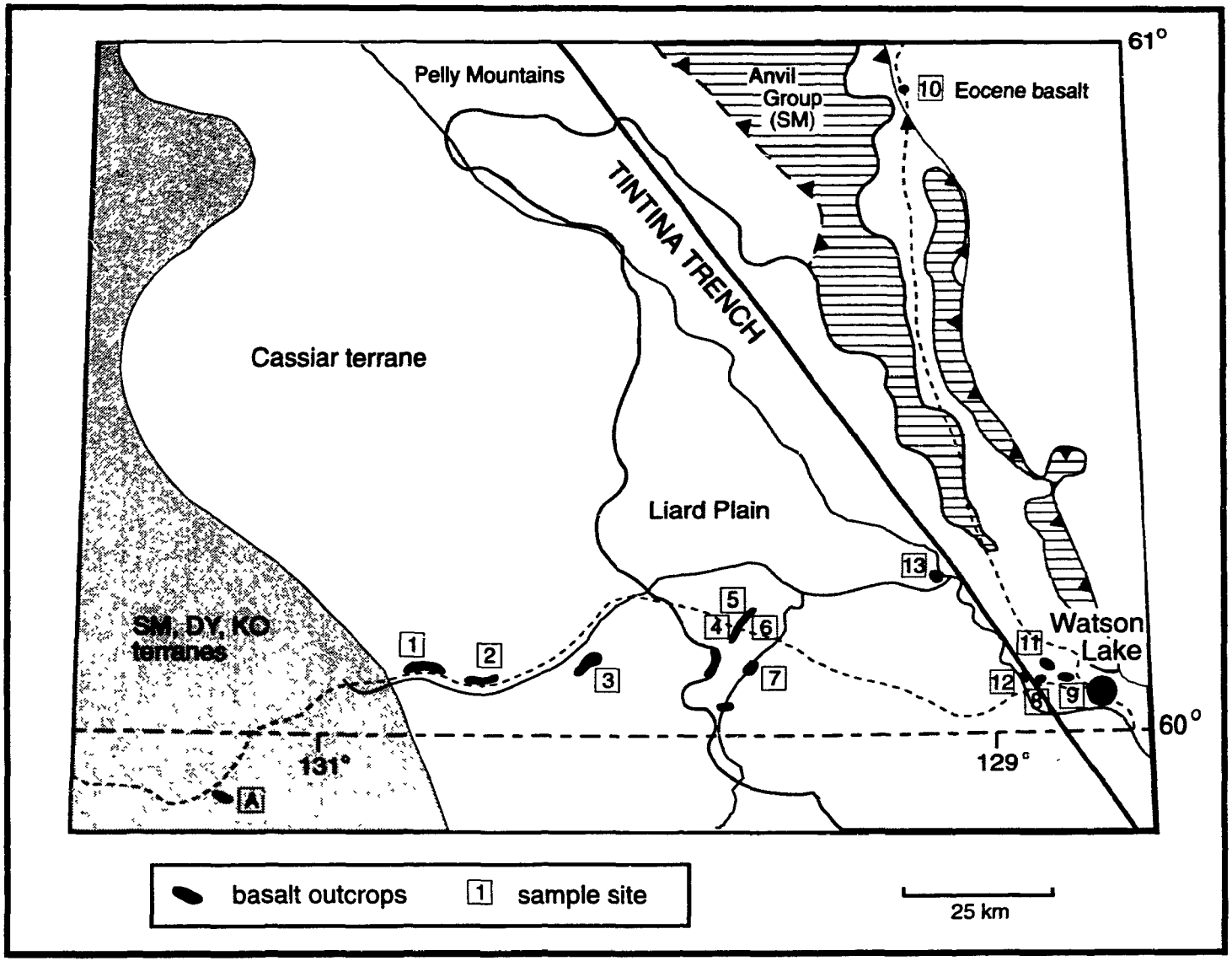
61°
Pelly Mountains
Anvil
Group
(SM)
10 Eocene basalt
TINTINA TRENCH
Cassiar terrane
Liard Plain
13
5
4
6
1
2
3
7
SM, DY, KO
terranes
11
Watson
Lake
12
8
9
60°
131°
129°
A
basalt outcrops
1 sample site
25 km

meters, with strongly vesicular, ropy flow tops and massive columnar jointed interiors.

Eocene tholeiitic basalts have erupted in the Hoole River region along the east side of the Tintina Trench. These basalts unconformably overlie Devonian to Late Triassic volcanics and sediments of the Slide Mountain terrane, Late Proterozoic to possibly early Mesozoic cataclastic sedimentary, volcanic and intrusive rocks of the Kootenay terrrane, and Paleozoic rocks of the ancestral North American craton (Wheeler et al. 1991). The basalts are in turn covered by thick deposits of alluvium and glacial drift. The lavas are exposed over a 50 km^2 area east-southeast of the town of Ross River in a topographic depression which is bordered by the Pelly Mountains to the south-west. They occur along the banks of the Pelly and Hoole Rivers, north of Starr Lake, and at the northern end of Weasel Lake (Fig. 3). An isolated occurrence of columnar jointed basalt is also found on the eastern side of the Tintina Trench, 100 km north of Watson Lake (Fig. 6, site 10). Jackson et al. (1986) analyzed basalts in the Weasel Lake area as well as along Hoole River and Starr Creek and provided new whole rock K-Ar dates (46.4 ± 2.3 Ma to 55.4 ± 2.3 Ma), establishing an Eocene age for these basalts, which were formerly thought to be late Tertiary to Quaternary in age (Tempelman-Kluit 1977). Along Hoole and Pelly Rivers, the Eocene basaltic magmas have erupted to produce valley-filling lava flows and breccias. The flows range between 3 and 8 meters in thickness and have smooth, vesicular flow tops which are characteristically oxidized red (Fig. 4). The breccia found along the Hoole River is composed of massive to vesicular bombs with glassy rims (Fig. 5) suggesting rapid quenching by contact with ice or water, in a brownish clastic matrix

Figure 3: Simplified geological map of the Hoole region modified from Gabrielse et al. (1977) showing the location of sampled sites.

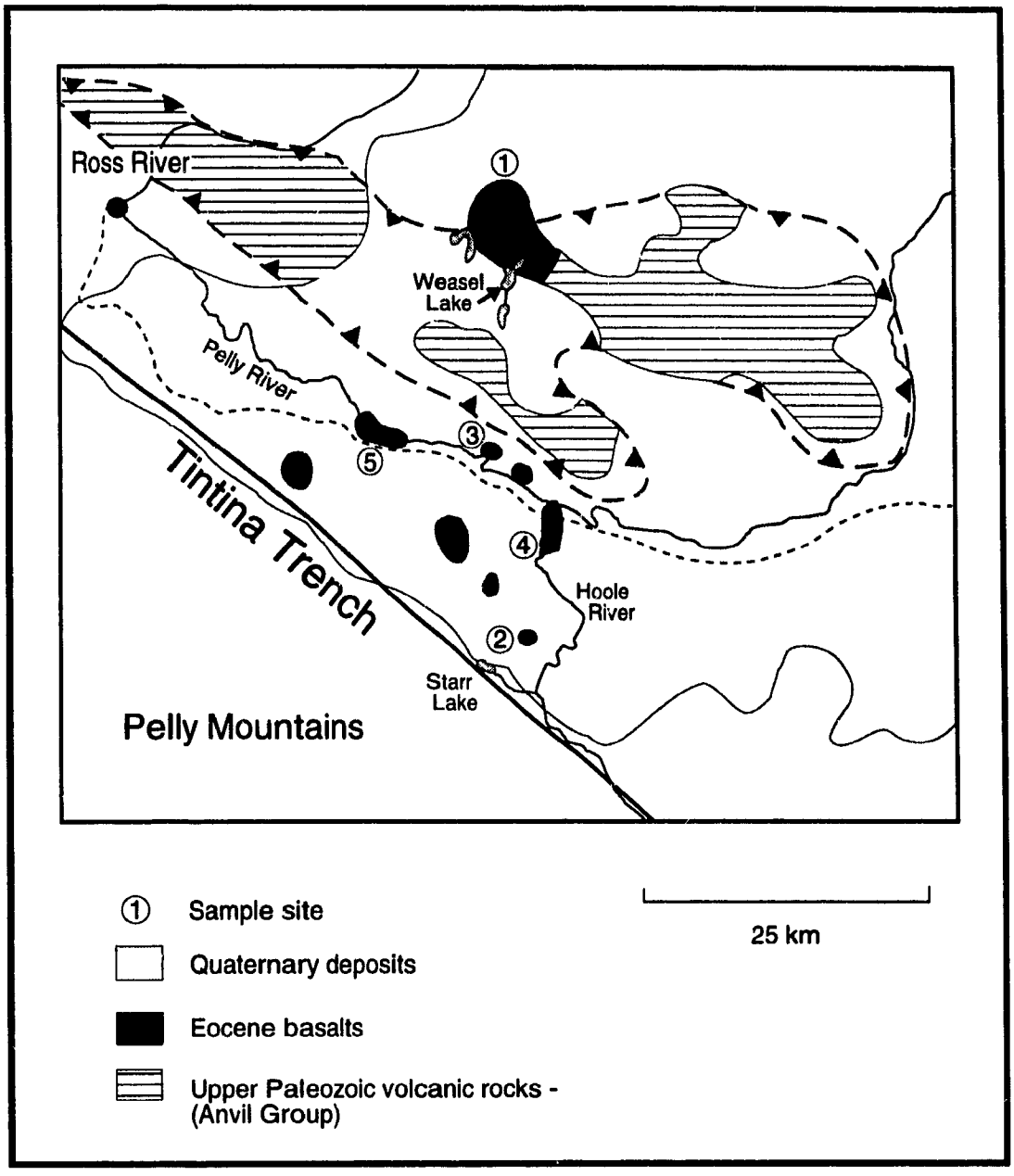
Ross River
Weasel Lake
Pelly River
Tintina Trench
Hoole River
Starr Lake
Pelly Mountains
① Sample site
Quaternary deposits
Eocene basalts
Upper Paleozoic volcanic rocks - (Anvil Group)
25 km

Figure 4: Valley-filling flows with oxidized tops along the Hoole River.

Figure 5: Massive to vesicular dark grey basaltic bomb with glassy rims from the breccia found along the Hoole River.

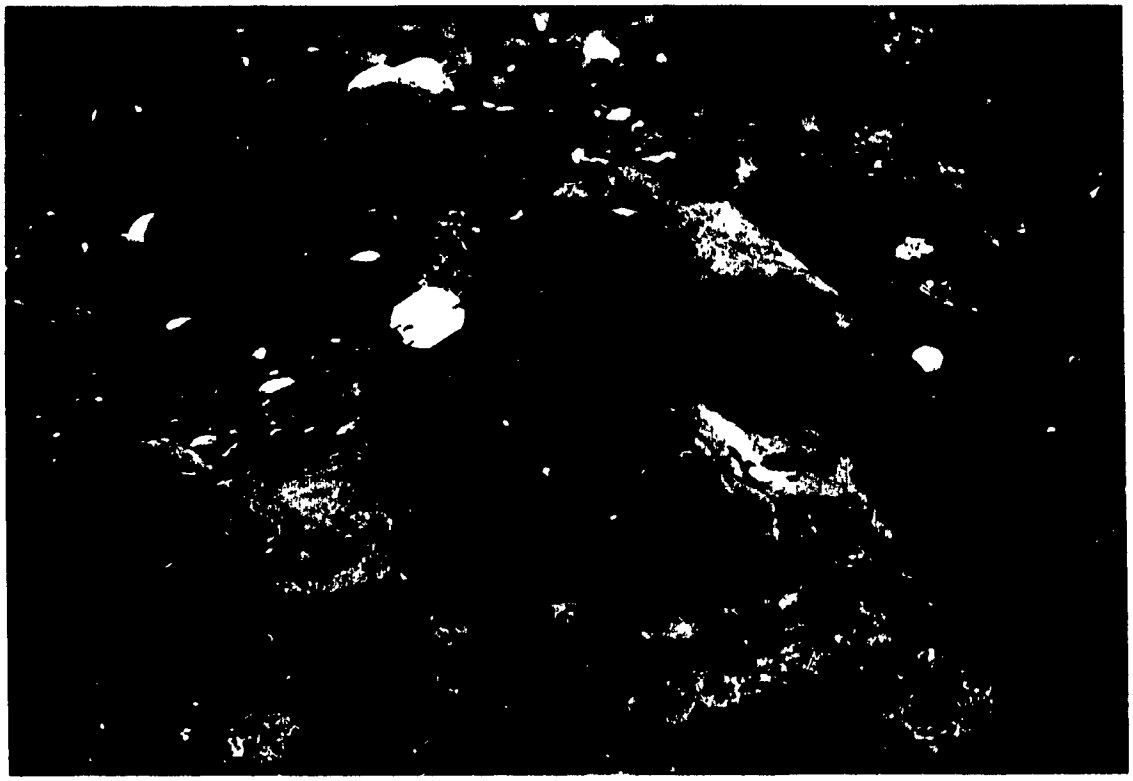

Figure 6: Weasel Lake basaltic occurrence, looking south-west. The Pelly Mountains are seen in the background. They are located on the southwestern side of the Tintina Trench.

Figure 7: Columnar joints of Weasel Lake, north-east side of the occurrence.

comprised of small, subrounded, glass fragments as well as sand-, block-, and pebble-size fragments of quartz, granite, and basalt. On the south bank of the Pelly River, the breccia consists of scattered 10-40 cm basaltic bombs in a purplish grey pebble-size matrix. Most of these bombs are massive, although some appear to have glassy selvages. The thickest occurrences of basalt in the Hoole region are located north of Weasel Lake and north-east of Starr Lake. The Weasel Lake occurrence consists of a 75 meter section of basalt which exhibits remarkably continuous columnar joints (Figs. 6 and 7). This basaltic occurrence has been interpreted as a volcanic neck by Jackson et al. (1986), however, the chemical variation across the section indicates that it is comprised of two thick (30 to 45 meters) lava flows (will be further discussed).

BASALTS OF THE RANCHERIA REGION

Petrography

The most silica-poor (44-46 wt% SiO_2) Rancheria lavas are basanites (BASAN) with normative nepheline contents between 5 and 15 wt%. These lavas are medium to dark grey in colour and range in MgO content from 8 to 11 wt%. They are characterized by abundant euhedral to skeletal olivine phenocrysts (5 to 12 vol%), with cores reaching Fo_{83}, set in a groundmass of plagioclase laths (An_{69} to An_{53}), granular clinopyroxene (En_{42-43}, Fs_{11-14}, Wo_{45-46}), olivine, and small equant crystals of oxides. More silica-rich alkaline olivine basalts (AOB) (45-48 wt% SiO_2) and hypersthene-normative transitional basalts (HYN) (47-50 wt% SiO_2) are also abundant in the Rancheria region with normative

nepheline between 0 and 5 wt% and 0 and 13 wt% normative hypersthene respectively. The AOB and HYN basalts are lighter grey in colour than the basanites. The Mg contents of the AOB range between 10-12 wt% MgO, and between 8-12 wt% MgO in the HYN lavas, although one AOB sample appears to have accumulated olivine and reaches 16 wt% MgO. The AOB and HYN basalts are also olivine-phyric (5 to 15 vol%) (Fo_{83} cores), but the abundance and size of zoned plagioclase laths (AOB: An_{63-65} and HYN: An_{48-65}) increases systematically in the groundmass from the AOB to the HYN basalts. Clinopyroxene (AOB: En_{40-46}, Fs_{11-17}, Wo_{43-44} and HYN: En_{41-47}, Fs_{15-21}, Wo_{38-41}) occurs as zoned granular to prismatic crystals in the groundmass, crystallizing after plagioclase.

The lava samples from the east side of the Tintina Fault, near the town of Watson Lake, are alkaline olivine basalts (AOB) with 48 wt% SiO_2. Their MgO contents range between 8 and 9 wt%, slightly lower than the MgO contents of the Rancheria AOB lavas on the west side of the fault. However, the Watson Lake AOB have clinopyroxene (En_{40-44}, Fs_{13-17}, Wo_{42-43}) phenocrysts (15 to 20 vol%), which have crystallized before plagioclase (An_{60}), and phenocrysts of olivine (5 to 7 vol%) with core compositions of Fo_{75} to Fo_{80}.

Geochemistry

The alkaline character of the Rancheria basalts is evident in a total alkalies (Na + K) versus silica cation plot (Fig. 8a), in which the lava compositions fall on the silica-undersaturated side of the plagioclase compositional line. Other alkaline basalts of the Yukon and northern British Columbia, such as those from Fort Selkirk (Francis and

Table 1. Selected analyses of basalts from the Rancheria region

Sample:	RA-3	RA-14	RA-11	RA-17	RA-16	RA-19	RA-20	RA-21	RA-22
Rock:	*BASAN*	*BASAN*	*AOB*	*AOB*	*HYN*	*HYN*	*AOB*	*AOB*	*AOB*
Site:	1	3	2	6	5	7	8(WT)	9(WT)	9(WT)
Wt% Ne:	15.72	5.20	2.98	0.17	0.00	0.00	2.17	3.36	1.70
Major Elements in wt%									
SiO2	44.01	46.30	46.40	48.28	47.47	48.69	48.01	47.94	47.79
TiO2	2.49	2.08	2.02	1.92	1.74	1.68	2.15	2.15	2.12
Al2O3	13.84	13.35	13.21	13.72	12.57	13.85	13.59	13.88	13.77
Fe2O3	14.01	13.35	13.42	13.46	12.87	13.58	14.38	14.19	14.51
MgO	8.29	10.82	10.96	9.58	12.42	10.11	9.08	8.29	8.89
MnO	0.20	0.18	0.18	0.17	0.18	0.16	0.16	0.16	0.16
CaO	11.05	9.53	9.39	9.40	8.61	8.69	8.05	8.07	7.98
Na2O	4.07	3.12	2.86	3.07	2.75	3.00	3.62	3.82	3.51
K2O	1.67	1.27	1.19	0.92	0.87	0.85	1.26	1.39	1.31
P2O5	0.76	0.44	0.43	0.35	0.30	0.25	0.50	0.53	0.52
LOI	0.01	0.01	0.01	0.01	0.01	0.01	0.01	0.01	0.01
Total	100.39	100.44	100.07	100.88	100.79	100.87	100.81	100.43	100.57
Trace Elements in ppm									
Rb	31	27	25	17	17	19	25	26	24
Sr	902	589	576	459	405	395	604	639	633
Ba	565	445	367	402	301	252	216	325	328
Sc	22.1	23.7	23.2	-	22.0	-	16.7	16.7	-
V	246	249	230	203	185	203	209	186	189
Cr	211	356	396	354	397	354	280	256	278
Ni	117	237	258	220	322	194	245	215	226
Y	25	21	21	20	19	18	18	19	19
Zr	213	144	139	130	111	106	185	200	194
Nb	60	35	34	27	23	17	31	34	33
Hf	5.1	3.7	3.8	-	3.0	-	4.7	5.3	-
Ta	3.2	2.1	1.8	-	1.1	-	1.8	2.0	-
Cs	0.6	0.0	0.0	-	0.5	-	0.4	0.0	-
Co	51	59	58	-	64	-	62	58	-
Th	5.4	3.7	3.5	-	2.8	-	2.9	3.7	-
U	1.8	0.7	1.2	-	0.2	-	1.2	1.6	-
Rare Earth Elements in ppm									
La	46.3	27.3	25.1	-	20.0	-	26.1	29.0	-
Ce	88.0	54.1	47.9	-	39.3	-	53.6	57.5	-
Nd	41.1	28.0	24.6	-	19.9	-	24.9	25.7	-
Sm	8.60	6.40	5.93	-	4.79	-	6.46	7.25	-
Eu	2.75	1.98	1.92	-	1.62	-	2.11	2.30	-
Tb	0.85	0.72	0.66	-	0.65	-	0.79	0.64	-
Yb	1.93	1.70	1.61	-	1.73	-	1.42	1.44	-
Lu	0.21	0.19	0.29	-	0.25	-	0.12	0.20	-

Major elements and V, Cr, Ni, Ba were analyzed by X-ray fluorescence at McGill University with a Philips PW 1400 using fused discs and a x-coefficient technique Analytical precisions for the major elements are Si 0 05, Ti 0 003, Al 0 03, Mg 80 058, Fe 0 01, Mn 0 001, Ca 0 01, Na 0 06, K 0 001, P 0.004 (in wt%) Rb, Sr, Zr, Nb, and Y were analyzed by XRF at McGill University on pressed-powder pellets using a Rh-Kb Compton scatter matrix correction The precision for these elements is estimated to be 5% Other trace elements and REE were analyzed by INAA at the Université de Montréal using a SLOWPOKE II reactor and two Ge detectors The analytical precisions for La, Sm, Eu, Yb, Sc, and Co are estimated to be <5%, while those for Ce, Nd, Tb, Lu, and Ta are estimated to be between 5 and 10% The site number refers to the position of the samples in Fig 2 WT refers to samples from Watson Lake Total Fe is calculated as Fe_2O_3

Ludden 1990) and Alligator Lake (Eiché et al. 1987; Francis 1987), define a similar compositional spectrum (Fig. 8b), ranging from transitional hypersthene-normative basalt lying near the plagioclase line to alkali olivine basalt, basanite and nephelinite which lies to the silica-poor side of the olivine - Na-clinopyroxene join. The Rancheria BASAN lavas fall between the olivine-albite and olivine - Na-clinopyroxene joins, whereas AOB lavas lie between the olivine-albite join and the plagioclase line. The AOB samples on the east side of the Tintina Trench near Watson Lake are distinct in having higher total alkalies than the other Rancheria AOB lavas at similar MgO contents. There is a slight increase in Fe content with decreasing Mg content, with the Watson Lake AOB lavas on the east side of the Tintina Trench exhibiting slightly higher Fe contents (Fig. 9). The most primitive lavas have compositions which would equilibrate with olivine of composition of only Fo_{86}, assuming an olivine-liquid K_D of 0.30 (Roeder and Emslie 1970) and an Fe^{3+}/Fe_{total} ratio of 0.15. The Al, Ca, Ti, and P contents of the Rancheria lavas generally increase with decreasing Mg (Fig. 10). However, the rates of increase in Ca, Ti, and P decrease with increasing Si-activity of the lavas. The Watson Lake AOB have distinctly lower Ca and Sc (Table 1) contents than the AOB lavas to the west of the Tintina Trench.

The Rancheria basalts display fractionated rare earth element (REE) profiles and are enriched in light rare-earth elements (LREE) and high field strength (HFS) elements, such as Zr, Hf, Nb and Ta, in a chondrite-normalized spider diagram (Fig. 12a), but are increasingly depleted in large ion lithophile (LIL) elements, K, Rb, and Ba. The BASAN

Figure 8: **(a)** Alkalies versus silica plot in cation units of Rancheria and Hoole basalts. In the Rancheria suite, basanites are represented by squares, alkaline olivine basalts by crosses, hypersthene-normative basalts by diamonds, and alkaline olivine basalts from Watson Lake by grey asterisks. The tholeiites from the Hoole region are represented by black triangles. **(b)** Alkalies versus silica plot in cation units of alkaline lavas from the Fort Selkirk complex (Francis and Ludden 1990) and the Alligator Lake complex (Eiché et al. 1987). Symbols as in (a), with the addition of nephelinites which are represented by circles.

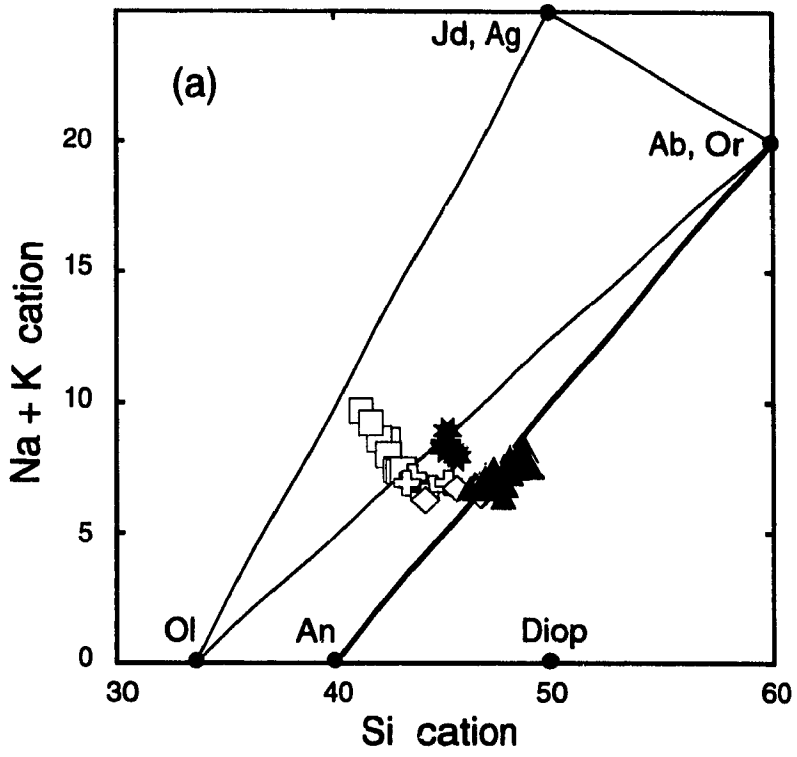
(a)
Jd, Ag
Ab, Or
Ol
An
Diop
Na + K cation
Si cation
0
5
10
15
20
30
40
50
60

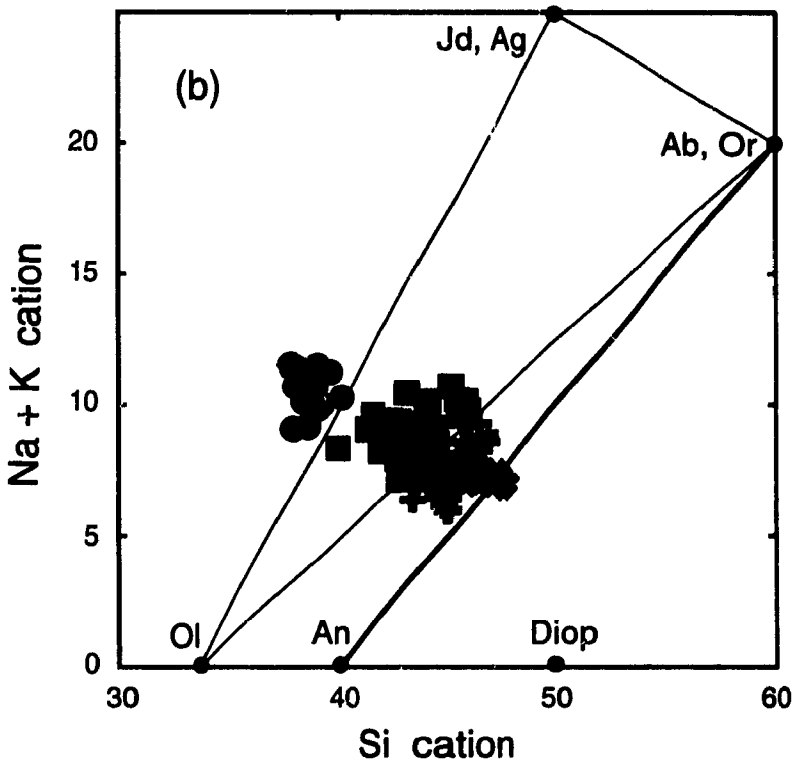
(b)
Jd, Ag
Ab, Or
Ol
An
Diop
Na + K cation
Si cation
0
5
10
15
20
30
40
50
60

Figure 9: Mg versus Fe in cation units for the Rancheria and Hoole basalts. Symbols as in Figure 8 (a). Lines radiating from the origin represent the locii of liquids which would coexist with the indicated olivine compositions, assuming that Fe^{3+} is 15% of Fe_{total} and an Fe/Mg distribution coefficient of 0.3 (Roeder and Emslie 1970).

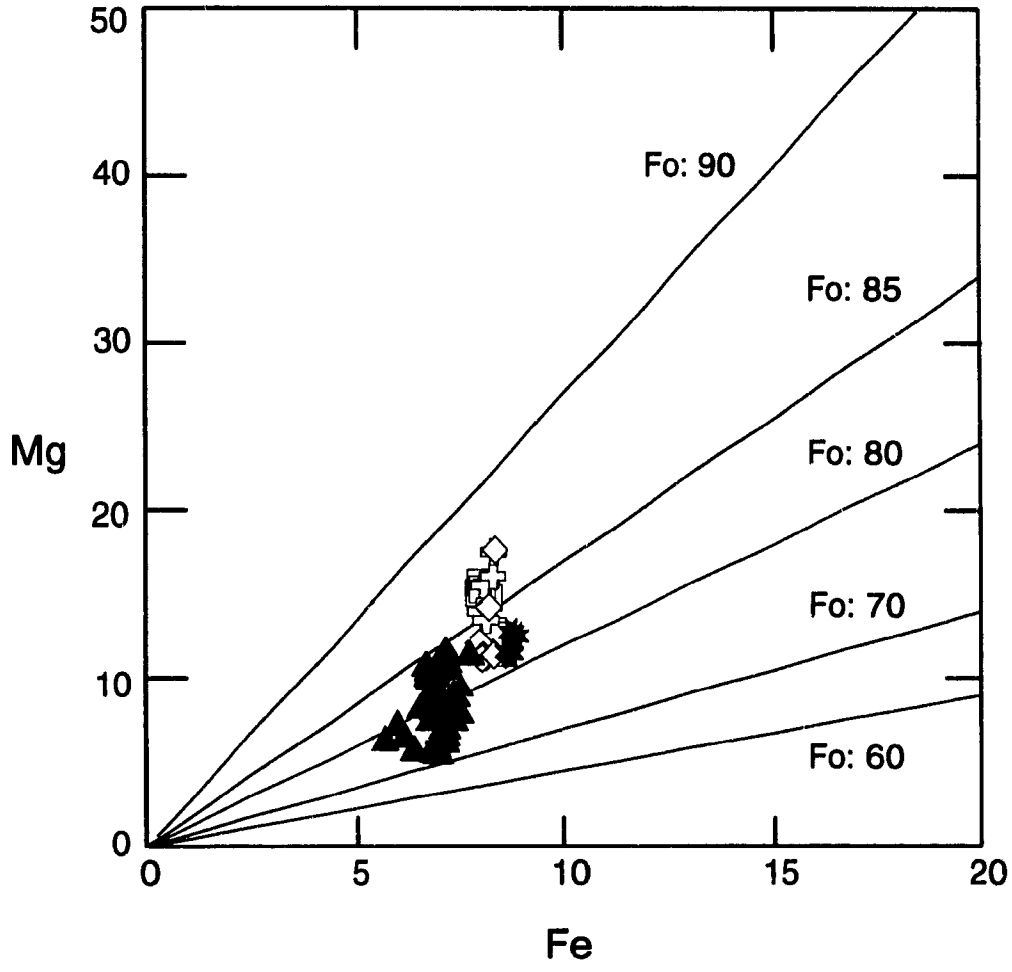
50
40
30
20
10
0
Mg
0
5
10
15
20
Fe
Fo: 90
Fo: 85
Fo: 80
Fo: 70
Fo: 60

Figure 10: Major element variation diagrams in cation units: **(a)** Al vs Mg, **(b)** Ca vs Mg, **(c)** P vs Mg, and **(d)** Ti vs Mg for the Hoole basalts. The lavas and bombs from the Hoole and Pelly Rivers are represented as grey diamond and coarsed grained basalts from the Weasel Lake and Starr Lake, as black triangles. **(e)** Ca vs Mg, **(f)** Al vs Mg, **(g)** P vs Mg, and **(h)** Ti vs Mg for the Rancheria basalts. In the Rancheria suite, basanites are represented by squares, alkaline olivine basalts by crosses, hypersthene-normative basalts by diamonds, and alkaline olivine basalts from Watson Lake by grey asterisks.

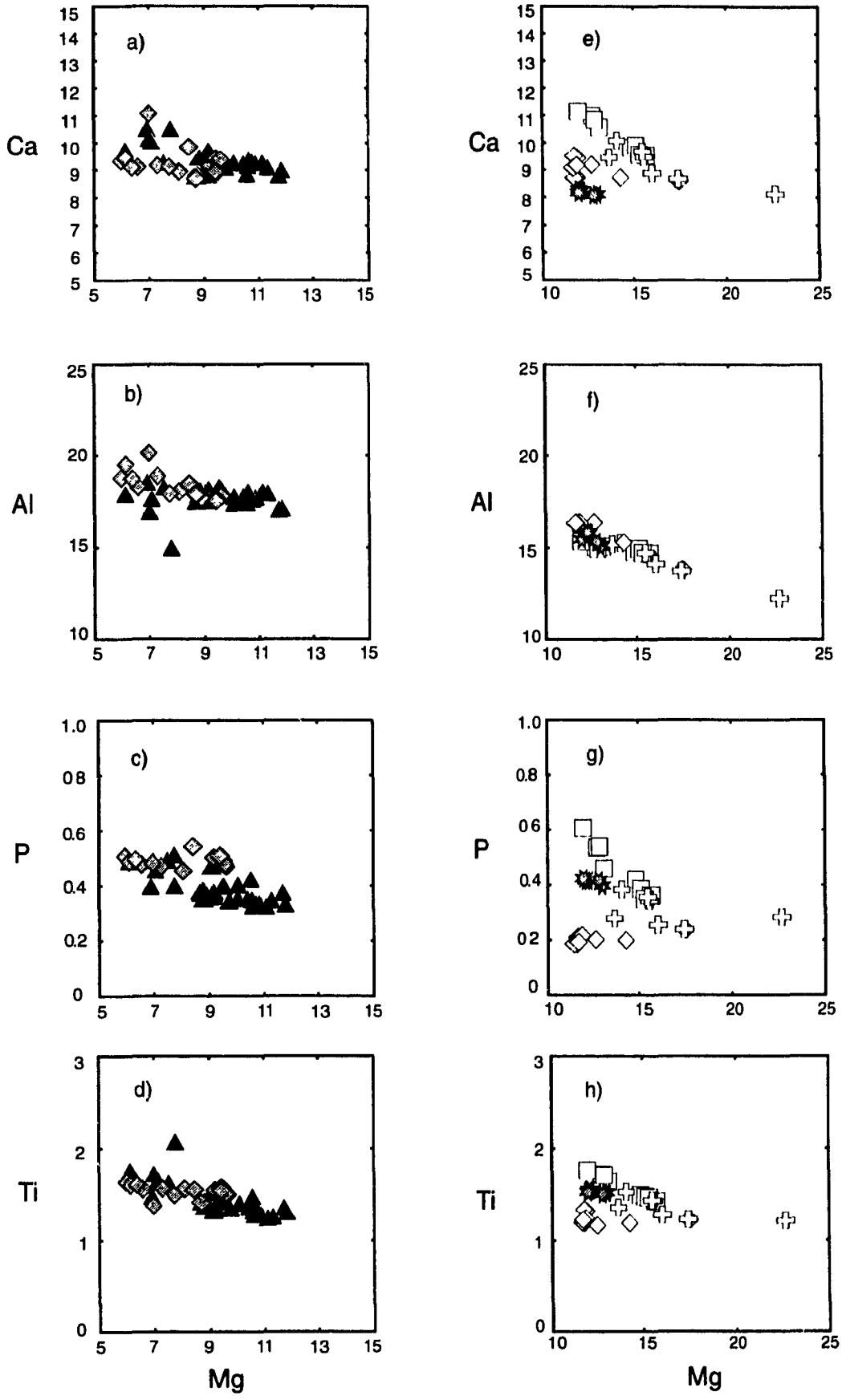
a)
b)
c)
d)
e)
f)
g)
h)
Ca
Al
P
Ti
Mg
Mg

Figure 11: Al versus Si in cation units for the Rancheria and the Hoole basalts. Symbols as in Figure 8 (a).

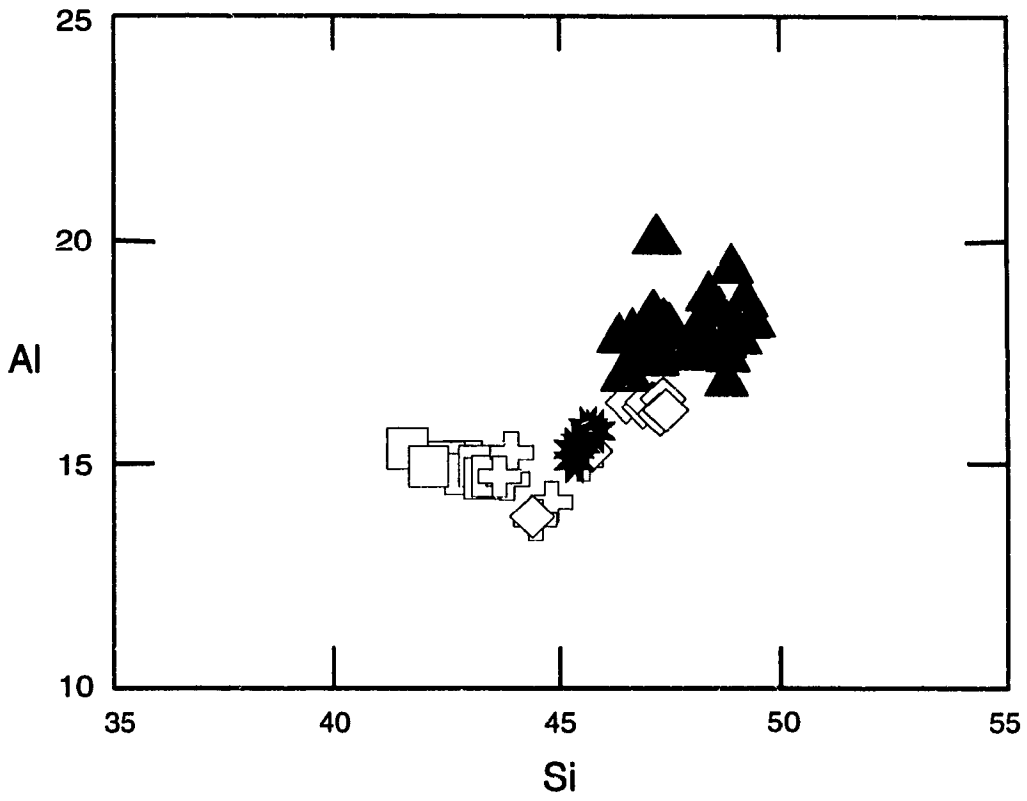
25
20
15
10
Al
35
40
45
50
55
Si

Figure 12: Chondrite-normalized extended spider diagram for **(a)** Rancheria lavas, and **(b)** Hoole basalts. Symbols as in Figure 8 (a).

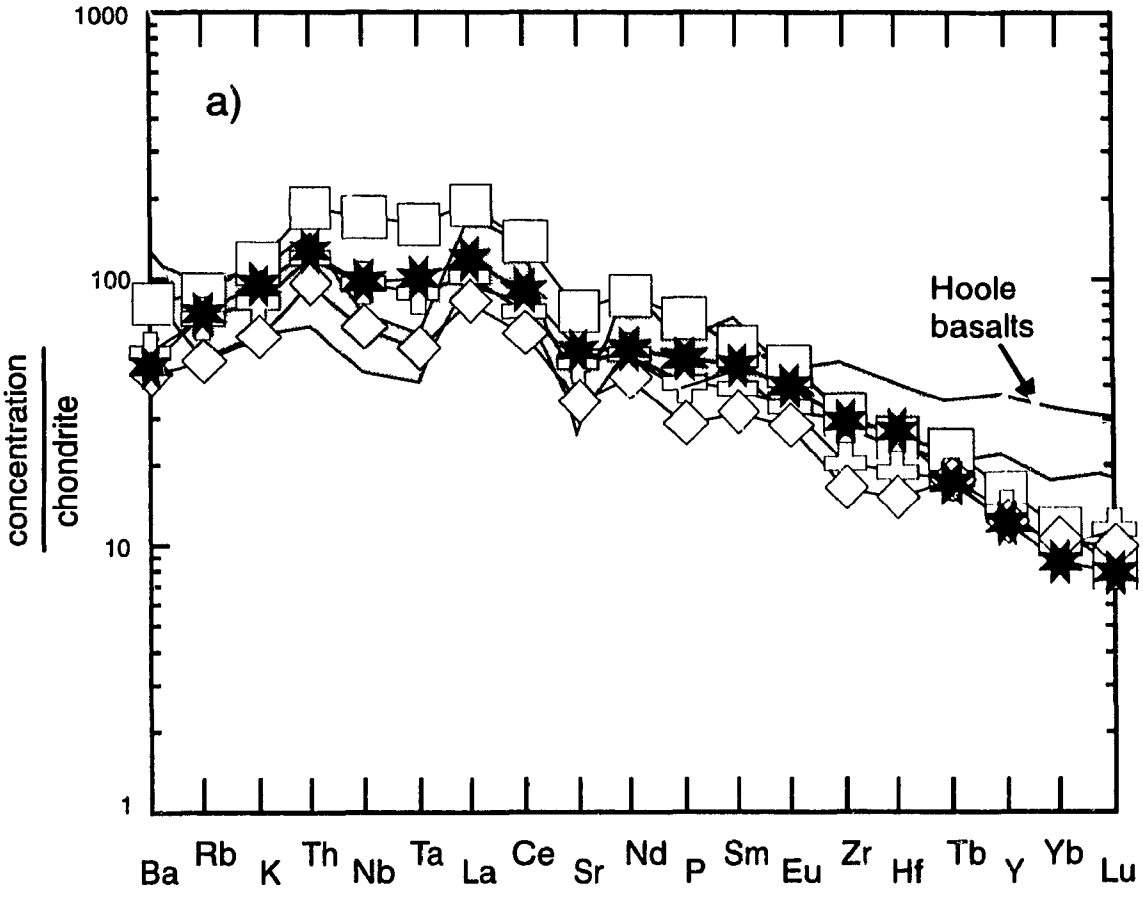
1000
100
10
1
a)
concentration
chondrite
Hoole
basalts
Ba
Rb
K
Th
Nb
Ta
La
Ce
Sr
Nd
P
Sm
Eu
Zr
Hf
Tb
Y
Yb
Lu

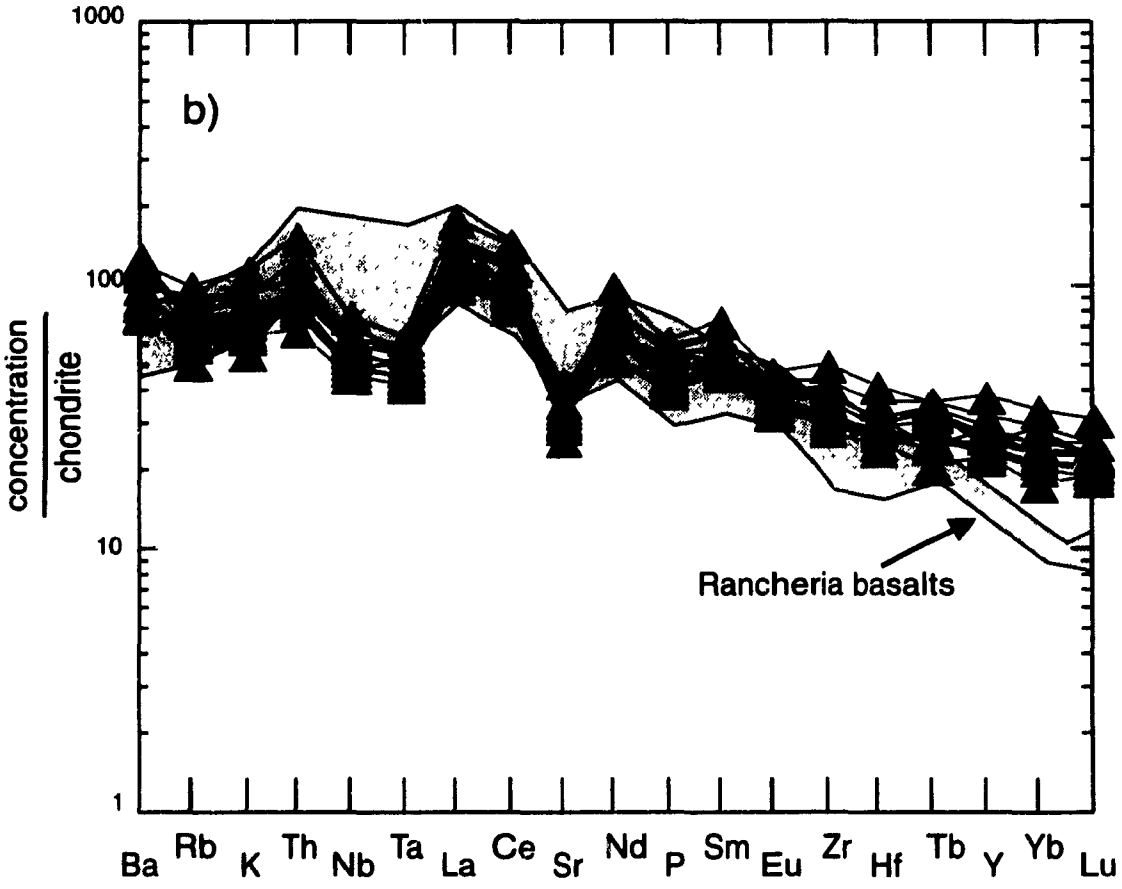
b)
1000
100
10
1
concentration / chondrite
Rancheria basalts
Ba
Rb
K
Th
Nb
Ta
La
Ce
Sr
Nd
P
Sm
Eu
Zr
Hf
Tb
Y
Yb
Lu

Figure 13: Nb versus Zr in ppm for the Rancheria and Hoole basalts. Symbols as in Figure 8 (a).

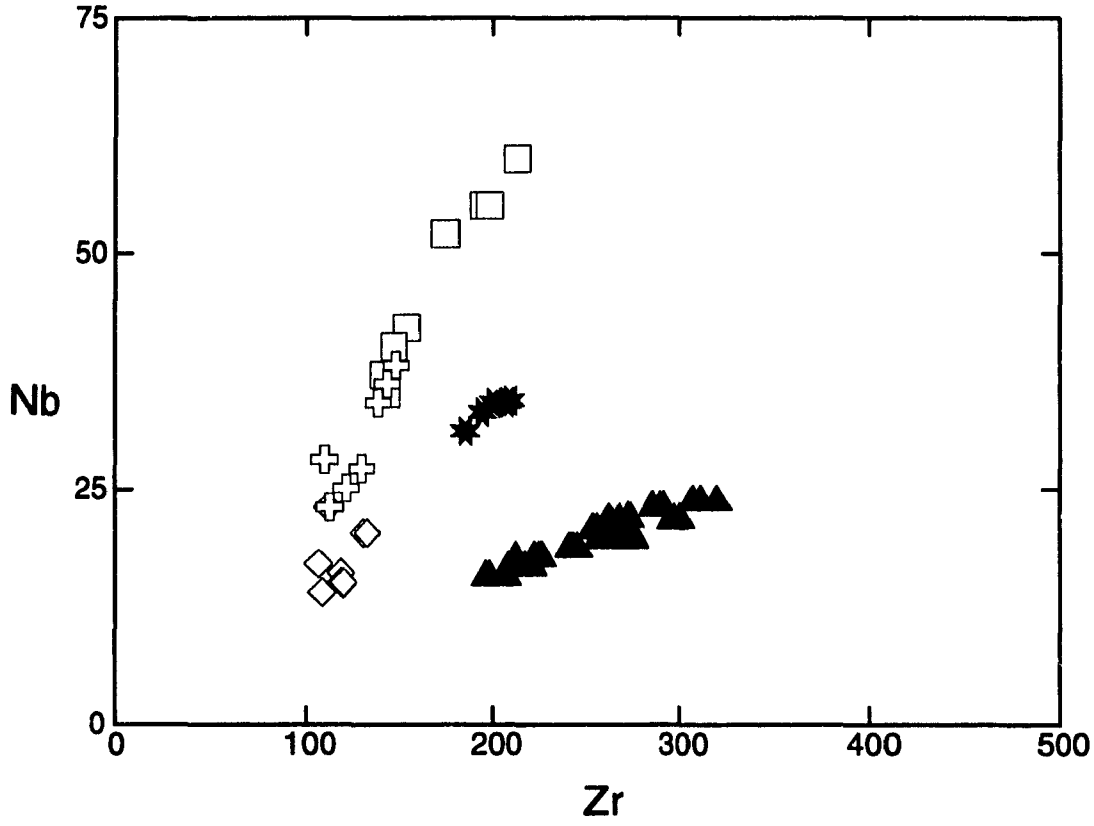
75
50
25
0
Nb
0
100
200
300
400
500
Zr

lavas contain the highest contents of the most incompatible elements, but the REE profilesof the AOB lavas nearly parallel those of the BASAN lavas. The HYN basalts exhibit slight depletions in Nb and Ta and their HREE are less fractionated than those of the AOB and BASAN lavas. In a diagram of Nb versus Zr (Fig. 13), most of the lavas of the Rancheria region define a trend of decreasing Nb with decreasing Zr content which does not pass through the origin. The Watson Lake AOB samples, however, have distinctly higher Zr contents than AOB samples from the west side of the Tintina Trench, at equivalent Nb contents.

BASALTS OF THE HOOLE REGION

Petrography

The valley-filling lavas along the Hoole and Pelly Rivers are brownish grey and plagioclase-phyric in hand sample. Phenocrysts of euhedral to subhedral zoned labradorite (25 to 50 vol%) are ubiquitous in the lavas. Equant or subhedral microphenocrysts of partly or completely iddingsitized olivine (5 to 15 vol%) are also common, with core compositions ranging from Fo_{55} to Fo_{72}. The phenocrysts are set in a groundmass composed of anhedral augite crystals, plagioclase laths, rare anhedral olivine, and equant to acicular oxides. The augite crystals frequently enclose plagioclase laths forming a subophitic texture. Light green spinel has been observed in one sample. The bombs in the breccias along the Hoole and Pelly Rivers are dark grey and very fine-grained in hand sample. Plagioclase occurs as abundant (50 vol%) lath-shaped

microphenocrysts with subordinate equant euhedral olivine microphenocrysts (5-10 vol%). In thin section, the groundmass of the bombs consists of plagioclase microlites and granular olivine in a submicroscopic brownish mesostasis. Thick sections of basalt at Weasel Lake and Starr Lake, however, are coarser grained and lack phenocrysts. Some basalt samples are composed mainly of euhedral plagioclase laths (55 vol%), of partly iddingsitized subhedral olivine (15 vol%), and small grained interstitial phases (30 vol%) including acicular oxides, prismatic clinopyroxene, and feldspar. Other basalt samples are composed of subhedral to anhedral olivine (10 to 25 vol%), ramdomly oriented, concentrically zoned plagioclase laths (50 vol%) which are generally enclosed in bigger clinopyroxene crystals forming a well developed subophitic texture, along with smaller prismatic clinopyroxene (15 to 25 vol%), acicular oxides (2 to 5 vol%), and an interstitial fine grained brownish matrix (5 vol%).

Geochemistry

The basalts from the Hoole region range in composition from 48 to 52 wt% SiO_2 (Table 2) and contain hypersthene (10-22 wt%) and olivine (0-12.5 wt%) or minor quartz (0-2 wt%) in their normative mineralogy. They range from 4 to 8 wt% MgO, with the quartz-normative samples having the lowest MgO contents. The most primitive basalts would equilibrate with olivine of composition of Fo_{85}, assuming an olivine-liquid K_D of 0.30 (Roeder and Emslie 1970) and an Fe^{3+}/Fe_{total} ratio of 0.15. Although the lavas and the bombs along the Hoole and Pelly Rivers reach lower MgO contents than the coarser grained basalts of the Weasel Lake and Starr Lake occurrences, they are geochemicallly

Table 2. Selected analyses of basalts from the Hoole region

Sample:	Ho-1	Ho-8	WL-37	WL-41	WL-8	WL-12	WL-18	WL-27	WL-34
Rock:	*qz thol*	*ol thol*	*ol thol*	*ol thol*	*ol thol*	*ol thol*	*ol thol*	*ol thol*	*ol thol*
Type:	lava	bomb	bomb	lava	coarse	coarse	coarse	coarse	coarse
Site:	4	5	4	3	1	1	1	1	2
Major Elements in wt%									
SiO2	49.33	49.76	48.56	49.42	50.19	48.80	49.31	48.56	49.61
TiO2	2.08	2.14	2.07	2.15	1.97	1.83	1.85	1.76	2.12
Al2O3	15.58	15.55	15.56	15.56	15.68	15.29	16.13	16.02	15.37
Fe2O3	11.29	11.82	11.94	12.08	11.02	11.84	11.26	11.88	11.60
MgO	4.38	6.35	6.63	6.53	6.33	8.29	7.37	7.90	6.21
MnO	0.22	0.20	0.19	0.17	0.17	0.17	0.17	0.17	0.18
CaO	8.55	8.88	9.01	8.71	8.67	8.85	9.01	8.95	8.50
Na2O	3.03	2.75	3.14	3.16	3.14	2.96	3.03	2.88	2.97
K2O	1.16	1.20	0.83	1.12	1.30	0.98	0.99	0.96	1.25
P2O5	0.57	0.62	0.58	0.63	0.47	0.42	0.44	0.44	0.58
LOI	3.87	0.97	1.59	1.39	1.54	1.24	0.00	1.47	2.10
Total	100.06	100.24	100.20	100.92	100.48	100.67	99.56	100.99	100.49
Trace Elements in ppm									
Rb	18	25	23	22	31	22	23	21	31
Sr	432	415	426	436	363	357	375	394	396
Ba	797	662	496	690	601	535	539	595	652
Sc	25.7	-	-	26.8	25.3	24.6	25.0	21.9	-
V	198	209	215	244	194	182	201	154	186
Cr	147	155	124	116	129	196	184	200	188
Ni	43	47	74	69	50	75	78	96	68
Y	39	40	45	46	43	37	38	35	43
Zr	283	272	255	266	256	208	214	208	264
Nb	23	22	21	22	20	17	17	17	20
Hf	6.0	-	-	6.2	6.3	5.3	5.2	5.1	-
Ta	1.1	-	-	1.1	1.2	0.9	0.9	1.0	-
Cs	0.7	-	-	0.9	1.3	0.6	0.0	1.0	-
Co	37	-	-	39	35	42	39	43	-
Th	2.8	-	-	2.8	3.6	2.5	2.5	2.4	-
U	1.1	-	-	1.6	1.6	0.7	0.6	0.6	-
Rare Earth Elements in ppm									
La	37.0	-	-	37.1	30.8	24.4	26.0	25.0	-
Ce	61.8	-	-	76.9	63.7	53.5	56.3	52.5	-
Nd	30.7	-	-	37.7	37.3	25.2	30.6	25.6	-
Sm	8.91	-	-	9.90	8.24	7.11	7.64	7.18	-
Eu	2.28	-	-	2.48	2.13	1.91	2.05	1.92	-
Tb	0.92	-	-	1.28	1.24	0.95	0.97	0.77	-
Yb	4.81	-	-	4.04	3.83	3.59	3.44	2.93	-
Lu	0.56	-	-	0.56	0.60	0.52	0.53	0.48	-

Analytical precisions as in Table 1 Total Fe is calculated as Fe_2O_3 Site numbers refer to the position of the samples in Fig 3

indistinguishable at equivalent MgO contents. In a total alkalies (Na+K) versus silica plot (Fig. 8a), the Hoole basalts fall mainly on the Si-rich side of the plagioclase composition line with average total alkalies of 4 wt% (Na_2O+K_2O). The Hoole basalts are poorer in both Mg and Fe (Fig. 9) and richer in Al and Si than the Rancheria alkaline basalts (Fig. 11). They generally exhibit increasing contents of Ca, Al, P, and Ti with decreasing Mg (Fig. 10), although some lavas and bombs from the Hoole and Pelly Rivers have higher P and Ti contents at similar Mg contents than the basalts from the Weasel and Starr Lakes (e.g. Ho-8 and WL-8, Table 2).

The variations of Mg and Si in a 75 meter section sampled at Weasel Lake (Fig. 14) indicate the presence of two distinct cooling units in which Mg increases and Si decreases up section, making it unlikely that this occurrence represents a volcanic neck (Jackson et al. 1986). The concommitant increase in Mg, the decrease in K, Si, and high field strength elements, such as Zr, up section in each unit, however, is inconsistent with in situ crystal fractionation. These units may represent thick ponded flows which preserved inverted fractionation sequences which were developed in deeper magmatic reservoirs.

The Hoole basalts have fractionated LREE profiles (Fig.12b), but relatively flat unfractionated HREE profiles compared to the Rancheria alkaline basalts. They exhibit distinct negative anomalies in Sr, Nb and Ta with respect to LREE and LIL elements. In addition, the LIL elements are relatively undepleted and thus the Hoole basalts contain

Figure 14: Stratigraphy (meters) vs Mg, Si, and K (cations) and Zr (ppm) for the Weasel Lake section. The inferred upper cooling unit is represented by filled triangles and the lower cooling unit by dotted triangles.

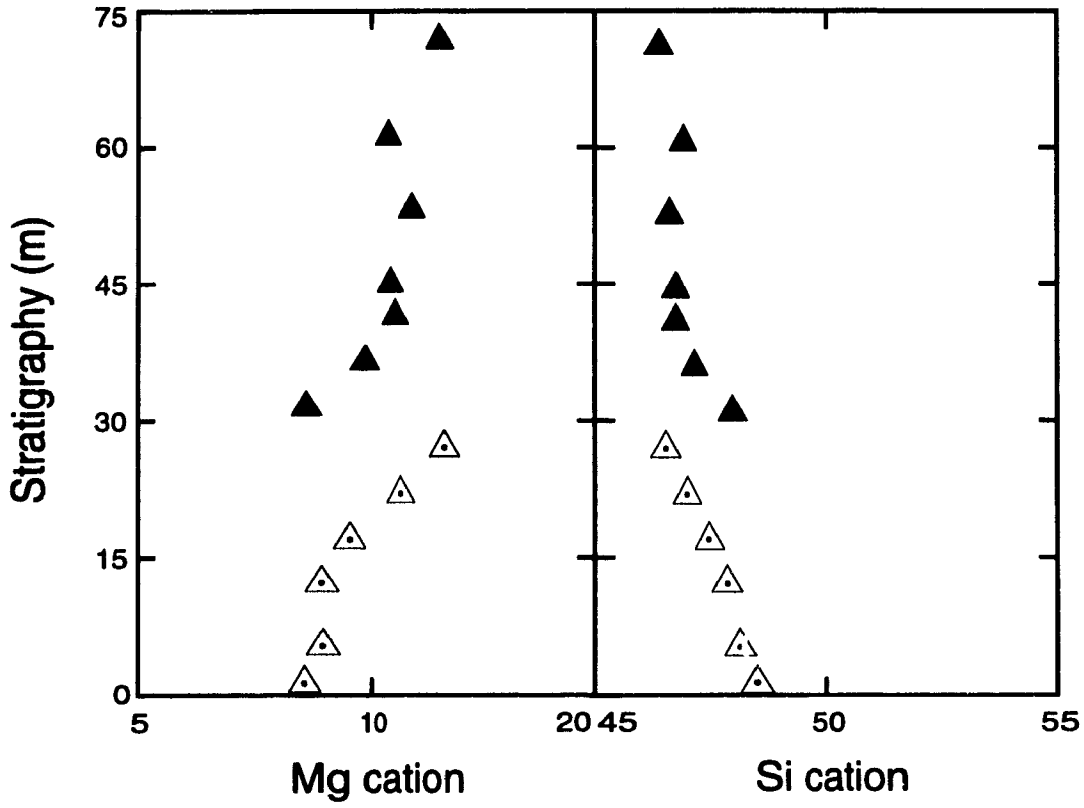
Stratigraphy (m)
75
60
45
30
15
0
5
10
20
45
50
55
Mg cation
Si cation

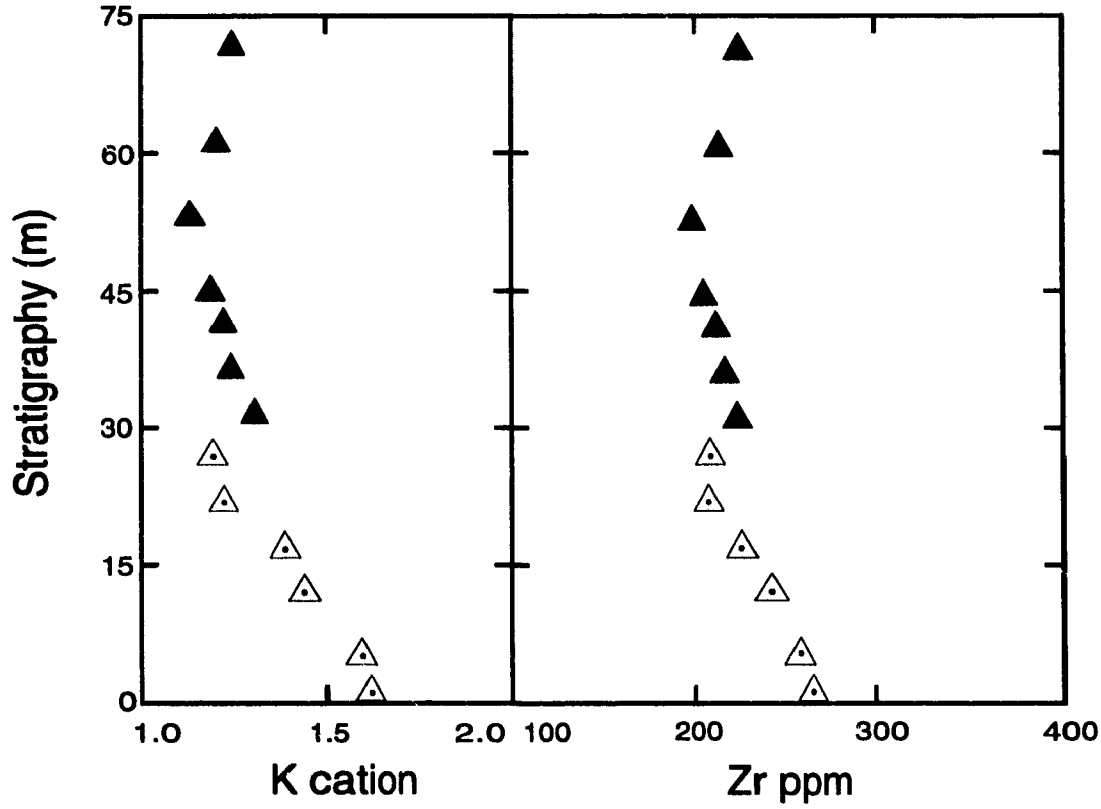
Stratigraphy (m)
75
60
45
30
15
0
1.0
1.5
2.0
100
200
300
400
K cation
Zr ppm

significantly higher Ba contents than the Rancheria alkaline basalts. The Hoole basalts have Cr and Ni contents which are well correlated with Mg content (Table 2), although some samples have anomalously high Cr and Ni contents at relatively low Mg contents. In a plot of Nb versus Zr (Fig. 13), the Hoole basalts also differ from the Rancheria basalts in having significantly higher Zr contents and low Nb contents, defining a linear array which passes through the origin.

DISCUSSION

Petrogenesis of the alkaline basalts of the Rancheria region

The basalts of the Rancheria suite are unlikely to represent primary mantle melts. Although the lavas have MgO contents greater than 8 wt% and most have Ni contents > 150 ppm, the most primitive lavas of the suite would only coexist with an olivine with a composition of Fo_{86}. These basalts thus probably represent derived liquids which have fractionated from more magnesian parental magmas. The fact that olivine is the only phenocryst phase in the basalts on the west side of the Tintina Trench and the systematic increase in Ca and Al with decreasing Mg content (Fig. 10) suggest that plagioclase, clinopyroxene, Fe-Ti oxides and apatite have not fractionated from these magmas and that olivine was the only phase involved in the fractionation process. The Watson Lake AOB lavas, however, have clinopyroxene phenocrysts and lower abundances of Ca and Sc at equivalent Mg contents suggesting that they may have fractionated clinopyroxene as well

as olivine.

The distinct Nb/Zr ratios of the BASAN, AOB, and HYN lavas (Fig. 15a) indicate that they cannot be related by any crystal fractionation process because such processes are not efficient in changing the ratios of these elements (Miyashiro 1978; Pearce and Norry 1979). Furthermore, the trend defined by the Rancheria suite is difficult to produce by different degrees of partial melting of a common mantle source because the rate of change in Nb/Zr ratio decreases with increasing Nb from the HYN to the BASAN lavas, a feature which is characteristic of the late Tertiary to Quaternary alkaline lavas of the Canadian Cordillera (Fig. 15b). In contrast, partial melting of an anhydrous mantle source should produce the greatest fractionation of Nb from Zr at the smallest degree of partial melting, that is at the highest Nb contents. The normalized (see explanations in the caption of Fig. 16) compositional array of the Rancheria basalts, however, approximates a binary mixing array between the BASAN (RA-3) and the HYN (RA-19) lavas in terms of Nb and Zr (Fig. 16). The Watson Lake AOB lavas, however, clearly fall off the calculated mixing curve for the Rancheria suite to the west of the Tintina Trench.

As previously documented by Francis and Ludden (1990), the Fort Selkirk compositional array is approximated by a binary mixing array between the nephelinite and transitional hypersthene-normative basalt end members. In their model, the nephelinite is derived by the melting of amphibole - garnet - clinopyroxenite veins within the

Figure 15: Plots of Nb/Zr versus Nb in ppm for **(a)** Rancheria and Hoole basalts, **(b)** Fort Selkirk (Francis and Ludden 1990), Alligator Lake (Eiché et al. 1987) and Minto alkaline volcanic complexes in the Yukon Territory and Mount Edziza in northern BC (Francis and Ludden, unpublished data). In **(a)** the symbols for the Rancheria and Hoole basalts are as in Figure 8 (a); in **(b)**, the nephelinites are represented in black, the basanites, in light grey, the alkaline olivine basalts, in white, and the hypersthene-normative basalts, in dark grey. The different symbols represent lavas from different suites: circles - Alligator Lake, asterisks - Fort Selkirk, triangles - Edziza, and squares - Minto.

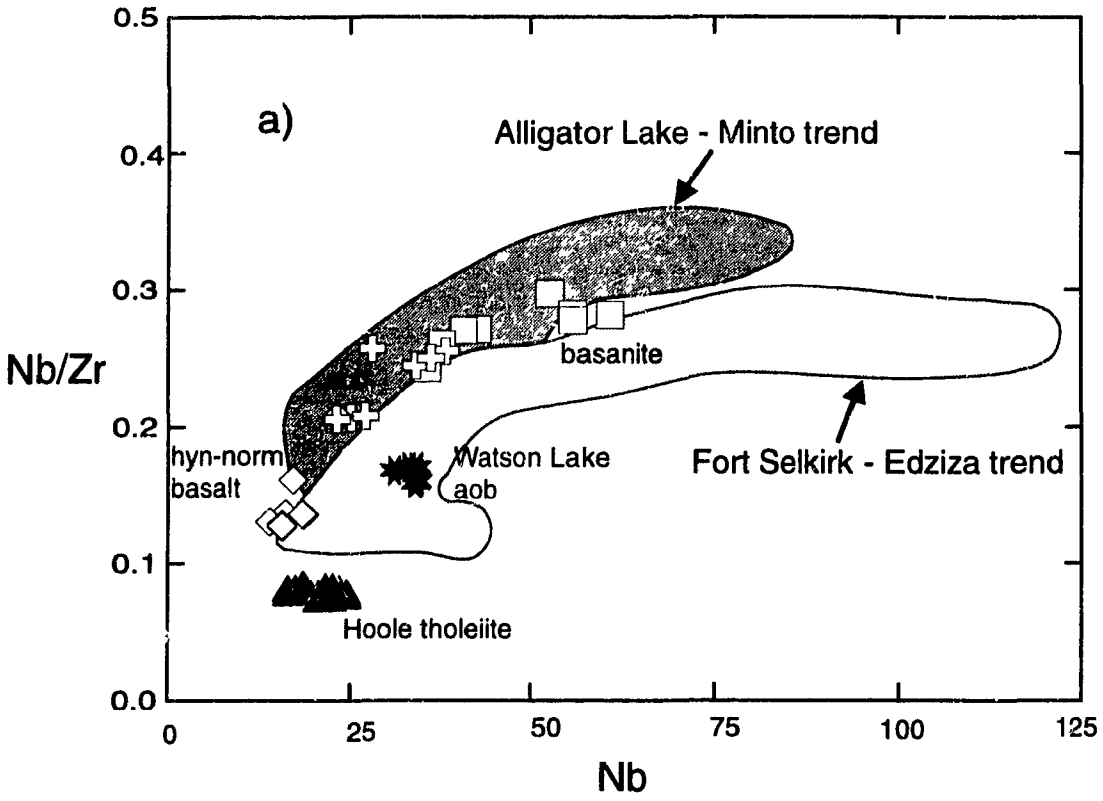
a)
Alligator Lake - Minto trend
basanite
Fort Selkirk - Edziza trend
hyn-norm
basalt
Watson Lake
aob
Hoole tholeiite
Nb/Zr
Nb
0.0
0.1
0.2
0.3
0.4
0.5
0
25
50
75
100
125

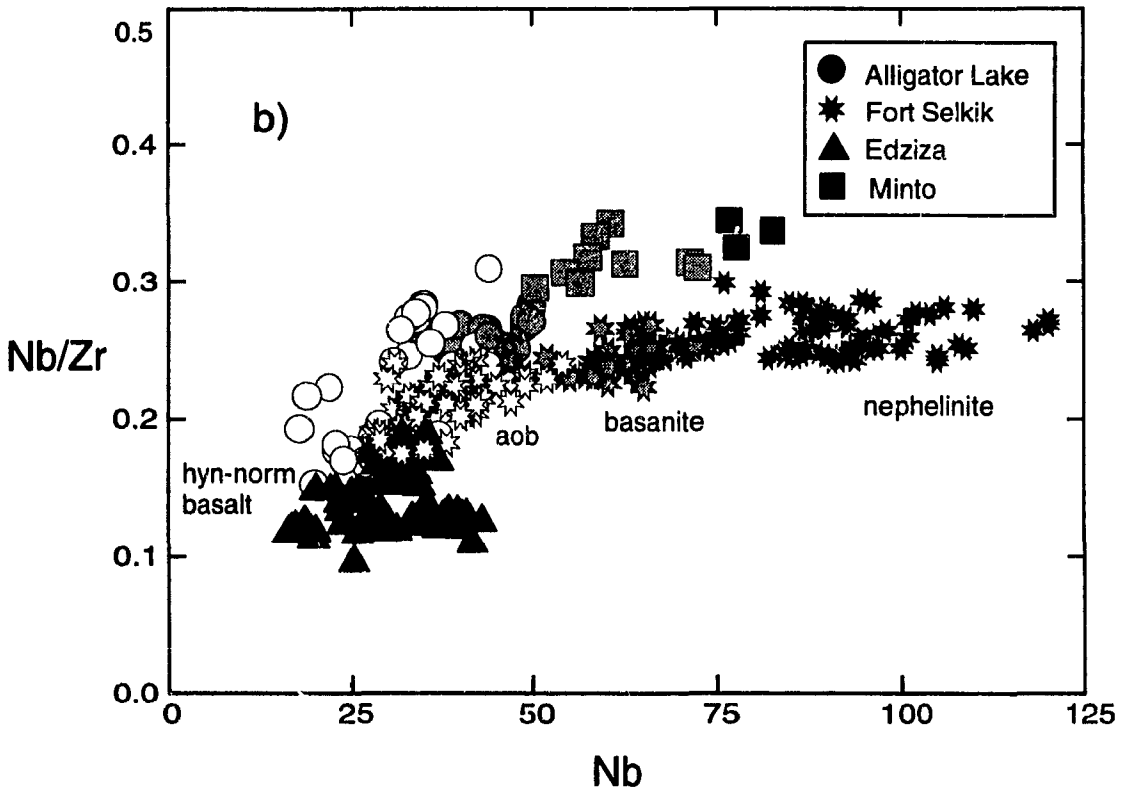
b)
Alligator Lake
Fort Selkik
Edziza
Minto
aob
basanite
nephelinite
hyn-norm
basalt
Nb/Zr
Nb
0.0
0.1
0.2
0.3
0.4
0.5
0
25
50
75
100
125

Figure 16: Nb/Zr versus Nb plot (ppm) of Rancheria and Hoole basalts normalized to 9 wt% MgO. The Rancheria basalts were corrected for olivine accumulation or fractionation by adding or substracting equilibrium olivine in small increments to normalize their compositions to an MgO content of 9 wt%, which corresponds to the average MgO content of the lavas in the suite. The Hoole basalts have also been normalized to an MgO content of 9 wt%. Symbols as in Figure 8 (a). The thick curve represents a mixing curve between a basanite RA-3 and a hypersthene-normative basalt RA-19, both from the Rancheria region. Increments of 10% mixing are indicated by tics along the curve.

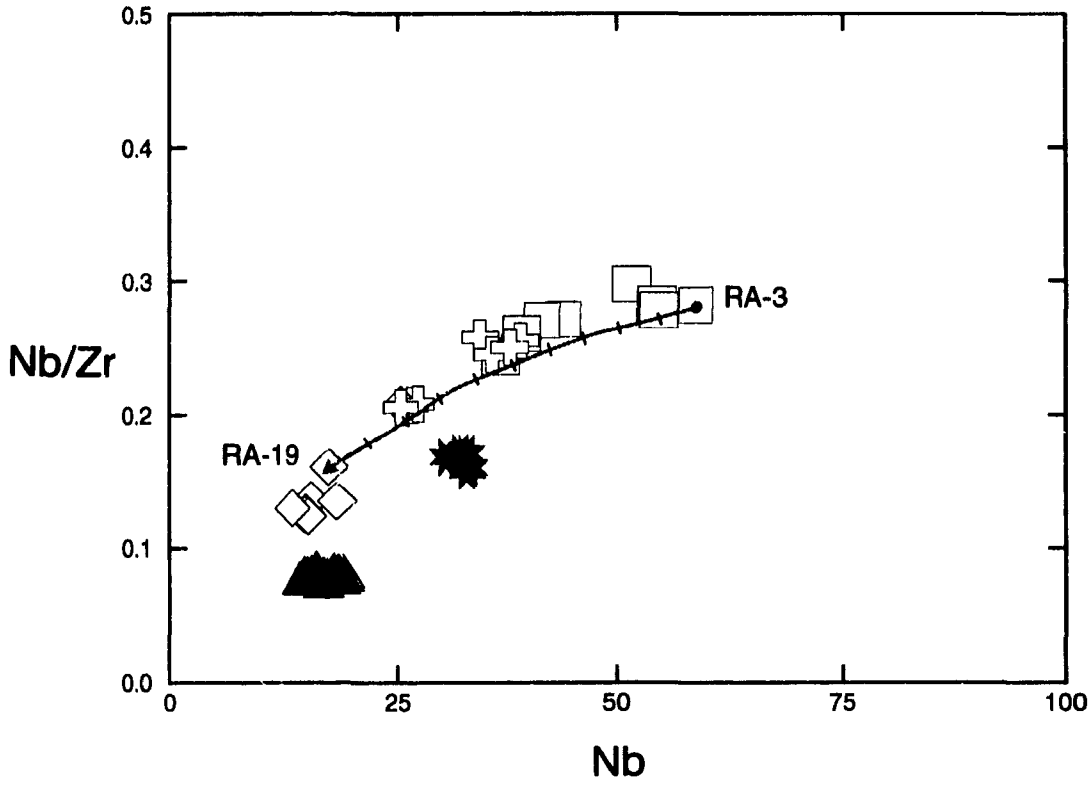
0.5
0.4
0.3
0.2
0.1
0.0
Nb/Zr
RA-3
RA-19
0
25
50
75
100
Nb

lithosphere, whereas the AOB represents more extensive melting of the host lherzolite. The attraction of this model is that it eliminates the requirement of extremely small degrees of partial melting to generate nephelinitic magmas and calls upon a single heterogeneous source to produce the different alkaline magma types without requiring the mixing of magmas from spatially isolated sources. More recently, however, Francis and Ludden (1994) have observed that large-ion lithophile (LIL) and high-field-strength (HFS) elements systematics at a number of alkaline volcanic centres in the Canadian Cordillera indicate that their compositional spectra are not simple binary mixing lines, which are better explained by progressive melting of an amphibole-bearing mantle source.

In a plot of a LIL element, such as K, versus a highly incompatible element, such as La (Fig. 17), the Rancheria alkaline basalts show increasing K with increasing La, but there is a marked change in the slope of the BASAN lavas with respect to AOB and HYN basalts. Similarly, olivine nephelinites of the Canadian Cordillera exhibit constant or decreasing K with increasing La, indicating that the bulk K_D of K is > or = 1, suggesting the presence of residual amphibole in their mantle source (Francis and Ludden 1994). The fact that the Rancheria BASAN lavas define a linear array which cuts the K axis indicates that the bulk K_D for K is larger than that of La, and suggests that a K-bearing phase, such as amphibole, was also involved in the petrogenesis of the Rancheria BASAN lavas. In contrast, the fact that the HYN and AOB lavas lie along a line passing through the origin, indicate that both K and La were highly incompatible elements in these lavas. The involvement of amphibole as a residual mantle phase requires that the geochemical

Figure 17: Binary plot of K (element weight) vs La (ppm) showing the different slopes (thick lines) within the Rancheria basalts. The thick lines are visual best fit lines. The basanites are represented by squares, the alkaline olivine basalts by crosses, the hypersthene-normative basalts by diamonds, and the alkaline basalts from Watson Lake by grey asterisks.

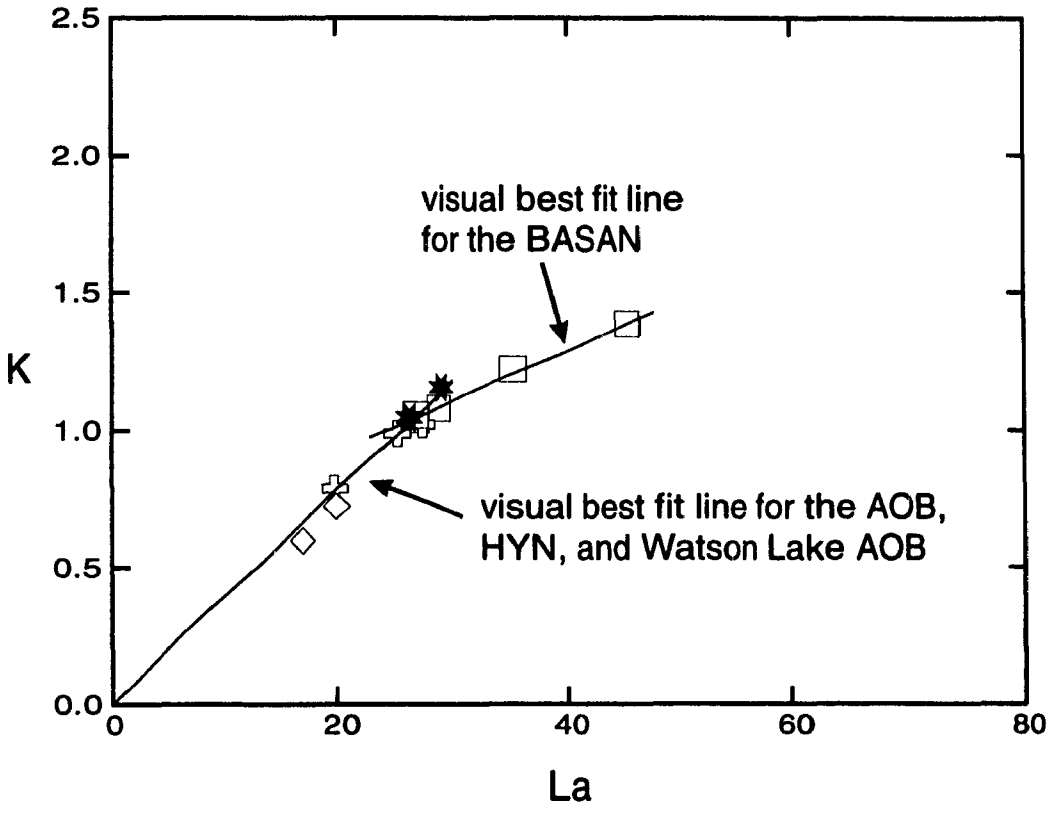
2.5
2.0
1.5
1.0
0.5
0.0
K
0
20
40
60
80
La
visual best fit line
for the BASAN
visual best fit line for the AOB,
HYN, and Watson Lake AOB

characteristics of the Rancheria BASAN magmas are inherited in the lithosphere, where amphibole is stable. If amphibole is the primary control in the partitioning of Nb and Zr, as suggested by Francis and Ludden (1994), then the increasing fractionation of Nb from Zr at lower Nb contents in the Rancheria alkaline lavas could be explained by the exhaustion of amphibole in the mantle source at the transition from basanitic to AOB magma compositions.

Petrogenesis of the tholeiitic basalts from the Hoole region

The Hoole basalts are characterized by fractionated LREE, but flat HREE profiles, and relative depletions in Nb, Ta and Sr. Although Jackson et al. (1986) have assigned a calc-alkaline to transitional tholeiitic affinity to the basalts of the Hoole region, these lavas are clearly not subduction-related. The Nb contents of the Hoole basalts range between 16 and 24 ppm, significantly higher than those typical of subduction-related calc-alkaline lavas (0 - 5 ppm) (B.S.V.P. 1981, p. 202). The Nb contents of the Hoole basalts are more similar to those of the Rancheria HYN basalts, which range between 14 and 23 ppm. Futhermore, the negative Sr anomaly displayed by the Hoole basalts is not typical of calc-alkaline basalts, which are commonly characterized by positive Sr anomalies. The chemical features of the Hoole basalts are more typical of continental tholeiites and their tectonic setting suggests that they are related to transtension along the Tintina Fault (Souther 1977; Pride 1988).

The basalts of the Hoole region have MgO contents below 8 wt% and most have Ni contents < 100 ppm, suggesting that they do not represent primary mantle melts. In fact, the most primitive basalts of the suite would only coexist with an olivine composition of Fo_{85}. Therefore, these basalts must have fractionated from a more magnesian parental magma. The constant Nb/Zr ratio (Fig. 15a) of the Hoole basalts is consistent with closed-system crystal fractionation, as these elements have similar mineral-melt partition coefficients for likely fractionating phases. The basalts also exhibit nearly constant LILE/HFSE ratios (e.g. K/Zr, Sr/Zr) indicating that they may have evolved from a common parental magma. The Hoole basalts show increasing contents of Al, Ca, P, and Ti with decreasing Mg content (Fig. 10) suggesting that plagioclase, clinopyroxene, apatite, and oxides have not fractionated from these magmas, despite their relatively low Mg content. A relatively constant to slightly decreasing Fe content with decreasing Mg content indicate that the Hoole magmas were dominated by olivine fractionation, although there is some scatter in the data especially between 9 and 12 Mg (cat%). However, phenocrysts of plagioclase exceed olivine in size and abundance in the Hoole lavas and bombs, indicating that the Hoole magmas were saturated in plagioclase. Although a small proportion of plagioclase may have been fractionated, the increase of Al with decreasing Mg indicates that plagioclase could not have been the dominant fractionating phase. The abundance of plagioclase might be attributed to flotation, thus although it was crystallizing, was not significantly fractionated.

Figure 18: Mg versus **(a)** Al, **(b)** Ti, **(c)** Ca, and **(d)** Fe (in cation units) for the Hoole basalts showing the low-pressure closed-system crystal fractionation trend which has been calculated by the removal of 100% olivine from a parental magma with one of the most primitive magma composition within the Hoole and Pelly River lavas and bombs (WL-41, Table 3). The extent of crystallization reaches 7%. The lavas and bombs are represented by light grey diamonds and the coarser grained basalts from the Weasel Lake and Starr Lake, by black triangles. The Fe^{3+}/Fe_{total} ratio in the model was initially fixed at 0.15.

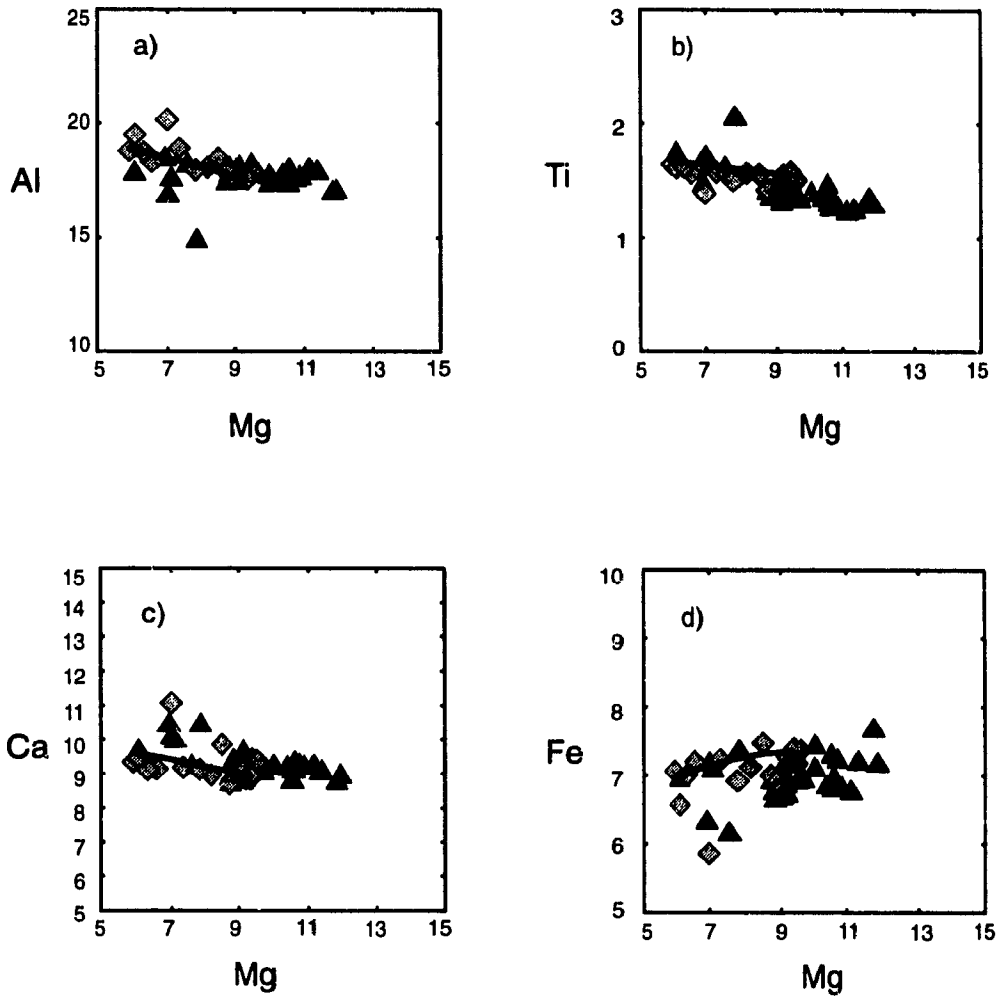
a)
Al
Mg
25
20
15
10
5
7
9
11
13
15
b)
Ti
Mg
3
2
1
0
c)
Ca
Mg
15
14
13
12
11
10
9
8
7
6
5
d)
Fe
Mg
10
9
8
7
6
5

In order to assess the effects of low-pressure closed-system crystal fractionation within the Hoole tholeiitic basalts, we used a computer program employing a finite difference algorithm in which the compositions of the fractionating phases were determined using the two-lattice activity-temperature model of Nielsen & Dungan (1983) and Nielsen (1988). The range of many major and trace elements observed within the more evolved lavas and bombs can be closely reproduced by 7% closed-system crystal fractionation of olivine (Fig. 18) from a common parental magma (WL-41) (Table 3). However, two samples appear to have Ca contents which are too high to be reached with the inferred crystal fractionation model. Although a parental magma composition with greater Ca contents could explain the higher Ca contents of those samples, higher Ca contents could be attributed to an increased content of carbonate filling the vesicles.

Despite the fact that the tholeiitic basalts of the Hoole region have Mg numbers ($Mg/[Mg+Fe^{3+}]$ = 0.41 - 0.58) which are too low for primary mantle melts, they are sufficiently primitive to constrain the trace element composition of their mantle source. The similarity of trace and REE abundances between the lavas, the bombs and the coarse grained basalts suggests that they are cogenetic. The flat unfractionated profile of HREE in the Hoole magmas suggests that residual garnet was not present in their mantle source, and that the primary magma from which the Hoole magmas may have been derived by partial melting within the spinel lherzolite stability field of the upper mantle. Simple equilibrium and fractional melting models were evaluated to constrain the composition of the mantle source of the Hoole magmas. An estimate of the composition of the

Table 3. Parental magma and estimated primary magma compositions

Sample:	WL-41	WL-19	WL-12	WLprFo$_{90}$
Major Elements in wt%				
SiO2	49.42	48.43	48.80	47.60
TiO2	2.15	1.89	1.83	1.54
Fe2O3	12.08	12.62	11.84	12.58
Al2O3	15.56	15.17	15.29	12.62
MgO	6.53	8.17	8.29	15.33
MnO	0.17	0.19	0.17	0.18
CaO	8.71	8.62	8.85	7.37
Na2O	3.16	2.84	2.96	2.40
K2O	1.12	1.02	0.98	0.83
P2O5	0.63	0.47	0.42	0.36
LOI	1.39	1.49	1.24	0.18
Total	100.92	99.84	99.66	99.92
Trace Elements in ppm				
Rb	22	22	22	18
Sr	436	382	357	306
Ba	691	640	535	487
Y	46	38	37	31
Zr	266	225	208	180
Nb	22	18	17	14
V	244	189	182	154
Cr	116	207	196	167
Co	39	-	42	96
Ni	69	114	75	715
Sc	24.8	-	24.6	21.3
Th	2.8	-	2.5	2.1
U	1.6	-	0.7	0.6
Rare Earth Elements in ppm				
La	37.1	-	24.4	20.2
Ce	74.9	-	53.5	44.4
Nd	37.7	-	25.2	20.9
Sm	9.90	-	7.11	5.89
Eu	2.48	-	1.91	1.58
Tb	1.28	-	0.95	0.79
Yb	4.04	-	3.59	2.99
Lu	0.56	-	0.52	0.43

Total Fe is calculated as Fe_2O_3. WL-41 lava is the parental composition used in the crystal fractionation model. WLprFo$_{90}$ is the estimated primitive magma composition which has been calculated as the average of WL-12 and WL-19 magma compositions and then normalized to a composition which would coexist with a Fo$_{90}$ olivine.

primary magma of the Hoole basalts was calculated by incrementally adding olivine to the average composition of the two most primitive magma compositions of the suite (WL-12 and WL-19, Table 3) until it would coexist with an olivine composition of Fo_{90}. The resultant estimate of the primary magma composition contained approximately 15 wt% MgO ($WLprFo_{90}$, Table 3). The flat HREE profile of the Hoole primary magma can be generated by 10-15% non-modal equilibrium melting (Fig. 19a) or 15% fractional melting (Fig. 19b) of a spinel lherzolite source with a primitive mantle composition (Sun and McDonough 1989). Although the HREE of the Hoole basalts are consistent with either equilibrium or fractional melting of a dry spinel lherzolite source, the calculated LREE, LILE and incompatible element abundances do not match those observed in the estimated Hoole primary magma. The LREE and LILE compositions of the Hoole basalts require a mantle source which was enriched with respect to estimated compositions of the primitive upper mantle, suggesting that the mantle source for the Hoole basalts was enriched lithosphere beneath the ancestral North America or that the primary magmas have been contaminated by the lower crust before they underwent low-pressure crystal fractionation. The ancestral North American craton may have experienced a history of incompatible element enrichment through previous subduction events and remained isolated from the underlying convecting asthenosphere.

Figure 19: Chondrite-normalized diagrams showing the calculated non-modal **(a)** equilibrium and **(b)** fractional melting models (dashed lines) for 1%, 5%, 10% and 15% partial melting of a spinel lherzolite source using the equations of Shaw (1970) and the partition coefficients are listed in Table 4. Thick line represents the calculated primary magma for the Hoole basalts (WLprfo90, Table 3). Source modal mineralogy: olivine 56%, orthopyroxene 22%, clinopyroxene 19%, and spinel 3% (McDonough 1990).

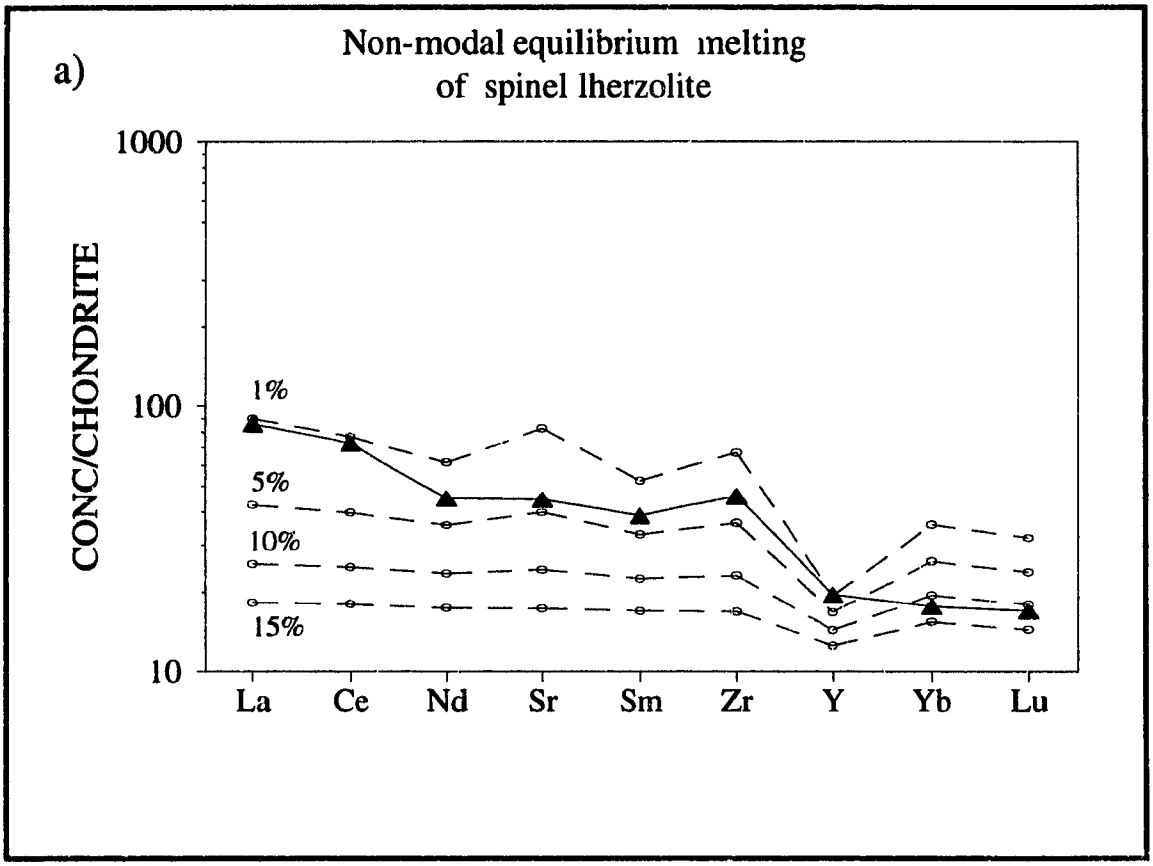
a)
Non-modal equilibrium melting
of spinel lherzolite
CONC/CHONDRITE
1000
100
10
1%
5%
10%
15%
La
Ce
Nd
Sr
Sm
Zr
Y
Yb
Lu

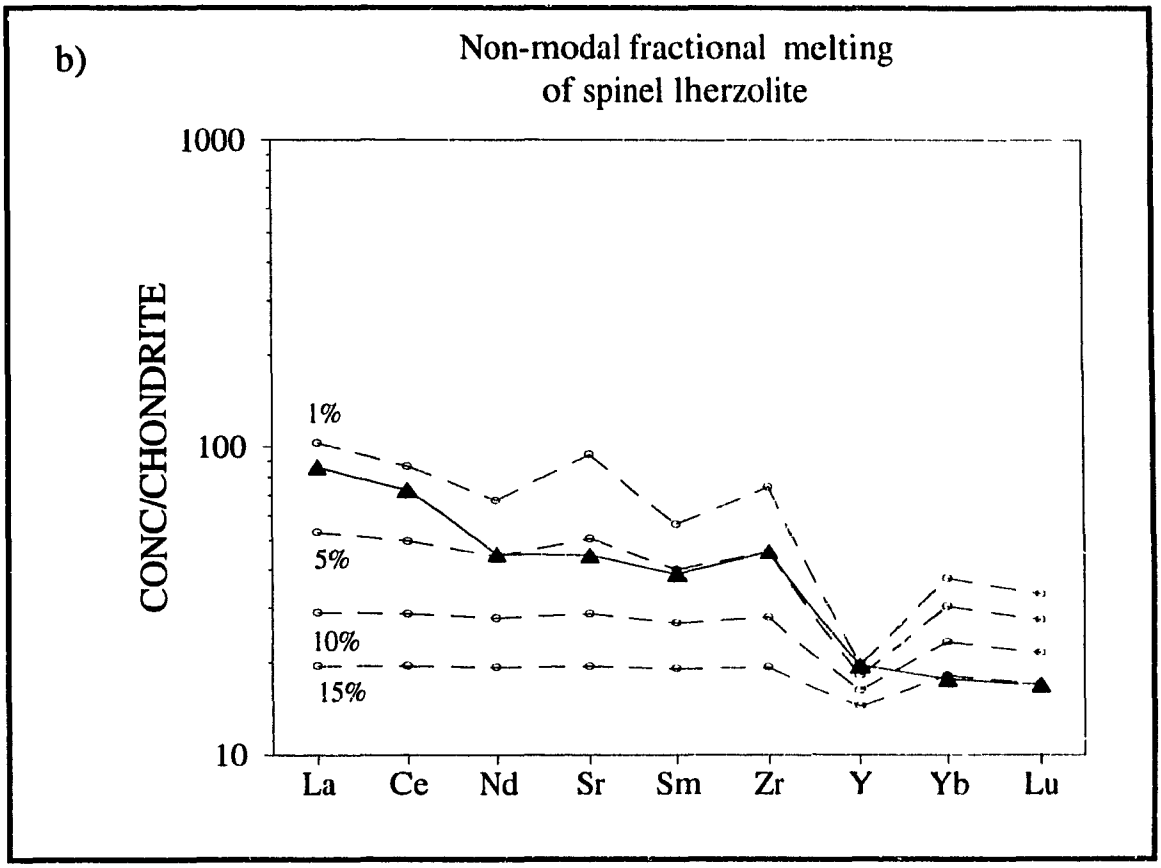
b)
Non-modal fractional melting
of spinel lherzolite
CONC/CHONDRITE
1000
100
10
1%
5%
10%
15%
La
Ce
Nd
Sr
Sm
Zr
Y
Yb
Lu

Table 4. Mineral - liquid partition coefficients

	Olivine	*Opx*	*Cpx*	*Spinel*
La	0.0004[c]	0.0012[c]	0.12[c]	0.0002[c]
Ce	0.0003[c]	0.0016[c]	0.15[c]	0.0002[c]
Nd	0.0002[c]	0.0028[c]	0.20[c]	0.0001[c]
Sr	0.0100[b]	0.0400[d]	0.06[d]	0.0010
Sm	0.0002[c]	0.0054[c]	0.24[c]	0.0001[c]
Zr	0.0100[a]	0.0300[a]	0.10[a]	0.1000[e]
Y	0.0100[a]	0.2000[a]	0.50[a]	0.0010
Yb	0.0052[c]	0.0600[c]	0.30[c]	0.0012[c]
Lu	0.0085[c]	0.0703[c]	0.31[c]	0.0004[c]

Source data: [a]Pearce and Norry (1979); [b]Le Roex et al. (1981); [c]Prinzhofer and Allègre (1985); [d]Green et al. (1989); [e]Viereck et al. (1989).

The Watson Lake Basalts

Although the Watson Lake alkaline basalts are contemporaneous with the Rancheria suite, they have distinctive Nb/Zr ratios and lower Ca and Sc contents than the Rancheria AOB to the west of the Tintina Fault. The latter two features combined with the presence of clinopyroxene phenocrysts suggest that, unlike the Rancheria alkaline basalts on the western side of the Tintina Fault, the Watson Lake AOB have experienced the fractionation of clinopyroxene. The differences between the Watson Lake AOB and the Rancheria alkaline suite suggest a chemical contrast between the lithospheric component in these magmas across the Tintina Trench. The Tintina Fault, therefore, juxtaposes continental lithospheric mantles which have different contents of Zr. In this regard, it is interesting to note that the high Zr contents of the Watson Lake AOB lavas are similar to those of the Eocene tholeiitic lavas on the east side of the Tintina Fault, further to the north. Mixing of 40% basanitic magma (RA-3) from the Rancheria suite with primitive tholeiitic magma from the Hoole region (WL-12) reproduces much of the trace element character of the Watson Lake AOB lavas (Fig. 20). The HREE contents of the calculated mixture, however, are higher than the HREE contents of the Watson Lake lavas (Fig. 21) and suggest that, unlike the Hoole tholeiitic magmas, the lithospheric component for the Watson Lake magmas was generated in the garnet lherzolite stability field. Furthermore, the HREE abundances of the Watson Lake AOB are even lower than those of the Rancheria BASAN lavas, suggesting that the source of the Watson Lake alkaline magmas had a greater proportion of garnet than that of the Rancheria alkaline

Figure 20: Nb/Zr versus Nb (ppm) plot showing a mixing line between a Rancheria basanite (RA-3) and a Hoole primitive tholeiitic basalt (WL-12) all normalized to 9 wt% MgO. Symbols as in Figure 8 (a). Increments of 10% mixing are indicated by tics along the line.

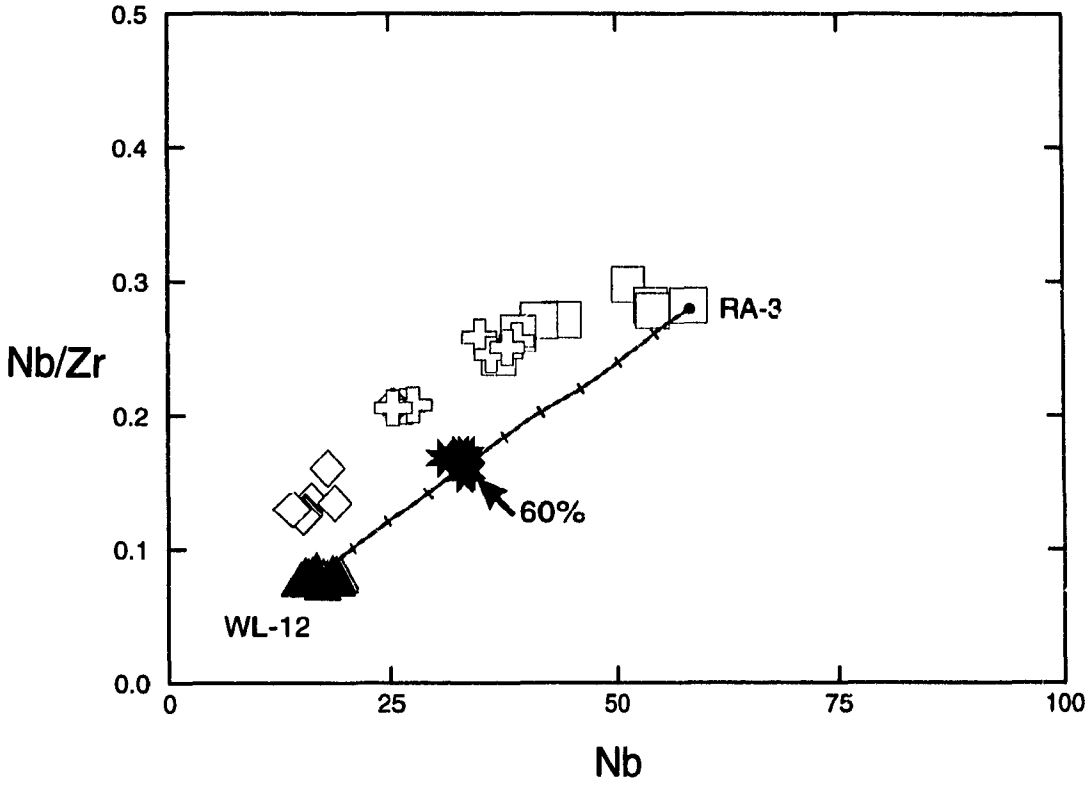
0.5
0.4
0.3
0.2
0.1
0.0
Nb/Zr
0
25
50
75
100
Nb
RA-3
60%
WL-12

Figure 21: Chondrite-normalized spider diagram of the average composition of the Watson Lake AOB (asterisks) and the calculated composition of the liquid produced by 60% mixing (stars) of a Rancheria basanite, RA-3, and a Hoole primitive tholeiitic basalt, WL-12. The data have been previously normalized to 9 wt% MgO.

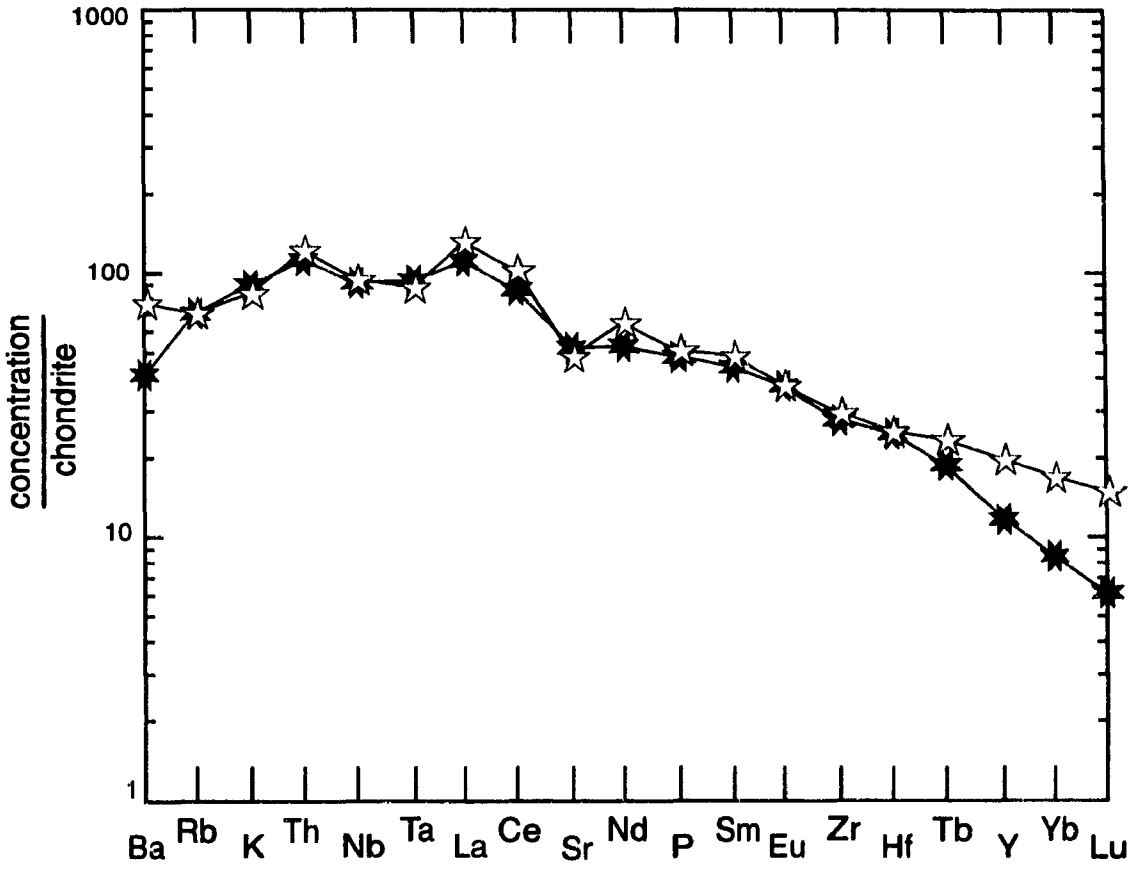
1000
100
10
1
concentration
chondrite
Ba
Rb
K
Th
Nb
Ta
La
Ce
Sr
Nd
P
Sm
Eu
Zr
Hf
Tb
Y
Yb
Lu

magmas. The dramatic increase in Zr in the Quaternary alkaline basalts from the Rancheria suite across the Tintina Trench reflects the contribution of chemically distinct continental lithospheric mantles on either side of the Trench, indicating that the Tintina Fault is a steeply dipping suture which penetrates the lithospheric mantle.

CONCLUSION

The Quaternary alkaline basalts from the Rancheria region do not represent primary mantle melts, but rather residual liquids resulting from the fractionation of olivine of more magnesian parental magmas. The BASAN, AOB, and HYN lavas forming the Rancheria alkaline suite all display fractionated HREE profiles, suggesting that they were produced in the garnet stability field. Because the rate of change in the Nb/Zr ratio decreases with increasing Nb content from the HYN to the BASAN lavas, they cannot be produced by different degrees of partial melting of a common mantle source, and cannot be related by any crystal fractionation process. However, the compositional array of the alkaline volcanics along the Rancheria River on the west side of the Tintina Trench can be explained by a model involving the partial melting of an amphibole-bearing mantle source. The systematics of LILE in the BASAN magmas of the Rancheria suite require the presence of amphibole as a residual mantle phase in their source, whereas the HYN basalts may have been produced after amphibole was completely melted in the lithospheric mantle beneath the Omenica Belt. The range in composition from the most

primitive AOB to the HYN basalts on the western of the Tintina Trench may be the result of mixing between partial melts of amphibole and melts derived from the lherzolite after amphibole was exhausted. The involvement of amphibole in the petrogenesis of the Rancheria alkaline basalts indicates that these magmas were generated within the lithosphere, where amphibole is a stable phase.

In contrast, on the east side of the Tintina Trench, Eocene tholeiitic basalts from the Hoole River region also have fractionated LREE, but flat HREE profiles, and distinctive relative depletions in Nb, Ta, and Sr. Much of the variation in the major and trace elements of the Hoole lavas and bombs can be explained by closed-system crystal fractionation of olivine at low-pressure. The LREE and LILE compositions of the Hoole basalts require a mantle source which was enriched with respect to estimated compositions of the primitive upper mantle. Furthermore, the flat unfractionated HREE profile of the Hoole tholeiitic basalts suggests that residual garnet was not present in their mantle source, and that the primary magma for the Hoole volcanics may have been produced by partial melting within the spinel lherzolite stability field of the upper mantle. Therefore, the mantle source for the Hoole basalts, on the eastern side of the Tintina Trench, may have been enriched lithosphere beneath the ancestral North America.

The distinctive Nb - Zr systematics of the AOB from the Watson Lake region, on the east side of the Tintina Trench, at the eastern end of the Rancheria region indicate that they may be derived by mixing between melts produced by melting of an amphibole

dominated residue and a lithospheric mantle similar in composition to that which produced the Hoole Eocene tholeiitic basalts erupted on the eastern side of the Tintina Trench. The dramatic increase in Zr in the alkaline olivine basalts across the Tintina Fault and the similar high Zr contents of Eocene tholeiitic basalts on the northeast side of the Fault in the Hoole River region suggests that the Tintina Fault represents a major lithospheric suture that juxtaposes contrasting compositions of mantle lithospheres, and that the compositional differences in the Quaternary alkaline basalts from the Rancheria suite across the Tintina Trench reflects the contribution of two chemically distinct continental mantle lithospheres.

ACKNOWLEDGMENTS

This research was funded by a scholarship from the Fonds pour la Formation de Chercheurs et l'Aide à la Recherche to V. H. and by grants from the Natural Sciences and Engineering Research Council of Canada and by a Northern Scientific Traineeship from the Department of Indian and Northern Affairs. We would like to thank Tariq Ahmedali for performing the XRF analyses, Jean-Luc Bastien and Brigitte Dionne for their valuable help during the instrumental neutron-activation analyses, and Glenn Poirier for assistance on electron probe microanalysis. Special thanks to Anne Charland, Claude Dalpé, and Pierre Hudon for helpful discussions and encouraging comments.

GENERAL SUMMARY

This study has demonstrated that there is an abrupt increase in Zr and decrease in Ca and Sc in recent alkaline olivine basalts across the Tintina Fault, and that the anomalously high Zr contents of the Watson Lake lavas on the east side of the fault are strikingly similar to those of Eocene tholeiitic basalts, also on the northeast side of the Fault in the Hoole River region. We have argued that this chemical discontinuity across the Tintina Fault reflects a contrast in the compositions of the mantle lithospheres from which the alkaline magmas were derived. If this interpretation is correct, then the Tintina Fault must have a steep dip and represent a major lithospheric suture.

The significance of the compositional differences in the Rancheria alkaline basalts across the Tintina Trench should be further explored with isotopic studies of the Rancheria and Hoole basalts to better constrain the relative character of the asthenospheric and lithospheric mantle components in these basalts. The change in chemical composition across the Tintina Trench necessitate a significant involvement of the lithospheric mantle in the genesis of these alkaline basalts. The asthenospheric contribution appears to be restrained to the introduction of amphibole in the lithosphere by asthenosphere-derived magmas and fluids prior to the magmatic event which generated the recent alkaline magmas. The trace element systematics of the Rancheria alkaline magmas on the west side of the Tintina Trench indicate that the lithospheric mantle beneath the Omenica Belt is an amphibole-bearing lherzolite. In contrast, the high concentrations in Zr of the

Watson Lake alkaline basalts indicate that the lithospheric mantle on the east side of the Tintina Fault is similar in Zr to that which produced the Eocene tholeiitic basalts from the Hoole River region. The fractionated LREE profiles, the distinctive relative depletions in HFSE, such as Nb and Ta, and the high co.'tents of Zr of the Eocene tholeiitic basalts, erupted on the east side of the Tintina Trenc.h, indicate that the lithospheric mantle beneath ancestral North America is also enriched in incompatible elements relative to estimated compositions of the primitive upper mantle, but is significantly different from the lithospheric mantle on the west side of the Tintina Fault in terms of Nb, Ta, and Zr contents.

The fact that the HREE abundances of the Watson Lake AOB are more fractionated and depleted than those of the Rancheria BASAN lavas suggests that the source of the Watson Lake alkaline magmas had a greater proportion of garnet than that of the Rancheria alkaline magmas, on the west side of the Tintina Trench, and therefore the Watson Lake AOB may have been produced by melting of the lithospheric mantle at greater depths than the Rancheria BASAN. This indicates that the depth at which melting occurred in the lithosphere on the east side of the Tintina Fault is greater than that on the west side of the fault. This change in the depth of melt segregation could reflect a change in the lithopheric thickness across the Tintina Fault.

The results of this thesis suggest that a regional comparison of the major and trace element character of the numerous recent alkaline eruption centres along the northern

Cordillera would provide an important tool for probing the depth extension of the sutures between the disparate accreted terranes of northwestern North America. This will be one of the objectives of the Slave-Northern Cordillera Lithospheric Evolution (SNORCLE) Transect of the LITHOPROBE project during the next few years. The chemical variation in the Quaternary to Recent alkaline volcanism of the northern Canadian Cordillera provides valuable information for the characterization and definition of the accreted terranes and may provide one of the most valuable constraints for interpreting the results of the planned SNORCLE seismic reflection survey.

REFERENCES

Allègre CJ, Lambert B, Richard P (1981) The subcontinental versus the sub-oceanic debate - I. Lead-neodymium-strontium isotopes in primary alkali basalts from a shield area: the Ahaggar volcanic suite. Earth Planet Sci Lett 52:85-92

Bailey DK (1982) Mantle metasomatism - continuing chemical change within the Earth. Nature 296:525-530

Bailey DK (1987) Mantle metasomatism - perspective and prospect. *In*: Fitton JG & Upton BGJ (eds) Alkaline Igneous Rocks, 1-13

Basaltic Volcanism Study Project (BSVP) (1981) Basaltic Volcanism on the Terrestrial Planets. New York: Pergamon Press, 1286 pp.

Chen CY and Frey FA (1985) Trace element and isotopic geochemistry from Haleakala Volcano, East Maui, Hawaii: implications for the origin of Hawaiian basalts. JGR 90:8743-8768

Christie AB, Duke JL, Rushton R (1992) Grew Creek epithermal gold-silver deposit, Tintina Trench, Yukon. *In*: Yukon Geology, Vol. 3; Exploration and Geological Services Division, Yukon, Indian and Northern Affairs, Canada. 223-259

Clowes RM (ed) (1993) LITHOPROBE Phase IV Proposal - Studies of the Evolution of a Continent. Published by the LITHOPROBE Secretariat, The University of British Columbia, Vancouver, B.C. 290 pp.

Dawson GM (1888) The Yukon River and British Columbia. Geological and Natural History Survey of Canada Annual Report, Vol. III, Part IB'

Duke JL and Godwin CI (1986) Geology and alteration of the Grew Creek epithermal gold-silver prospect, south-central Yukon. *In*: Yukon Geology, Vol. 1; Exploration and Geological Services Division, Yukon, Indian and Northern Affairs, Canada. 72-82

Eiché G, Francis D, Ludden J (1987) Primary alkaline magmas associated with the Quaternary Alligator Lake volcanic complex, Yukon Territory, Canada. Contrib Mineral Petrol 95:191-201

Erdmer P (1987) Blueschist and eclogite in mylonitic allochthons, Ross River and Watson Lake areas, southeastern Yukon. Can J Earth Sci 1439-1449

Fitton JG (1987) The Cameroon Line, west Africa: a comparison between oceanic and continental alkaline volcanism. *In*: Fitton JG & Upton BGJ (eds) Alkaline Igneous Rocks, 273-291

Fitton JG, Dunlop HM (1985) The Cameroon line, west Africa, and its bearing on the origin of oceanic and continental basalt. Earth Planet Sci Lett 72:23-38

Fitton JG, James D, Kempton PD, Ormerod DS, Leeman WP (1988) The role of lithospheric mantle in the generation of late Cenozoic basic magmas in the Western United States. J Petrol, Special Lithosphere Issue, 331-349

Francis DM (1987) Mantle-Melt interaction recorded in spinel lherzolite xenoliths from the Alligator Lake Volcanic Complex, Yukon, Canada. J Petrol 28:569-597

Francis D and Ludden J (1990) The mantle source for olivine nephelinite, basanite, and alkaline olivine basalt at Fort Selkirk, Yukon, Canada. J Petrol 31:371-400

Francis D and Ludden J (1994) The chemical signature of amphibole in mafic alkaline lavas. Submitted to Contrib Mineral Petrol

Gabrielse H (1966) Geology of the Watson Lake map-area. Geological Survey of Canada, map 19-1966

Gabrielse H, Tempelman-Kluit DJ, Blusson SL, Campbell RB (1977) Geological compilation, Macmillan River, Yukon Territory. Geological Survey of Canada, map 1398A

Gabrielse H (1985) Major dextral transcurrent displacements along the northern Rocky Mountain Trench and related lineaments in north-central British Columbia. Geol Soc Am Bull 96:1-14

Green TH, Sie SH, Ryan CG, Cousens DR (1989) Proton microprobe-determined partitioning of Nb, Ta, Zr, Sr and Y between garnet, clinopyroxene and basaltic magma at high pressure and temperature. Chem Geol 74:201-216

Hawkesworth CJ, Rogers NW, Van Calsteren PWC, Menzies MA (1984) Mantle enrichment processes. Nature 311:331-335

Jackson LE, Gordey SP, Armstrong RL, Harakal JE (1986) Bimodal Paleogene volcanics near Tintina Fault, east-central Yukon, and their possible relationship to placer gold. *In*: Yukon Geology, Vol. 1; Exploration and Geological Services Division, Yukon, Indian and Northern Affairs, Canada. 139-147

Klassen RW (1987) The Tertiary Pleistocene stratigraphy of the Liard Plain, southeastern Yukon Territory. Geological Survey of Canada Paper 86-17

Leat PT, Thompson RN, Morrison MA, Hendry GL, Dickin AP (1988) Compositionally-diverse Miocene-Recent rift-related magmatism in Northwest Colorado: partial melting, and mixing of mafic magmas from 3 different asthenospheric and lithospheric mantle sources. J Petrol, Special Lithosphere Issue, 351-377

Le Roex AP, Erlank AJ, Needham HD (1981) Geochemical and mineralogical evidence for the occurence of at least three distinct magma types in the "Famous region". Contrib Mineral Petrol 77:24-37

Lord CS (1944) Geological reconnaissance along the Alaska Highway between Watson Lake and the Teslin River, Yukon and British Columbia. Geological Survey of Canada Paper 44-25

Lowey GW and Lowey JF (1986) Geology of Spencey Creek (105 B/1) and Daughney Lake (105 B/2) map areas, Rancheria district, southeast Yukon, Canada. Exploration and Geological Services Division, Yukon, Indian and Northern Affairs Canada. Open file report 1986-1

McDonough WF (1990) Constraints on the composition of the continental lithopheric mantle. Earth Planet Sci Lett 101:1-18

Menzies M (1983) Mantle ultramafic xenoliths in alkaline magmas: evidence for mantle heterogeneity modified by magmatic activity. *In*: Hawkesworth CJ and Norry MJ (eds) Continental Basalts and Mantle Xenoliths, 92-110

Menzies M (1987) Alkaline rocks and their inclusions: a window on the Earth's interior. *In*: Fitton JG and Upton BGJ (eds) Alkaline igneous rocks, 15-27

Miyashiro A (1978) Nature of alkalic volcanic rock series. Contrib Mineral Petrol 66:91-104

Nielsen RL, Dungan MA (1983) Low pressure mineral-melt equilibria in natural anhydrous mafic systems. Contrib Mineral Petrol 84:310-326

Nielsen RL (1988) A model for the simulation of combined major and trace element liquid lines of descent. Geochim Cosmochim Acta 52:27-38

Pearce JA and Norry MJ (1979) Petrogenetic implications of Ti, Zr, Y, and Nb variations in volcanic rocks. Contrib Mineral Petrol 69:33-47

Pride MJ (1988) Bimodal volcanism along the Tintina Trench, near Faro and Ross River. *In*: Yukon Geology, Vol. 2; Exploration and Geological Services Division, Yukon, Indian and Northern Affairs Canada. 69-80

Prinzhofer A and Allègre CJ (1985) Residual peridotites and the mechanisms of partial melting. Earth Planet Sci Lett 74:251-265

Roddick JA (1967) Tintina Trench. J Geol 75:23-33

Roeder MF, Emslie RF (1970) Olivine-liquid equilibrium. Contrib Mineral Petrol 29:275-289

Shaw DM (1970) Trace element fractionation during anatexis. Geochim Cosmochim Acta 34:237-243

Souther JG (1977) Volcanic and tectonic environments in the Canadian cordillera - a second look. *In*: Baragar WRA, Coleman LC, & Hall JM (eds) Volcanic regimes in Canada. Geol Assoc Canada Spec Pap 16:3-24

Souther JG, Brew DA, Okulitch AV (1974) Geological compilation, Iskut River, British Columbia-Alaska. Geological Survey of Canada, map 1418A

Sun SS and McDonough WF (1989) Chemical and isotopic systematics of oceanic basalts: implications for mantle compositions and processes. In: Saunders AD and Norry MJ (eds) Magmatism in the Ocean Basins. Geol Soc Lond Spec Publ 42:313-345

Tempelman-Kluit DJ (1972) Geology and origin of the Faro, Vangorda, and Swim concordant zinc-lead deposits, Central Yukon Territory. Geological Survey of Canada Bulletin 208. 73 pp.

Tempelman-Kluit DJ (1977) Geology of the Quiet Lake (105 F) and Finlayson Lake (105 G) map areas. Geological Survey of Canada Open File Report 486

Tempelman-Kluit DJ (1980) Evolution of physiography and drainage in southern Yukon. Can J Earth Sci, vol. 17, 9:1189-1203

Viereck LG, Flower MFJ, Hertogen J, Schmincke M-V, Jenner GA (1989) The genesis and significance of N-MORB sub types. Contrib Mineral Petrol 102:112-126

Wheeler JO, Green LH, Roddick JA (1960) Geology of Quiet Lake map area and Finlayson Lake area. Geological Survey of Canada, maps 7-1960 and 8-1960

Wheeler JO, Brookfield AJ, Gabrielse H, Monger JWH, Tipper HW, Woodsworth GJ (1991) Terrane map of the Canadian Cordillera. Geological Survey of Canada, map 1713A

APPENDIX A AND B:

Major, trace and rare earth element compositions

for the Rancheria basalts and the Hoole basalts

APPENDIX A. COMPOSITION OF RANCHERIA BASALTS (1)

Sample:	RA-1	RA-2	RA-3	RA-4	RA-5	RA-6	RA-7	RA-8
Rock:	*BASAN*	*BASAN*	*BASAN*	*BASAN*	*BASAN*	*BASAN*	*AOB*	*HYN*
Site:	1	1	1	1	1	1	1	A
Major Elements in wt%								
SiO2	45.55	44.80	44.01	45.61	46.36	46.47	44.82	49.12
TiO2	2.32	2.42	2.49	2.12	2.11	2.04	1.73	1.74
Al2O3	13.64	13.55	13.84	13.40	13.67	13.42	11.21	14.69
Fe2O3	13.76	13.91	14.01	13.60	13.35	13.40	14.73	13.61
MgO	9.18	8.83	8.29	10.48	10.76	11.17	16.31	8.26
MnO	0.19	0.19	0.20	0.18	0.19	0.18	0.19	0.17
CaO	10.52	10.87	11.05	9.78	9.95	9.59	8.18	9.06
Na2O	3.60	3.60	4.07	3.42	3.17	3.13	2.15	3.06
K2O	1.47	1.47	1.67	1.30	1.24	1.25	0.95	0.72
P2O5	0.58	0.67	0.76	0.53	0.49	0.46	0.36	0.27
LOI	0.01	0.52	0.01	0.01	0.01	0.01	0.01	0.01
Total	100.82	100.81	100.39	100.43	101 30	101.12	100.64	100.71
Trace Elements in ppm								
Rb	29	32	31	26	27	28	20	14
Sr	726	1024	902	679	662	620	529	370
Ba	588	564	565	408	491	476	434	215
Sc	21.9	-	22.1	23.2	-	23.3	21.5	23.6
V	230	263	246	238	248	229	203	201
Cr	278	244	211	315	309	352	548	253
Ni	167	148	117	213	215	237	381	139
Y	23	25	25	21	21	21	17	20
Zr	175	195	213	155	148	142	109	118
Nb	52	55	60	42	40	37	28	16
Hf	4.7	-	5.1	3.9	-	3.7	2.9	3.6
Ta	2.6	-	3.2	2.2	-	2.1	1.4	0.9
Cs	0.3	-	0.6	0.5	-	0.3	0.4	0.5
Co	53	-	51	59	-	61	76	55
Th	4.6	-	5.4	4.0	-	3.7	2.6	2.4
U	2.6	-	1.8	1.3	-	0.7	1.0	0.8
Rare Earth Elements in ppm								
La	36.2	-	46.3	29.4	-	27.3	20.0	16.9
Ce	66.5	-	88.0	59.8	-	52.7	39.4	32.7
Nd	31.4	-	41.1	27.2	-	22.0	16.4	20.4
Sm	7.41	-	8.60	6.20	-	6.45	4.96	4.57
Eu	2.32	-	2.75	2.01	-	1.93	1.56	1.65
Tb	0.67	-	0.85	0.71	-	0.63	0.53	0.43
Yb	2.07	-	1.93	1.62	-	1.97	1.29	1.90
Lu	0.23	-	0.21	0.20	-	0.21	0.14	0.27

APPENDIX A. COMPOSITION OF RANCHERIA BASALTS (2)

Sample:	RA-9	RA-10	RA-11	RA-12	RA-13	RA-14	RA-15	RA-16
Pock:	*HYN*	*BASAN*	*AOB*	*AOB*	*AOB*	*BASAN*	*AOB*	*HYN*
Site:	A	2	2	3	3	3	4	5
Major Elements in wt%								
SiO2	49.93	44.78	46.40	46.42	46.53	46.30	47.75	47.47
TiO2	1.68	2.43	2.02	2.15	2.04	2.08	1.82	1.74
Al2O3	14.74	13.57	13.21	13.72	13.36	13.35	12.85	12.57
Fe2O3	13.41	13.90	13.42	13.20	13.41	13.35	13.80	13.87
MgO	8.16	9.02	10.96	9.85	10.97	10.82	11.36	12.42
MnO	0.17	0.20	0.18	0.18	0.18	0.18	0.18	0.18
CaO	9.00	10.81	9.39	9.97	9.66	9.53	8.87	8.61
Na2O	3.05	3.90	2.86	2.91	2.87	3.12	2.97	2.75
K2O	0.71	1.60	1.19	1.33	1.23	1.27	0.92	0.87
P2O5	0.24	0.68	0.43	0.48	0.45	0.44	0.32	0.30
LOI	0.01	0.01	0.01	0.33	0.01	0.01	0.01	0.01
Total	101.10	100.90	100.07	100.54	100.71	100.44	100.85	100.79
Trace Elements in ppm								
Rb	15	32	25	29	25	27	18	17
Sr	332	833	576	633	600	589	415	405
Ba	221	514	367	390	497	445	259	301
Sc	-	-	23.2	-	24.0	23.7	-	22
V	194	267	230	245	236	249	216	185
Cr	251	259	396	348	374	356	363	397
Ni	136	131	258	208	232	237	268	322
Y	21	24	21	22	21	21	20	19
Zr	108	198	139	149	144	144	121	111
Nb	14	55	34	38	36	35	25	23
Hf	-	-	3.8	-	4.0	3.7	-	3.0
Ta	-	-	1.8	-	2.0	2.1	-	1.1
Cs	-	-	0.0	-	0.4	0.0	-	0.5
Co	-	-	58	-	60	59	-	64
Th	-	-	3.5	-	3.8	3.7	-	2.8
U	-	-	1.2	-	0.7	0.7	-	0.2
Rare Earth Elements in ppm								
La	-	-	25.1	-	27.3	27.3	-	20.0
Ce	-	-	47.9	-	50.8	54.1	-	39.3
Nd	-	-	24.6	-	24.2	28.0	-	19.9
Sm	-	-	5.93	-	6.42	6.40	-	4.79
Eu	-	-	1.92	-	2.11	1.98	-	1.62
Tb	-	-	0.66	-	0.63	0.72	-	0.65
Yb	-	-	1.61	-	1.53	1.70	-	1.73
Lu	-	-	0.29	-	0.26	0.19	-	0.25

APPENDIX A. COMPOSITION OF RANCHERIA BASALTS (3)

Sample:	RA-17	RA-18	RA-19	WT-3	WT-4	WT-5	WT-6	WT-7
Rock:	*AOB*	*AOB*	*HYN*	*HYN*	*HYN*	*HYN*	*HYN*	*HYN*
Site:	6	6	7	13	13	13	12	12
Major Elements in wt%								
SiO2	48.28	47.39	48.69	49.68	49.78	50.06	49.70	49.85
TiO2	1.92	1.74	1.68	1.61	1.75	1.66	1.86	1.89
Al2O3	13.72	12.49	13.85	14.64	14.75	14.80	14.43	14.51
Fe2O3	13.46	13.83	13.58	13.23	13.17	13.20	13.59	13.23
MgO	9.58	12.31	10.11	8.79	8.08	8.18	8.24	8.07
MnO	0.17	0.17	0.16	0.18	0.18	0.17	0.17	0.18
CaO	9.40	8.66	8.69	9.05	9.36	9.30	8.58	8.68
Na2O	3.07	2.82	3.00	2.80	3.04	2.74	2.90	2.95
K2O	0.92	0.88	0.85	0.63	0.64	0.67	0.91	0.96
P2O5	0.35	0.30	0.25	0.24	0.23	0.24	0.26	0.26
LOI	0.01	0.01	0.01	0.00	0.00	0.00	0.00	0.00
Total	100.88	100.59	100.87	100.84	100.98	101.02	100.66	100.58
Trace Elements in ppm								
Rb	17	18	19	13	13	23	13	24
Sr	459	409	395	369	376	381	374	379
Ba	402	378	252	304	285	271	338	349
Sc	-	-	-	27.0	22.0	21.0	18.0	20.0
V	203	211	203	184	206	209	197	194
Cr	354	406	354	272	266	272	270	272
Ni	220	328	194	181	148	155	178	180
Y	20	18	18	20	20	21	21	21
Zr	130	112	106	119	118	142	120	145
Nb	27	23	17	15	15	19	15	19
Hf	-	-	-	-	-	-	-	-
Ta	-	-	-	-	-	-	-	-
Cs	-	-	-	-	-	-	-	-
Co	-	-	-	55	59	69	59	62
Th	-	-	-	1.2	1.2	1.7	1.6	1.4
U	-	-	-	-	-	-	-	-
Rare Earth Elements in ppm								
La	-	-	-	-	-	-	-	-
Ce	-	-	-	35.0	33.0	13.0	40.0	25.0
Nd	-	-	-	-	-	-	-	-
Sm	-	-	-	-	-	-	-	-
Eu	-	-	-	-	-	-	-	-
Tb	-	-	-	-	-	-	-	-
Yb	-	-	-	-	-	-	-	-
Lu	-	-	-	-	-	-	-	-

APPENDIX A. COMPOSITION OF RANCHERIA BASALTS (4) (BASALTS FROM WATSON LAKE)

Sample:	RA-20	RA-21	RA-22	WT-1	WT-2
Rock:	*AOB*	*AOB*	*AOB*	*AOB*	*AOB*
Site:	8	9	9	11	11

Major Elements in wt%

SiO2	48.01	47.94	47.79	48.22	48.05
TiO2	2.15	2.15	2.12	2.17	2.17
Al2O3	13.59	13.88	13.77	14.10	14.16
Fe2O3	14.38	14.09	14.51	14.31	14.26
MgO	9.08	8.29	8.89	8.42	8.34
MnO	0.16	0.16	0.16	0.17	0.17
CaO	8.05	8.07	7.98	8.07	8.13
Na2O	3.62	3.82	3.51	3.30	3.41
K2O	1.26	1.39	1.31	1.34	1.33
P2O5	0.50	0.53	0.52	0.52	0.52
LOI	0.01	0.01	0.01	0.00	0.00
Total	100.81	100.43	100.57	100.62	100.54

Trace Elements in ppm

Rb	25	26	24	25	24
Sr	604	639	633	637	648
Ba	216	325	328	443	473
Sc	16.7	16.7	-	15.0	17.0
V	209	186	189	176	179
Cr	280	256	278	247	253
Ni	245	215	226	217	208
Y	18	19	19	21	20
Zr	185	200	194	214	217
Nb	31	34	33	34	34
Hf	4.7	5.3	-	-	-
Ta	1.8	2.0	-	-	-
Cs	0.4	0.0	-	-	-
Co	62	58	-	67	66
Th	2.9	3.7	-	1.2	1.5
U	1.2	1.6	-	-	-

Rare Earth Elements in ppm

La	26.1	29.0	-	-	-
Ce	53.6	57.5	-	61.0	60.0
Nd	24.9	25.7	-	-	-
Sm	6.46	7.25	-	-	-
Eu	2.11	2.30	-	-	-
Tb	0.79	0.64	-	-	-
Yb	1.42	1.44	-	-	-
Lu	0.12	0.20	-	-	-

APPENDIX B. COMPOSITION OF HOOLE BASALTS (1)

Sample:	Ho-1	Ho-2	Ho-3	Ho-4	Ho-5	Ho-6	Ho-7	Ho-8
Rock:	*qz thol*	*qz thol*	*qz thol*	*qz thol*	*qz thol*	*ol thol*	*ol thol*	*ol thol*
Type:	lava	lava	lava	lava	lava	lava	bomb	bomb
Site:	4	4	4	4	4	4	5	5
Major elements in wt%								
SiO2	49.33	50.55	48.78	48.20	50.06	49.74	48.67	49.76
TiO2	2.08	2.25	2.14	2.09	2.19	2.15	2.08	2.14
Al2O3	15.58	16.44	16.59	16.05	16.25	15.85	15.66	15.55
Fe2O3	11.29	11.39	10.29	11.32	11.19	11.53	11.53	11.82
MgO	4.38	4.07	4.06	4.87	4.30	5.61	6.51	6.35
MnO	0.22	0.19	0.22	0.16	0.22	0.17	0.20	0.20
CaO	8.55	8.99	8.84	8.58	8.68	8.65	8.92	8.88
Na2O	3.03	3.26	3.13	2.91	3.18	3.22	2.69	2.75
K2O	1.16	1.17	1.06	1.12	1.14	1.20	1.17	1.20
P2O5	0.57	0.62	0.58	0.56	0.60	0.56	0.60	0.62
LOI	3.87	1.67	4.01	4.06	2.10	1.55	1.49	0.97
Total	100.06	100.60	99.70	99.92	99.91	100.23	99.52	100.24
Trace Elements in ppm								
Rb	18	22	12	14	27	28	20	25
Sr	432	467	468	441	459	395	413	415
Ba	797	895	826	849	837	790	564	662
Sc	25.7	-	-	-	-	-	-	-
V	198	206	184	171	203	208	200	208
Cr	147	96	89	86	88	136	166	155
Ni	43	38	37	35	32	47	56	47
Y	39	43	42	40	42	42	39	40
Zr	283	309	299	290	307	291	266	272
Nb	23	24	22	23	24	23	22	22
Hf	6.0	-	-	-	-	-	-	-
Ta	1.1	-	-	-	-	-	-	-
Cs	0.7	-	-	-	-	-	-	-
Co	37	-	-	-	-	-	-	-
Th	2.8	-	-	-	-	-	-	-
U	1.1	-	-	-	-	-	-	-
Rare Earth Elements in ppm								
La	37.0	-	-	-	-	-	-	-
Ce	61.8	-	-	-	-	-	-	-
Nd	30.7	-	-	-	-	-	-	-
Sm	8.91	-	-	-	-	-	-	-
Eu	2.28	-	-	-	-	-	-	-
Tb	0.92	-	-	-	-	-	-	-
Yb	4.81	-	-	-	-	-	-	-
Lu	0.56	-	-	-	-	-	-	-

APPENDIX B. COMPOSITION OF HOOLE BASALTS (2)

Sample:	Ho-9	WL-36	WL-37	WL-38	WL-40	WL-41
Rock:	*qz thol*	*ol thol*	*ol thol*	*ol thol*	*ol thol*	*ol thol*
Type:	bomb	bomb	bomb	bomb	lava	lava
Site:	5	4	4	4	3	3

Major Elements in wt%

SiO2	48.54	48.16	48.56	48 58	49.29	49.42
TiO2	2.13	2.12	2.07	2.08	2.14	2.15
Al2O3	15.28	16.07	15.66	15.63	15.54	15.56
Fe2O3	11.54	11.98	11.94	11.89	11 93	12.08
MgO	6.36	5.79	6.63	6.59	6.51	6.53
MnO	0.20	0.21	0.19	0.20	0.17	0.17
CaO	8.94	9.43	9.01	9.07	8.66	8.71
Na2O	2.64	3.07	3.14	3.13	3.11	3.16
K2O	0.88	0.54	0.83	0.81	1.14	1 12
P2O5	0.61	0.66	0.58	0.59	0.63	0.63
LOI	2.80	2.71	1.59	1.74	1.69	1.39
Total	99.92	100.74	100.20	100.31	100.81	100.92

Trace Elements in ppm

Rb	18	15	23	23	24	22
Sr	409	446	426	429	436	436
Ba	653	511	496	548	743	691
Sc	-	-	-	27.5	-	26.8
V	193	221	215	220	222	244
Cr	181	142	124	125	120	116
Ni	43	71	74	77	68	69
Y	41	45	45	43	46	46
Zr	273	261	255	253	266	266
Nb	22	22	21	21	22	22
Hf	-	-	-	5.8	-	6.2
Ta	-	-	-	1.1	-	1.1
Cs	-	-	-	0.9	-	0.9
Co	-	-	-	40	-	39
Th	-	-	-	2.7	-	2.8
U	-	-	-	0.8	-	1.6

Rare Earth Elements in ppm

La	-	-	-	33.6	-	37.1
Ce	-	-	-	74.4	-	76.9
Nd	-	-	-	38.3	-	37.7
Sm	-	-	-	8.65	-	9.90
Eu	-	-	-	2.40	-	2.48
Tb	-	-	-	1.13	-	1.28
Yb	-	-	-	4.16	-	4.04
Lu	-	-	-	0.64	-	0.56

APPENDIX B. COMPOSITION OF HOOLE BASALTS (3)

Sample:	WL-1	WL-2	WL-3	WL-4	WL-5	WL-6	WL-7	WL-8
Rock:	*qz thol*	*ol thol*	*ol thol*	*ol thol*	*ol thol*	*ol thol*	*ol thol*	*ol thol*
Site:	1	1	1	1	1	1	1	1
Meter:	-	-	-	-	-	-	1.20	5.20

Major Elements in wt%

SiO2	50.49	50.04	49.59	48.69	49.12	49.08	50.57	50.19
TiO2	2.42	2.04	2.24	1.96	1.88	1.89	1.99	1.97
Al2O3	15.70	16.28	15 44	15.35	15.72	15.79	15.78	15.68
Fe2O3	11.28	10.28	11.47	12.12	10.79	11.24	11.08	11.02
MgO	4.13	4.71	4.81	6.90	6.13	7.19	6.07	6.33
MnO	0.18	0.17	0.18	0.18	0.16	0.16	0.16	0.17
CaO	9.39	10.14	9.67	8.96	9.05	9.01	8.56	8.67
Na2O	3.37	3.18	3.28	3.04	3.00	3.00	3.10	3.14
K2O	1.31	1.06	1.22	1.09	1.12	1.05	1.32	1.30
P2O5	0.60	0.49	0.56	0.50	0.44	0.44	0.48	0.47
LOI	1.10	1 78	2.01	1.44	2.94	1.59	1.31	1.54
Total	99.97	100.17	100.47	100.23	100.35	100.44	100.43	100.48

Trace Elements in ppm

Rb	26	25	25	23	27	24	32	31
Sr	386	411	389	388	370	363	354	363
Ba	2067	883	958	496	889	536	551	601
Sc	-	31.9	-	-	25.7	-	-	25.3
V	242	240	238	204	192	188	197	194
Cr	269	214	244	220	138	167	165	129
Ni	192	83	106	58	72	82	69	50
Y	49	42	46	40	38	39	44	43
Zr	295	243	275	242	217	221	263	256
Nb	22	19	20	19	17	17	21	20
Hf	-	6.0	-	-	5.7	-	-	6.3
Ta	-	1.0	-	-	1.0	-	-	1.2
Cs	-	0.8	-	-	1.1	-	-	1.3
Co	-	31	-	-	38	-	-	35
Th	-	2.4	-	-	2.6	-	-	3.6
U	-	0.8	-	-	0.8	-	-	1.6

Rare Earth Elements in ppm

La	-	27.8	-	-	27.5	-	-	30.8
Ce	-	59.4	-	-	56.8	-	-	63.7
Nd	-	34.2	-	-	33.6	-	-	37.3
Sm	-	8.30	-	-	7.90	-	-	8.24
Eu	-	2.40	-	-	2.04	-	-	2.13
Tb	-	1.21	-	-	1.28	-	-	1.24
Yb	-	3.78	-	-	3.52	-	-	3.83
Lu	-	0.57	-	-	0.50	-	-	0.60

APPENDIX B. COMPOSITION OF HOOLE BASALTS (4)

Sample:	WL-9	WL-10	WL-11	WL-12	WL-13	WL-14	WL-15	WL-16
Rock:	*ol thol*	*ol thol*	*ol thol*	*ol thol*	*ol thol*	*ol thol*	*ol thol*	*ol thol*
Site:	1	1	1	1	1	1	1	1
Meter:	12.10	16.80	21.80	26.90	31.40	36.40	41.40	44.90

Major Elements in wt%

SiO2	49.72	49.40	49.08	48.80	50.04	48.97	48.84	48.78
TiO2	1.90	1.87	1.79	1.83	1.90	1.94	1.85	1.78
Al2O3	15.76	15.78	15.75	15.29	16.03	15.69	15.68	15.94
Fe2O3	11.21	11.34	11.20	11.84	10.91	11.60	11.89	11.44
MgO	6.29	6.69	7.53	8.29	6.09	6.90	7.44	7.35
MnO	0.17	0.16	0.17	0.17	0.17	0.17	0.18	0.17
CaO	8.83	8.85	9.04	8.85	9.21	9.00	9.10	9.16
Na2O	3.15	3.10	2.95	2.96	3.11	3.00	2.92	2.97
K2O	1.18	1.14	1.00	0.98	1.07	1.01	1.00	0.97
P2O5	0.45	0.43	0.42	0.42	0.44	0.44	0.42	0.41
LOI	1.94	1.87	1.79	1.24	1.77	1.88	1.49	1.72
Total	100.60	100.63	100.72	100.67	100.74	100.60	100.81	100.68

Trace Elements in ppm

Rb	27	26	23	22	25	23	22	22
Sr	365	358	367	357	371	361	363	377
Ba	513	579	551	535	605	510	638	529
Sc	-	-	-	24.6	25.9	-	-	-
V	214	198	198	182	201	206	199	180
Cr	126	123	172	196	206	170	198	199
Ni	68	75	97	75	64	93	97	89
Y	42	40	37	37	39	40	37	36
Zr	241	226	207	208	224	217	212	205
Nb	19	18	16	17	18	17	18	16
Hf	-	-	-	5.3	5.5	-	-	-
Ta	-	-	-	0.9	0.9	-	-	-
Cs	-	-	-	0.6	0.5	-	-	-
Co	-	-	-	42	39	-	-	-
Th	-	-	-	2.5	2.7	-	-	-
U	-	-	-	0.7	0.8	-	-	-

Rare Earth Elements in ppm

La	-	-	-	24.4	26.6	-	-	-
Ce	-	-	-	53.5	57.3	-	-	-
Nd	-	-	-	25.2	32.2	-	-	-
Sm	-	-	-	7.11	7.54	-	-	-
Eu	-	-	-	1.91	2.13	-	-	-
Tb	-	-	-	0.95	0.98	-	-	-
Yb	-	-	-	3.59	3.84	-	-	-
Lu	-	-	-	0.52	0.58	-	-	-

APPENDIX B. COMPOSITION OF HOOLE BASALTS (5)

Sample:	WL-17	WL-18	WL-19	WL-21	WL-23	WL-25
Rock:	*ol thol*	*ol thol*	*ol thol*	*ol thol*	*qz thol*	*ol thol*
Site:	1	1	1	1	1	1
Meter:	53.10	61.10	71.70	-	-	-

Major Elements in wt%

SiO2	48.82	49.31	48.43	50.45	50.15	49.72
TiO2	1.74	1.85	1.89	1.97	2.04	1.94
Al2O3	16.08	16.13	15.17	15.66	15.61	15.66
Fe2O3	11.16	11.26	12.62	11.23	11.10	11.29
MgO	7.74	7.37	8.17	6.16	5.30	5.97
MnO	0.17	0.17	0.19	0.17	0.16	0.16
CaO	9.09	9.01	8.62	8.60	8.73	8.36
Na2O	2.96	3.03	2.84	3.19	2.99	3.15
K2O	0.93	0.99	1.02	1.31	1.35	1.33
P2O5	0.41	0.44	0.47	0.46	0.49	0.46
LOI	1.63	0.00	1.49	1.36	2.59	2.24
Total	100.73	99.56	100.92	100.56	100.51	100.28

Trace Elements in ppm

Rb	20	23	22	31	31	32
Sr	375	375	382	351	343	344
Ba	580	539	640	624	647	694
Sc	-	25.0	-	-	-	25.9
V	187	201	189	198	203	197
Cr	155	184	207	120	133	157
Ni	99	78	114	59	65	70
Y	35	38	38	44	45	44
Zr	198	214	225	262	262	256
Nb	16	17	18	21	21	20
Hf	-	5.2	-	-	-	6.4
Ta	-	0.9	-	-	-	1.0
Cs	-	0.0	-	-	-	1.8
Co	-	39	-	-	-	36
Th	-	2.5	-	-	-	3.1
U	-	0.6	-	-	-	0.8

Rare Earth Elements in ppm

La	-	26.0	-	-	-	31.8
Ce	-	56.3	-	-	-	66.2
Nd	-	30.6	-	-	-	33.6
Sm	-	7.64	-	-	-	8.44
Eu	-	2.05	-	-	-	2.16
Tb	-	0.97	-	-	-	0.92
Yb	-	3.44	-	-	-	4.22
Lu	-	0.53	-	-	-	0.59

APPENDIX B. COMPOSITION OF HOOLE BASALTS (6)

Sample:	WL-26	WL-27	WL-28	WL-30	WL-31	WL-32	WL-33	WL-34	
Rock:	*ol thol*	*ol thol*	*ol thol*	*ol thol*	*qz thol*	*ol thol*	*ol thol*	*ol thol*	
Site:	1	1	1	1	1	1	1	2	
Meter:	-	-	-	-	-	-	-	-	
Major Elements in wt%									
SiO2	50.42	48.56	48.99	49.20	50.70	49.53	49.83	49.61	
TiO2	1.96	1.76	1.83	2.06	2.85	2.01	2.36	2.12	
Al2O3	15.42	16.02	15.98	15.51	13.15	16.29	14.78	15.37	
Fe2O3	11.28	11.88	11.36	12.01	11.95	11.42	11.57	11.60	
MgO	5.99	7.90	6.26	7.31	5.34	6.60	4.73	6.21	
MnO	0.16	0.17	0.17	0.18	0.19	0.17	0.18	0.18	
CaO	8.51	8.95	9.40	8.66	10.14	9.01	9.73	8.50	
Na2O	3.12	2.88	3.00	2.98	3.11	3.09	3.26	2.97	
K2O	1.40	0.96	1.04	1.12	1.37	1.07	1.29	1.25	
P2O5	0.47	0.44	0.46	0.53	0.63	0.50	0.60	0.58	
LOI	1.83	1.47	1.73	0.91	1.15	0.81	2.02	2.10	
Total	100.56	100.99	100.22	100.47	100.58	100.49	100.34	100.49	
Trace Elements in ppm									
Rb	35	21	22	24	29	22	27	31	
Sr	357	394	409	397	335	397	364	396	
Ba	644	595	703	614	917	588	769	652	
Sc	-	21.9	-	-	-	-	36.7	-	
V	207	154	179	187	314	188	241	186	
Cr	128	200	283	195	424	172	350	188	
Ni	65	96	86	91	33	69	48	68	
Y	45	35	38	42	55	41	50	43	
Zr	270	208	222	256	320	245	297	264	
Nb	21	17	18	20	24	19	22	20	
Hf	-	5.1	-	-	-	-	7.2	-	
Ta	-	1.0	-	-	-	-	1.2	-	
Cs	-	1.0	-	-	-	-	0.6	-	
Co	-	43	-	-	-	-	32	-	
Th	-	2.4	-	-	-	-	3.6	-	
U	-	0.6	-	-	-	-	1.2	-	
Rare Earth Elements in ppm									
La	-	25.0	-	-	-	-	33.9	-	
Ce	-	52.5	-	-	-	-	77.4	-	
Nd	-	25.6	-	-	-	-	40.2	-	
Sm	-	7.18	-	-	-	-	9.85	-	
Eu	-	1.92	-	-	-	-	2.54	-	
Tb	-	0.77	-	-	-	-	1.35	-	
Yb	-	2.93	-	-	-	-	4.88	-	
Lu	-	0.48	-	-	-	-	0.64	-	

APPENDIX B. COMPOSITION OF HOOLE BASALTS (7)

Sample:	WL-35	RA-23
Rock:	*qz thol*	*HYN*
Site:	2	10
Meter:	-	-

Major Elements in wt%

SiO2	50.19	48.35
TiO2	2.22	1.89
Al2O3	15.87	17.58
Fe2O3	9.90	9.42
FeO	7.57	7.21
MgO	5.10	4.77
MnO	0.14	0.14
CaO	8.87	10.63
Na2O	3.04	3.05
K2O	1.33	0.93
P2O5	0.60	0.59
LOI	3.54	3.13
Total	100.80	100.48

Trace Elements in ppm

Rb	34	18
Sr	418	513
Ba	636	627
Sc	-	28.2
V	194	188
Cr	163	257
Ni	74	42
Y	44	36
Zr	270	196
Nb	20	16
Hf	-	4.8
Ta	-	0.8
Cs	-	0.0
Co	-	25
Th	-	2.0
U	-	1.0

Rare Earth Elements in ppm

La	-	28.6
Ce	-	60.8
Nd	-	26.3
Sm	-	7.82
Eu	-	2.41
Tb	-	0.98
Yb	-	3.39
Lu	-	0.47

APPENDIX C:

Olivine microprobe analysis

for the Rancheria and Hoole basalts

APPENDIX C. OLIVINE MICROPROBE ANALYSIS (1)

Sample:	WL-12	WL-12	WL-12	WL-12	WL-12	WL-41	WL-41	WL-41
Rock:	*ol thol*	*ol thol*	*ol thol (rim)*	*ol thol (ctre)*	*ol thol (rim)*	*ol thol*	*ol thol (ctre)*	*ol thol (rim)*
Major Elements in wt%								
SiO2	37.48	36.97	37.05	36.84	37.35	35.88	36.24	36.65
Al2O3	0.00	0.00	0.00	0.00	0.00	0.00	0.00	0.00
TiO2	0.04	0.02	0.05	0.00	0.06	0.06	0.05	0.01
FeO	31.26	34.70	33.74	33.08	32.99	38.20	35.88	36.75
MgO	30.98	28.11	29.15	29.45	29.40	25.82	27.21	26.48
MnO	0.56	0.69	0.63	0.57	0.56	0.64	0.60	0.64
NiO	0.05	0.03	0.01	0.02	0.03	0.04	0.03	0.02
Cr2O3	0.00	0.00	0.00	0.00	0.00	0.01	0.00	0.00
CaO	0.22	0.16	0.18	0.26	0.14	0.26	0.31	0.26
Total	100.59	100.67	100.82	100.22	100.53	100.90	100.32	100.81
Cations normalized to 3 cations								
Si	1.017	1.020	1.015	1.012	1.024	1.004	1.009	1.021
Al	0.000	0.000	0.000	0.000	0.000	0.000	0.000	0.000
Ti	0.001	0.000	0.001	0.000	0.001	0.001	0.001	0.000
Fe	0.709	0.801	0.773	0.760	0.756	0.894	0.836	0.856
Mg	1.253	1.157	1.191	1.206	1.201	1.077	1.130	1.100
Mn	0.013	0.016	0.015	0.013	0.013	0.015	0.014	0.015
Ni	0.001	0.001	0.000	0.000	0.001	0.001	0.001	0.000
Cr	0.000	0.000	0.000	0.000	0.000	0.000	0.000	0.000
Ca	0.006	0.005	0.005	0.008	0.004	0.008	0.009	0.008
O	4.018	4.021	4.016	4.012	4.025	4.005	4.010	4.021
Fo (cat)	63.8	59.1	60.6	61.5	61.4	54.6	57.5	56.2

APPENDIX C. OLIVINE MICROPROBE ANALYSIS (2)

Sample:	WL-41	RA-21	RA-21	RA-21	RA-21	RA-21	RA-7	RA-7
Rock:	*ol thol*	*AOB*	*AOB*	*AOB (rim)*	*AOB (ctre)*	*AOB (rim)*	*AOB cum (rim)*	*AOB cum (ctre)*
Major Elements in wt%								
SiO2	38.47	38.83	39.36	38.81	39.81	38.70	39.81	40.37
Al2O3	0.00	0.00	0.00	0.00	0.00	0.00	0.00	0.00
TiO2	0.02	0.02	0.01	0.06	0.01	0.02	0.01	0.01
FeO	24.70	21.78	21.14	22.47	18.27	22.76	16.81	14.61
MgO	36.47	38.79	39.40	38.34	41.49	37.76	43.13	44.49
MnO	0.40	0.30	0.27	0.27	0.23	0.30	0.25	0.22
NiO	0.08	0.20	0.15	0.18	0.23	0.14	0.15	0.20
Cr2O3	0.02	0.00	0.02	0.01	0.05	0.01	0.00	0.02
CaO	0.24	0.29	0.24	0.20	0.21	0.29	0.26	0.15
Total	100.39	100.21	100.59	100.34	100.30	99.98	100.43	100.08
Cations normalized to 3 cations								
Si	1.011	1.008	1.014	1.009	1.016	1.012	1.005	1.014
Al	0.000	0.000	0.000	0.000	0.000	0.000	0.000	0.000
Ti	0.000	0.000	0.000	0.001	0.000	0.000	0.000	0.000
Fe	0.543	0.473	0.456	0.489	0.390	0.498	0.355	0.307
Mg	1.428	1.500	1.514	1.486	1.578	1.472	1.624	1.666
Mn	0.009	0.007	0.006	0.006	0.005	0.007	0.005	0.005
Ni	0.002	0.004	0.003	0.004	0.005	0.003	0.003	0.004
Cr	0.000	0.000	0.000	0.000	0.001	0.000	0.000	0.000
Ca	0.007	0.008	0.007	0.006	0.006	0.008	0.007	0.004
O	4.011	4.008	4.015	4.010	4.016	4.013	4.006	4.014
Fo (cat)	72.4	76.0	76.8	75.2	80.2	74.7	82.6	84.4

APPENDIX C. OLIVINE MICROPROBE ANALYSIS (3)

Sample:	RA-7	RA-7	RA-11	RA-11	RA-3	RA-3	RA-3	RA-3
Rock:	*AOB cum (rim)*	*AOB cum*	*AOB*	*AOB (grdm)*	*BASAN (rim)*	*BASAN (ctre)*	*BASAN (rim)*	*BASAN*
Major Elements in wt%								
SiO2	40.05	40.11	40.33	40.03	38.64	39.77	37.57	40.26
Al2O3	0.00	0.00	0.00	0.00	0.00	0.00	0.00	0.00
TiO2	0.02	0.00	0.02	0.04	0.01	0.01	0.00	0.00
FeO	15.03	16.88	15.90	17.03	22.75	17.77	27.31	16.31
MgO	43.96	42.83	43.18	42.62	38.01	41.74	33.99	43.25
MnO	0.18	0.23	0.23	0.28	0.36	0.30	0.49	0.20
NiO	0.20	0.16	0.13	0.12	0.05	0.07	0.04	0.11
Cr2O3	0.03	0.01	0.01	0.01	0.01	0.00	0.00	0.01
CaO	0.19	0.25	0.29	0.30	0.47	0.45	0.58	0.28
Total	99.66	100.47	100.09	100.43	100.29	100.11	99.98	100.42
Cations normalized to 3 cations								
Si	1.012	1.014	1.020	1.013	1.006	1.014	1.005	1.016
Al	0.000	0.000	0.000	0.000	0.000	0.000	0.000	0.000
Ti	0.000	0.000	0.000	0.001	0.000	0.000	0.000	0.000
Fe	0.318	0.357	0.336	0.361	0.495	0.379	0.611	0.344
Mg	1.656	1.614	1.628	1.608	1.476	1.587	1.356	1.626
Mn	0.004	0.005	0.005	0.006	0.008	0.006	0.011	0.004
Ni	0.004	0.003	0.003	0.002	0.001	0.001	0.001	0.002
Cr	0.001	0.000	0.000	0.000	0.000	0.000	0.000	0.000
Ca	0.005	0.007	0.008	0.008	0.013	0.012	0.017	0.008
O	4.013	4.014	4.020	4.014	4.007	4.014	4.005	4.016
Fo (cat)	83.9	81.9	82.9	81.7	74.9	80.7	68.9	82.5

APPENDIX C. OLIVINE MICROPROBE ANALYSIS (4)

Sample:	RA-19	RA-19	RA-19
Rock:	*HYN*	*HYN (rim)*	*HYN (ctre)*

Major Elements in wt%

SiO2	38.51	39.86	40.01
Al2O3	0.00	0.00	0.00
TiO2	0.04	0.02	0.00
FeO	25.33	17.19	16.07
MgO	36.12	42.30	43.40
MnO	0.34	0.23	0.20
NiO	0.09	0.16	0.25
Cr2O3	0.03	0.03	0.02
CaO	0.31	0.21	0.20
Total	100.77	100.00	100.14

Cations normalized to 3 cations

Si	1.011	1.014	1.011
Al	0.000	0.000	0.000
Ti	0.001	0.000	0.000
Fe	0.556	0.366	0.340
Mg	1.413	1.605	1.635
Mn	0.008	0.005	0.004
Ni	0.002	0.003	0.005
Cr	0.001	0.001	0.000
Ca	0.009	0.006	0.005
O	4.012	4.015	4.011
Fo (cat)	71.8	81.4	82.8

APPENDIX D:

Clinopyroxene microprobe analysis

for the Rancheria and Hoole basalts

APPENDIX D. CLINOPYROXENE MICROPROBE ANALYSIS (1)

Sample:	HO-1	HO-1	HO-1	WL-12	WL-12	WL-12	WL-12	WL-41
Rock:	*qz thol*	*qz thol*	*qz thol*	*ol thol*	*ol thol (rim)*	*ol thol (ctre)*	*ol thol (rim)*	*ol thol*
Major Elements in wt%								
SiO2	47.34	48.67	46.34	50.77	50.49	50.47	51.28	49.87
Al2O3	3.41	2.50	3.78	2.45	2.64	2.86	1.35	2.40
TiO2	3.24	2.08	3.73	1.30	1.33	1.35	0.92	1.68
FeO	13.32	13.35	13.20	8.22	8.44	7.99	11.34	11.06
MgO	11.18	11.42	10.70	15.49	15.72	15.39	14.36	14.44
MnO	0.29	0.28	0.26	0.22	0.22	0.17	0.35	0.30
NiO	0.00	0.00	0.01	0.02	0.00	0.03	0.01	0.01
Cr2O3	0.08	0.03	0.24	0.37	0.49	0.55	0.00	0.04
CaO	19.69	19.69	19.91	19.48	19.04	19.60	18.90	18.51
Na2O	0.46	0.33	0.48	0.31	0.34	0.31	0.35	0.37
Total	99.01	98.35	98.65	98.62	98.71	98.72	98.86	98.68
Cations normalized to 4 cations								
Si	1.823	1.883	1.795	1.906	1.892	1.892	1.941	1.889
Al	0.155	0.114	0.173	0.108	0.117	0.126	0.060	0.107
Ti	0.094	0.061	0.109	0.037	0.037	0.038	0.026	0.048
Fe	0.429	0.432	0.428	0.258	0.265	0.251	0.359	0.350
Mg	0.642	0.659	0.618	0.867	0.878	0.860	0.810	0.816
Mn	0.009	0.009	0.009	0.007	0.007	0.005	0.011	0.010
Ni	0.000	0.000	0.000	0.001	0.000	0.001	0.000	0.000
Cr	0.002	0.001	0.007	0.011	0.015	0.016	0.000	0.001
Ca	0.812	0.816	0.826	0.783	0.765	0.787	0.766	0.751
Na	0.034	0.025	0.036	0.023	0.025	0.023	0.026	0.027
O	5.978	5.989	5.975	5.991	5.983	5.990	5.984	5.978
En(mol%)	35.9	35.8	34.9	47.4	48.6	47.7	42.9	44.5
Fs(mol%)	23.0	22.6	23.3	12.8	12.6	12.3	17.9	17.5
Wo(mol%)	41.1	41.6	41.8	39.8	38.8	40.0	39.1	38.0

APPENDIX D. CLINOPYROXENE MICROPROBE ANALYSIS (2)

Sample:	WL-41	RA-21	RA-21	RA-21	RA-21	RA-7	RA-7	RA-7
Rock:	*ol thol*	*AOB*	*AOB*	*AOB (grdm)*	*AOB (grdm)*	*AOB cum*	*AOB cum (rim)*	*AOB cum (ctre)*
Major Elements in wt%								
SiO2	50.04	48.03	47.11	48.35	48.43	51.04	47.39	50.81
Al2O3	2.87	4.70	5.09	2.64	3.77	2.78	4.86	2.77
TiO2	1.30	2.34	2.93	2.92	2.45	1.19	3.02	1.24
FeO	8.84	8.70	10.08	13.01	10.06	6.66	9.28	6.47
MgO	15.21	13.10	12.37	10.65	12.41	15.35	12.14	15.29
MnO	0.23	0.17	0.16	0.27	0.19	0.15	0.16	0.15
NiO	0.02	0.01	0.03	0.01	0.01	0.00	0.01	0.00
Cr2O3	0.68	0.44	0.15	0.00	0.00	0.46	0.00	0.26
CaO	19.13	20.71	20.32	20.32	20.58	21.23	21.06	21.44
Na2O	0.31	0.52	0.56	0.71	0.54	0.33	0.66	0.36
Total	98.63	98.72	98.80	98.87	98.45	99.19	98.57	98.78
Cations normalized to 4 cations								
Si	1.883	1.815	1.789	1.863	1.847	1.899	1.801	1.896
Al	0.127	0.209	0.228	0.120	0.169	0.122	0.218	0.122
Ti	0.037	0.067	0.084	0.085	0.070	0.033	0.086	0.035
Fe	0.278	0.275	0.320	0.419	0.321	0.207	0.295	0.202
Mg	0.853	0.738	0.700	0.612	0.705	0.851	0.688	0.850
Mn	0.007	0.005	0.005	0.009	0.006	0.005	0.005	0.005
Ni	0.001	0.000	0.001	0.000	0.000	0.000	0.000	0.000
Cr	0.020	0.013	0.005	0.000	0.000	0.014	0.000	0.008
Ca	0.771	0.839	0.827	0.839	0.841	0.846	0.858	0.857
Na	0.023	0.038	0.041	0.053	0.040	0.024	0.049	0.026
O	5.982	5.974	5.969	5.981	5.982	5.988	5.972	5.982
En(mol%)	47.8	43.6	41.6	33.8	39.9	47.0	40.4	46.9
Fs(mol%)	13.1	13.4	16.2	22.4	16.8	9.8	15.2	9.4
Wo(mol%)	39.1	43.0	42.2	43.8	43.3	43.2	44.4	43.7

APPENDIX D. CLINOPYROXENE MICROPROBE ANALYSIS (3)

Sample:	RA-7	RA-7	RA-7	RA-7	RA-7	RA-11	RA-11	RA-11
Rock:	*AOBcum (rim)*	*AOBcum*	*AOBcum (rim)*	*AOBcum (ctre)*	*AOBcum (rim)*	*AOB*	*AOB*	*AOB*
Major Elements in wt%								
SiO2	48.63	50.75	49.83	50.25	47.64	48.82	49.12	49.74
Al2O3	4.50	2.97	2.63	2.83	4.71	2.51	4.17	2.56
TiO2	2.16	1.47	1.73	1.25	2.68	1.83	1.62	1.54
FeO	7.17	6.74	8.89	6.35	7.76	10.88	7.06	8.64
MgO	13.94	14.74	13.48	15.05	13.29	12.63	14.29	14.23
MnO	0.12	0.13	0.20	0.16	0.14	0.23	0.14	0.17
NiO	0.00	0.00	0.00	0.02	0.01	0.03	0.04	0.00
Cr2O3	0.07	0.09	0.00	0.30	0.03	0.00	0.34	0.01
CaO	21.65	21.59	21.18	21.83	21.67	20.90	21.14	21.13
Na2O	0.40	0.37	0.54	0.32	0.47	0.45	0.36	0.36
Total	98.63	98.85	98.48	98.36	98.41	98.28	98.28	98.38
Cations normalized to 4 cations								
Si	1.827	1.897	1.886	1.884	1.801	1.867	1.850	1.880
Al	0.199	0.131	0.117	0.125	0.210	0.113	0.185	0.114
Ti	0.061	0.041	0.049	0.035	0.076	0.053	0.046	0 044
Fe	0.225	0.211	0.281	0.199	0.245	0.348	0.222	C.273
Mg	0.781	0.822	0.761	0.841	0.749	0.720	0.802	0.802
Mn	0.004	0.004	0.006	0.005	0.004	0.007	0.004	0.005
Ni	0.000	0.000	0.000	0.001	0.000	0.001	0.001	0.000
Cr	0.002	0.003	0.000	0.009	0.001	0.000	0.010	0.000
Ca	0.871	0.865	0.859	0.877	0.878	0.857	0.853	0.855
Na	0.029	0.027	0.040	0.023	0.034	0.033	0.026	0.026
O	5.974	5.992	5.974	5.975	5.966	5.960	5.980	5.968
En(mol%)	44.9	45.0	42.0	46.7	43.7	39.8	46.0	44.0
Fs(mol%)	10.9	10.8	13.7	8.7	11.6	16.6	10.7	12.6
Wo(mol%)	44.2	44.2	44.3	44.6	44.7	43.6	43.3	43.4

APPENDIX D. CLINOPYROXENE MICROPROBE ANALYSIS (4)

Sample:	RA-3	RA-3	RA-3	RA-3	RA-19	RA-19	RA-19	RA-19
Rock:	*BASAN (rim)*	*BASAN (ctre)*	*BASAN (rim)*	*BASAN (ctre)*	*HYN (rim)*	*HYN*	*HYN*	*HYN*
Major Elements in wt%								
SiO2	43.13	46.21	43.90	45.25	50.06	49.31	50.32	49.33
Al2O3	9.84	6.99	8.24	7.72	2.23	2.64	2.76	3.20
TiO2	3.91	2.55	4.07	3.08	1.57	1.75	1.47	1.58
FeO	8.27	7.97	10.15	8.24	13.01	10.48	9.28	9.36
MgO	10.88	12.22	9.23	11.58	13.33	14.22	14.46	14.74
MnO	0.08	0.10	0.18	0.08	0.32	0.21	0.19	0.19
NiO	0.00	0.02	0.01	0.01	0.00	0.02	0.03	0.01
Cr2O3	0.14	0.10	0.02	0.00	0.01	0.10	0.14	0.38
CaO	21.73	22.30	21.97	22.21	18.23	19.59	19.92	19.27
Na2O	0.50	0.47	0.67	0.50	0.46	0.35	0.31	0.37
Total	98.48	98.93	98.44	98.66	99.22	98.67	98.88	98.43
Cations normalized to 4 cations								
Si	1.639	1.740	1.690	1.713	1.901	1.867	1.895	1.863
Al	0.441	0.310	0.374	0.344	0.100	0.118	0.122	0.142
Ti	0.112	0.072	0.118	0.088	0.045	0.050	0.042	0.045
Fe	0.263	0.251	0.327	0.261	0.413	0.332	0.292	0.296
Mg	0.617	0.686	0.530	0.654	0.755	0.803	0.812	0.830
Mn	0.003	0.003	0.006	0.003	0.010	0.007	0.006	0.006
Ni	0.000	0.001	0.000	0.000	0.000	0.001	0.001	0.000
Cr	0.004	0.003	0.001	0.000	0.000	0.003	0.004	0.011
Ca	0.885	0.900	0.906	0.901	0.742	0.795	0.804	0.780
Na	0.037	0.034	0.050	0.037	0.034	0.026	0.023	0.027
O	5.955	5.952	5.970	5.955	5.979	5.965	5.988	5.971
En(mol%)	42.0	43.0	34.4	41.6	41.1	44.3	44.4	46.8
Fs(mol%)	13.6	11.4	18.6	12.8	20.1	15.7	14.9	13.9
Wo(mol%)	44.4	45.6	47.0	45.6	37.9	40.0	40.7	39.3

APPENDIX E:

Plagioclase microprobe analysis

for the Rancheria and Hoole basalts

APPENDIX E. PLAGIOCLASE MICROPROBE ANALYSIS (1)

Sample:	HO-1	HO-1	HO-1	HO-1	HO-1	HO-1	WL-12	WL-12
Rock:	*qz thol (rim)*	*qz thol (ctre)*	*qz thol (rim)*	*qz thol (rim)*	*qz thol (ctre)*	*qz thol (rim)*	*ol thol*	*ol thol (rim)*
Major Elements in wt%								
SiO2	51.77	51.96	58.10	54.92	52.97	53.38	51.52	51.64
Al2O3	28.98	29.55	24.32	27.43	29.12	29.21	30.14	29.32
FeO	0.90	0.41	0.85	0.48	0.45	0.54	0.54	0.75
MgO	0.38	0.16	0.17	0.14	0.16	0.14	0.08	0.22
Na2O	3.82	3.88	6.56	4.90	4.19	4.18	3.81	3.93
CaO	12.46	12.85	7.34	10.72	12.34	12.06	13.20	12.55
K2O	0.33	0.26	0.96	0.46	0.31	0.32	0.23	0.25
Total	98.65	99.08	98.30	99.05	99.54	99.83	99.51	98.67
Cations normalized to 5 cations								
Si	2.387	2.384	2.652	2.509	2.416	2.428	2.354	2.379
Al	1.575	1.598	1.308	1.477	1.565	1.566	1.623	1.592
Fe	0.035	0.016	0.032	0.018	0.017	0.021	0.021	0.029
Mg	0.026	0.011	0.012	0.010	0.011	0.009	0.005	0.015
Na	0.342	0.345	0.581	0.434	0.370	0.369	0.337	0.351
Ca	0.616	0.632	0.359	0.525	0.603	0.588	0.646	0.619
K	0.019	0.015	0.056	0.027	0.018	0.019	0.013	0.015
O	7.995	8.003	7.988	8.017	8.004	8.018	7.990	7.992
An (cat)	64.3	64.7	38.2	54.8	62.0	61.4	65.7	63.8

APPENDIX E. PLAGIOCLASE MIRCROPROBE ANALYSIS (2)

Sample:	WL-12	WL-12	WL-41	WL-41	WL-41	RA-21	RA-21	RA-21
Rock:	*ol thol (ctre)*	*ol thol (rim)*	*ol thol*	*ol thol*	*ol thol (grdm)*	*AOB*	*AOB*	*AOB*

Major Elements in wt%

SiO2	50.77	53.25	52.86	52.93	53.16	52.82	53.01	51.88
Al2O3	30.68	28.68	28.63	28.91	28.49	29.15	28.98	29.00
FeO	0.48	0.68	0.50	0.43	0.58	0.55	0.46	1.93
MgO	0.08	0.08	0.14	0.14	0.11	0.06	0.12	0.22
Na2O	3.44	4.52	4.44	4.25	4.43	4.53	4.43	4.27
CaO	13.80	11.71	11.89	12.16	11.58	11.84	11.80	11.85
K2O	0.21	0.34	0.36	0.33	0.36	0.25	0.31	0.27
Total	99.46	99.26	98.82	99.15	98.71	99.20	99.12	99.42

Cations normalized to 5 cations

Si	2.325	2.432	2.424	2.422	2.442	2.411	2.424	2.373
Al	1.656	1.544	1.547	1.559	1.543	1.569	1.562	1.563
Fe	0.018	0.026	0.019	0.016	0.022	0.021	0.018	0.074
Mg	0.005	0.005	0.010	0.010	0.008	0.004	0.008	0.015
Na	0.305	0.400	0.395	0.377	0.395	0.401	0.393	0.379
Ca	0.677	0.573	0.584	0.596	0.570	0.579	0.578	0.581
K	0.012	0.020	0.021	0.019	0.021	0.015	0.018	0.016
O	7.994	7.994	7.990	8.004	8.006	7.988	7.999	7.957
An (cat)	68.9	58.9	59.6	61.2	59.1	59.1	59.5	60.5

APPENDIX E. PLAGIOCLASE MICROPROBE ANALYSIS (3)

Sample:	RA-7	RA-7	RA-7	RA-7	RA-11	RA-11	RA-3	RA-3
Rock:	*AOBcum*	*AOBcum (rim)*	*AOBcum (ctre)*	*AOBcum (rim)*	*AOB*	*AOB*	*BASAN*	*BASAN*
Major Elements in wt%								
SiO2	52.35	52.46	51.77	51.49	51.22	51.99	50.55	50.36
Al2O3	29.38	29.48	30.38	30.10	29.82	29.25	30.57	30.76
FeO	0.65	0.58	0.62	0.69	0.62	0.79	0.54	0.59
MgO	0.07	0.06	0.08	0.05	0.10	0.16	0.03	0.04
Na2O	4.21	4.26	3.86	3.93	3.84	3.98	3.39	3.43
CaO	12.36	12.37	13.07	13.01	12.88	12.37	13.45	13.71
K2O	0.31	0.28	0.28	0.22	0.28	0.34	0.23	0.23
Total	99.33	99.48	100.06	99.49	98.75	98.88	98.76	99.12
Cations normalized to 5 cations								
Si	2.392	2.392	2.352	2.352	2.357	2.390	2.333	2.314
Al	1.582	1.584	1.627	1.620	1.617	1.585	1.663	1.666
Fe	0.025	0.022	0.024	0.026	0.024	0.030	0.021	0.023
Mg	0.005	0.004	0.005	0.003	0.007	0.011	0.002	0.003
Na	0.373	0.377	0.340	0.348	0.343	0.355	0.303	0.306
Ca	0.605	0.604	0.636	0.637	0.635	0.609	0.665	0.675
K	0.018	0.016	0.016	0.013	0.016	0.020	0.014	0.013
O	7.988	7.988	7.987	7.982	7.987	7.995	8.006	7.988
An (cat)	61.9	61.6	65.2	65.0	64.9	63.2	68.7	68.8

APPENDIX E. PLAGIOCLASE MICROPROBE ANALYSIS (4)

Sample:	RA-3	RA-19	RA-19	RA-19
Rock:	*BASAN (rim)*	*HYN*	*HYN*	*HYN*

Major Elements in wt%

SiO2	54.00	53.70	51.84	55.79
Al2O3	28.25	28.63	29.95	26.87
FeO	0.30	0.51	0.52	0.58
MgO	0.02	0.12	0.06	0.09
Na2O	4.99	4.68	3.93	5.64
CaO	10.34	11.43	12.95	9.59
K2O	0.58	0.32	0.24	0.53
Total	98.47	99.38	99.48	99.09

Cations normalized to 5 cations

Si	2.475	2.446	2.368	2.537
Al	1.526	1.537	1.612	1.440
Fe	0.012	0.019	0.020	0.022
Mg	0.001	0.008	0.004	0.006
Na	0.444	0.413	0.348	0.497
Ca	0.508	0.558	0.634	0.467
K	0.034	0.019	0.014	0.031
O	8.000	7.998	7.993	7.993
An (cat)	53.4	57.5	64.6	48.4